Air quality modeling ~~intercomparison~~inter-comparison and multi-scale ensemble chain for Latin America

Jorge E. Pachon[1], Mariel A. Opazo[2], Pablo Lichtig[3], Nicolas Huneeus[2], Idir Bouarar[4], Guy Brasseur[4*], Cathy W. Y. Li[4], Johannes Flemming[5], Laurent Menut[6], Camilo Menares[2], Laura Gallardo[2], Michael Gauss[7], Mikhail Sofiev[8], Rostislav Kouznetsov[8], Julia Palamarchuk[8], Andreas Uppstu[8], Laura Dawidowski[3], Nestor Y. Rojas[9], Maria de Fatima Andrade[10], Mario E. Gavidia-Calderón[10], Alejandro H. Delgado Peralta[10], Daniel Schuch[10,11]

[1] Department of Environmental Engineering, Universidad de La Salle, Bogotá, 111711, Colombia
[2] Department of Geophysics and Center for Climate and Resilience Research (CR2), Universidad de Chile, Santiago, 8320000~~, Chile & Center for Climate and Resilience Research (CR2)~~
[3] Consejo Nacional de Energía Atómica – CNEA, Buenos Aires, C1429BNP, Argentina
[4] Max Planck Institute for Meteorology, Hamburg, 20146, Germany
[5] European Centre for Medium-Range Weather Forecasts– ECMWF, Bonn, 53175, Germany
[6] Laboratoire de Météorologie Dynamique, Palaiseau, 91128, France
[7] Norwegian Meteorological Institute, Oslo, 0313, Norway
[8] Finnish Meteorological Institute, Helsinki, FI-00560, Finland
[9] Depa~~6~~rtment of Chemical and Environmental Engineering, Universidad Nacional de Colombia, Bogotá, 111321, Colombia
[10] Instituto de Astronomia, Geofísica e Ciências Atmosféricas, Universidad de São Paulo, São Paulo, 05508-09B, Brazil
[11] Civil and Environmental Engineering, Northeastern University, Boston, 02115, USA

Correspondence to: Guy Brasseur (guy.brasseur@mpimet.mpg.de)

Abstract. A multi-scale modeling ensemble chain has been assembled as a first step towards an Air Quality analysis and forecasting (AQF) system for Latin America. Two global and three regional models were tested and compared in retrospective mode over a shared domain (120W-28W, 60S-30N) for the months of January and July 2015. The objective of this experiment was ~~in order to to~~ understand their performance and characterize their errors~~simulate January and July of 2015~~. Observations from local air quality monitoring networks in Colombia, Chile, Brazil, México, Ecuador and Per~~ú~~ú were used for model evaluation. The models generally agreed with observations in large cities such as México City and São Paulo, whereas representing smaller urban areas, such as Bogotá and Santiago, was more challenging. For instance, in Santiago~~,~~ during wintertime, the simulations showed large discrepancies with observations. No single model demonstrated superior ~~had the best~~ performance over others or among pollutants and sites available. In general, ~~O~~ozone and NO_2 exhibited the lowest bias and errors, especially in ~~Sao Paulo~~São Paulo and Mexico City. For SO_2, the bias and error were close to 200%, except for ~~the of in Bogota~~Bogotá. ~~Ozone and NO_2 were reproduced better than other pollutants across sites whereas SO_2 was the most difficult.~~ The ensemble, created from the median value of all ~~the individual~~ models, was evaluated as well. In some cases, the ensemble outperformed the ~~showed better results over the~~ individual models and mitigated ~~the~~ extreme over- or underestimation ~~of certain models~~, ~~demonstrating the potential to establish an analysis and forecast system for Latin America.~~ However, more research is needed before concluding that the ensemble is the path for an AQF system in Latin America. This study identified certain limitations in the models and global emissions inventories, which should be addressed with the involvement and experience of local researchers.

Con formato: Superíndice
Con formato: Inglés (Estados Unidos)
Con formato: Inglés (Estados Unidos)
Con formato: Inglés (Estados Unidos)
Con formato: Francés (Francia)
Con formato: Subíndice
Con formato: Subíndice

1. Introduction

Latin America has some of the most populated urban areas in the world, notably, México City and São Paulo have populations exceeding 20 million, while Lima, Bogotá, Rio de Janeiro, and Buenos Aires have more than 10 million inhabitants each (United Nations, 2018). These densely populated regions often experience air pollution events due to large emission sources and due to atmospheric conditions. Other major cities, such as Santiago and Medellin, with a population of ~7 and ~3.5 million, respectively, are also affected by poor air quality. This urban air pollution not only has long lasting effects on the health of the population but also has a significant negative impact on the environment~~.~~, and possibly the regional climate (Busch et al., 2023; Gouveia et al., 2018; Molina et al., 2015; Rodríguez-Villamizar et al., 2018; Romieu et al., 2012). Latin America could greatly benefit from an air quality forecasting (AFC) system that informs the public about air pollution episodes and supports policy actions.

To better understand the causes of air pollution events in Latin America, it is important to consider the local emission sources. In addition to the usual urban pollution causes ~~sources~~ (e.g., industrial facilities, residential heating, energy production, and transportation sectors), plumes from biomass burning and long-range dust transport can occasionally reach major cities. In northern South America, increased pollution levels in the dry season have been associated with ~~wildfires~~ biomass burning (Ballesteros-González et al., 2020; Casallas et al., 2023; Mendez-Espinosa et al., 2019) and dust from the Sahara Desert (Mendez-Espinosa et al., 2020). The latter source also affects the Caribbean and central México in early spring (Kramer and Kirtman, 2021; Ramírez-Romero et al., 2021). Also, in the context of climate and land-use change, wildfires are a recurrent phenomenon in southern South America (Diaz Resquin et al., 2018; de la Barrera et al., 2018; Sarricolea et al., 2020). The Amazon is the largest forest in ~~Latin America~~the world and a significant source of biogenic volatile organic compounds (BVOCs), precursors of CO, ~~and secondary~~ ozone and secondary aerosols ~~being isoprene the dominant species~~ (Nascimento et al., 2022; Zimmerman et al., 1988)~~.~~.

Air quality management in Latin America and the Caribbean (LAC) has been traditionally focused on surveillance and building emission inventories (Franco et al., 2019). Modeling activities ~~for LAC~~ are less frequent than North America, Europe, or Asia, mainly due to limited computing resources and scarce information of emission sources. Of more than 30 regional AQF systems identified worldwide only one exists in Latin America (Zhang et al., 2012). In addition to the restrictions already mentioned, ~~Furthermore,~~ LAC has other challenges: complex terrain where cities are situated in the valleys and canyons of the Andes, varying meteorological conditions due to their proximity to mountains and coastlines, deep convection in the tropics, extensive biomass burning in the Orinoco and Amazonian basins, and the presence of densely populated megacities and urban areas, among others. Despite limitations for applying air quality models in LAC, regional models ~~in the literature~~ have been successfully implemented since ~~the year~~ 2000.

The coupled Aerosol and Tracer Transport model to the Brazilian development of the Regional Atmospheric Modeling System (CCATT-BRAMS) was developed in the region (Longo et al., 2013)~~(Longo et al., 2013)~~ to investigate the impact of the Amazonian wildfires on air quality in major Brazilian cities (Freitas et al., 2011; Pereira et al., 2011)~~(Freitas et al., 2011; Pereira et al., 2011)~~. The North American Community Multiscale Air Quality Model (CMAQ), coupled with the Weather Research and Forecasting (WRF) meteorological model, has been used in Colombia and Brazil to predict pollutant concentrations and assess reduction strategies ~~(~~(Albuquerque et al., 2019; East et al., 2021; Nedbor-Gross et al., 2018; Pachón et al., 2018; Pérez-Peña et al.,

2017)(Albuquerque et al., 2019; East et al., 2021; Nedbor-Gross et al., 2018; Pachón et al., 2018; Pérez-Peña et al., 2017). The WRF model coupled with Chemistry (WRF-Chem) online has been actively used to study the impact of regional sources on air quality in urban centers across Colombia (Ballesteros-González et al., 2020, 2022; Casallas et al., 2024; González et al., 2018; Mendez-Espinosa et al., 2019)(Ballesteros-González et al., 2020, 2022; Casallas et al., 2024; González et al., 2018; Mendez-Espinosa et al., 2019), Chile (Saide et al., 2016)(Saide et al., 2016) and São Paulo (Gavidia-Calderón et al., 2024)(Gavidia-Calderón et al., 2024). CHIMERE (Menut et al., 2013)(Menut et al., 2013) and MATCH (Andersson et al., 2015)(Andersson et al., 2015) have has been applied in Chile to assess pollutant chemical transformation and dispersion as well as emission reduction strategies (Gallardo et al., 2002; Lapere, 2018; Lapere et al., 2021; Mailler et al., 2017)(Gallardo et al., 2002; Lapere, 2018; Lapere et al., 2021; Mailler et al., 2017). Additionally, CAMS reanalysis data has been compared against air quality observations, observing well-captured temporal trends for PM_{10}, $PM_{2.5}$ and SO_2 but not for NO_X (Casallas et al., 2024)(Casallas et al., 2024).

This work conducts presents the first model inter-comparison effort and ensemble construction for Latin America, which was assembled under the Prediction of Air Pollutants in Latin America (PAPILA) project (https://papila-h2020.eu/papila). The aim of the projectPAPILA was to develop an air quality analysis and forecastAQF system for the region with increasing capabilities in major cities. This objective is in line with the WMO GAFIS initiative that supports the implementation of AQF systems, especially in countries and regions where they do not exist, such as Africa and South America (WMO, 2022)(WMO, 2022). This work is the first step towards such a system and seeks to examine the differences between the models in diagnostic mode to get an improved forecasting set-up. This manuscript presents a retrospective (hindcast) analysis and it's organized as follows: in Sect. 2 presents we provide model descriptions, the emission inventories utilized sed in the models, and the observations employed for model evaluationto evaluate the models. In Sect. 3 we analyze the model performance and conduct inter-comparisons in diagnostic mode for each pollutant (NO_2, O_3, CO, SO_2, $PM_{2.5}$). We also discuss the season variability of predictions and the analysis of large vs small urban areas. Finally, in Sect. 4 summarizes our wefindings and outlines directions for present our conclusions and future developments.

Con formato: Sin Superíndice / Subíndice

Con formato: Subíndice

Con formato: Subíndice

Con formato: Subíndice

Con formato: Subíndice

2. Methodology

The model intercomparisoninter-comparison and construction of the ensemble construction required several key relevant activities, such as: the execution of global and regional models in a common domain, harmonization of the model outputs, ensemble construction, collection of air quality observations, analysis of temporal and spatial variability, and model evaluation.

2.1. Description of the models and modeling set-up

For the model intercomparisoninter-comparison, two global models (CAMS and SILAM) and three regional models (CHIMERE, WRF-Chem, EMEP MSC-W) were selected based on the expertise of the research groups working on the PAPILA project (Table 1). WRF-Chem was implemented by two different groups, the Max Planck Institute for Meteorology (MPIM) in Germany and the University of São Paulo (USP) in Brazil, with different set-ups. The simulations analyzed hereby correspond to early simulation results that do not represent the best performance of each model in the LAC region or over individual urban areas. The different models are briefly described in the following paragraphs.

The Copernicus Atmosphere Monitoring Service (CAMS) provides state-of-the-art global atmospheric composition data based on the IFS (Integrated Forecasting System) model of the European Centre for Medium-Range Weather Forecasts (ECMWF) (Inness et al., 2019)(Inness et al., 2019). The chemical mechanism of IFS is an extended version of the Carbon Bond 2005 (CB05) and complements the MACC aerosol module (Morcrette et al., 2009) (Flemming et al., 2017; Morcrette et al., 2009)(Flemming et al., 2017; Morcrette et al., 2009). The CAMS reanalysis data used for this project is a combination of satellite observations of atmospheric composition and the IFS modeling setup. Anthropogenic emissions from the MACC/CityZen (MACCity) inventory (Granier et al., 2011)(Granier et al., 2011) (Granier et al., 2011) and biomass burning emissions from the Global Fire Assimilation System (GFASv1.2) (Kaiser et al., 2012)(Kaiser et al., 2012)(Kaiser et al., 2012) were used in the simulations (ref GFAS) (Table 1). The biogenic emissions were simulated off-line by the Model of Emissions of Gases and Aerosols from Nature (MEGAN) version 2.1 MEGAN2.1 model (Guenther et al., 2006)(Guenther et al., 2006) using an offline emission inventory (ECCAD, 2021)(ECCAD, 2021). CAMS has been extensively evaluated against ozone sondes, aircraft profiles, surface observations, and global satellite retrievals (Flemming et al., 2015)(Flemming et al., 2015).

The system for Integrated modelling of Atmospheric composition (SILAM, http://silam.fmi.fi) is a chemical transport model for global-to-local simulations of atmospheric composition and air quality developed at Finish Meteorological Institute (FMI) (Kouznetsov and Sofiev, 2012; Sofiev, 2002; Sofiev et al., 2006, 2010, 2015)(Kouznetsov and Sofiev, 2012; Sofiev, 2002; Sofiev et al., 2006, 2010, 2015). Briefly, SILAM employs the CBM-IV mechanism for gas-phase chemistry (Gery et al., 1989)(Gery et al., 1989). For further details on the The model characteristics, refer to are published elsewhere (METEO-FRANCE, 2020)(METEO-FRANCE, 2020)(CAMS-MeteoFrance). Briefly, SILAM uses the CBM-IV mechanism for gas-phase chemistry (Gery et al., 1989). For this work PAPILA,, the SILAM simulations were driven by the meteorological IFS model of ECMWF. Anthropogenic emissions were adopted from the CAMS global emission inventory v2.1 (version?), whereas the biomass burning emissions were generated by the Integrated Monitoring and Modeling System for Wildland fires (IS4FIRES) v1.0 (http://is4fires.fmi.fi, last access: 03 July 2024, (Soares and Sofiev, 2014; Sofiev et al., 2009)(Soares and Sofiev, 2014; Sofiev et al., 2009). The biogenic emissions were simulated off-line by the MEGAN v2.1 model (Guenther et al., 2006), particularly, isoprene and monoterpene emissions computed for the year 2010, as found on the MEGAN website (Table 1). The SILAM model has been extensively evaluated in numerous international retrospective studies (Blechschmidt et al., 2020; Kukkonen et al., 2012; Marécal et al., 2015; Petersen et al., 2019)(Blechschmidt et al., 2020; Kukkonen et al., 2012; Marécal et al., 2015; Petersen et al., 2019) and real-time operational applications. SILAM is included in the regional European forecasting system provided by CAMS together with CHIMERE, EMEP MSC-W and eight other models (Colette et al., 2020)(Colette et al., 2020).

CHIMERE is a Eulerian chemistry-transport model (CTM). It is able to perform simulations from urban to hemispheric scale. (Mailler et al., 2017).

CHIMERE is a Eulerian chemistry-transport model (CTM) and multi-scale from hemispheric to urban resolutions. The model can be used in offline or online mode and has meteorology forcing from the IFS model by the ECMWF data sets. The biogenic emissions were simulated off-line by the MEGAN v2.1 model (Guenther et al., 2006). Fire emissions are estimated by the CHIMERE module at each grid and time period (Menut et al., 2013). The model is used in research institutes and in operational centers for forecasting mainly in France and other European countries. In Latin America, CHIMERE has been widely used in Chile to assess pollutant chemical transformation and dispersion as well as emission reduction strategies (Lapere, 2018; Lapere et al.,

Comentado [PQJE1]: https://doi.org/10.1029/2008JD011235

Con formato: Resaltar

Con formato: Sin Resaltar

Con formato: Resaltar

Con formato: Fuente: (Predeterminada) Times New Roman, 10 pto

Con formato: Sin Resaltar

Con formato: Resaltar

Con formato: Resaltar

Con formato: Resaltar

Con formato: Espacio Antes: 12 pto

Con formato: Español (Colombia)

Con formato: Español (Colombia)

2021; Mailler et al., 2017; Menut et al., 2021)(Lapere, 2018; Lapere et al., 2021; Mailler et al., 2017; Menut et al., 2021). As previously discussed, CHIMERE is also included in the CAMS forecasting ensemble.

CHIMERE is ana Eulerian chemistry transport model (CTM). It is able to perform simulations from urban to hemispheric scale (Mailler et al., 2017). The model can be used online (with WRF only) or offline (with several meteorological modelforcings). The model characteristics are published elsewhere (METEO-FRANCE, 2020)(METEO-FRANCE, 2020)(CAMS-MeteoFrance). For this study, the meteorological forcing is the IFS global simulation provided by ECMWF. The biogenic emissions are online calculated using the MEGAN v2.1 model (Guenther et al., 2012)(Guenther et al., 2006)(Guenther et al., 2006) using the 30s horizontal resolution database. Fire emissions are those of CAMS (Kaiser et al., 2012)(Kaiser et al., 2012)(Kaiser et al 2012) and reformatted for CHIMERE using the dedicated preprocessor ((Menut et al., 2021)(Menut et al., 2021)Menut et al., 2021). The mineral dust areis calculated online using the (Alfaro and Gomes, 2001)(Alfaro and Gomes, 2001) (Alfaro and Gomes, 2011) scheme and the sea-salt emissions are also calculated online using the (Monahan, 1986)(Monahan, 1986)(Monahan, 1986) scheme. NOx by lightning are calculated using the scheme described in (Menut et al., 2020)(Menut et al., 2020)(Menut et al., 2020). CHIMERE

This model is used for analysis and forecast in tens of countries around the world and at various spatial scales, including the CAMS forecast. More specifically for Latin-America, it wa-s used for several studies about anthropogenic emissions, deposition of black carbon on snow, indirect effects and impact of megafires fires on clouds formation (Lapere, 2018; Lapere et al., 2021; Mailler et al., 2017)(Lapere, 2018; Lapere et al., 2021; Mailler et al., 2017). (Lapere et al., 2021; Mailler et al., 2017; Lapere, 2018) . For this exercise, CHIMERE were run for the 31 days of January and July of 2015, however due to problems in the output files 15 days were missing (5 days from January 14th to 18th and 10 days from July 11th to 19th and July 9th).

The EMEP MSC-W model ('EMEP model' hereafter) is an offline chemical transport model developed at the Norwegian Meteorological Institute (MET Norway), and can be run either globally or on regional domains. It is used to simulate photo-oxidants as well as organic and inorganic aerosols in scales ranging from local to global scales (Simpson et al., 2012)(Simpson et al., 2012) . Details regarding the model characteristics can be found in The model characteristics are published elsewhere (METEO-FRANCE, 2020)(METEO-FRANCE, 2020)(CAMS-MeteoFrance). For this study theThis model was driven byalso has meteorological dataforcing from the IFS model of the ECMWF. Gas phase chemistychemistry from the "EMEP scheme", comprising 70 species and 140 reactions (Andersson-Sköld and Simpson, 1999; Simpson et al., 2012)(Andersson-Sköld and Simpson, 1999; Simpson et al., 2012), inorganics from the MARS equilibrium module (Binkowski and Shankar, 1995)(Binkowski and Shankar, 1995) and organics from the CBM-Z mechanism (Zaveri and Peters, 1999)(Zaveri and Peters, 1999). Emissions from forest and vegetation fires are taken from the the Fire INventory from NCAR version 1.5 (FINN v1.0)FINN dataset (Wiedinmyer et al., 2011)(Wiedinmyer et al., 2011). Biogenic emissions of isoprene and (if required) monoterpenes are calculated in the model for every grid-cell (Simpson et al., 2012)(Simpson et al., 2012). The EMEP model has for several decades been the main tool for underpinning air quality policies under the UN ECE convention on long-range transboundary air pollution and it is also included

Con formato: Francés (Francia)

Con formato: Justificado, Espacio Antes: 12 pto, Después: 0 pto, Interlineado: 1.5 líneas

Con formato: Resaltar

Con formato: Resaltar

Con formato: Resaltar

Con formato: Resaltar

Con formato: Resaltar

Con formato: Resaltar

Con formato: Superíndice

Con formato: Superíndice

Con formato: Superíndice

Con formato: Superíndice

Con formato: Superíndice

Con formato: Sin Resaltar

Con formato: Resaltar

Con formato: Fuente: (Predeterminada) Times New Roman, 10 pto

Con formato: Fuente: (Predeterminada) Times New Roman, 10 pto

Con formato: Sin Resaltar

in the CAMS regional ensemble. However, it should be noted that the runs for this study were the very first EMEP model simulations ever conducted on a regional scale for LAC and should thus be considered only as a first demonstration of model capabilities. For PAPILA, the EMEP model was run by the modeling team at the University of Chile in Santiago with some support by MET Norway.

The WRF-Chem is the Weather Research and Forecasting (WRF) model coupled with Chemistry, developed at the National Center for Atmospheric Research (NCAR) with the purpose of simulating urban- to regional-scale fields of trace gasses and particulates. The air quality and meteorological components share the same transport and physics scheme, as well as horizontal and vertical grid (Fast et al., 2006; Grell et al., 2005)(Fast et al., 2006; Grell et al., 2005). The MPIM WRF-Chem uses version 3.6.1 to simulate meteorology and chemistry simultaneously online in South America at ~20 km horizontal resolution and 36 vertical levels extending from the surface to ~21 km altitude. The gas-phase chemistry is represented by the Model for Ozone and Related Chemical Tracers (MOZART-4) chemical scheme (Emmons et al., 2010)(Emmons et al., 2010). The Goddard Chemistry Aerosol Radiation and Transport (GOCART) bulk aerosol module coupled with MOZART is used in this study to consider the aerosol processes (Chin et al., 2002; Ginoux et al., 2001)(Chin et al., 2002; Ginoux et al., 2001). Boundary rder and initial conditions for the meteorology were set up from GFS, and for the chemical species concentrations from CAM-Chem. The anthropogenic emissions were from CAMS-GLOB-ANT v4.2, which consists of 0.1° x 0.1° gridmapsgrid maps of several species including CO, SO_2, NO, NMVOC, NH_3, BC and OC (Granier, 2019).(Granier, 2019). Daily varying emissions of trace species from biomass burning were taken from the (FINN v1.5) dataset (Wiedinmyer et al., 2011)(Wiedinmyer et al., 2011). Biogenic emissions of trace species from terrestrial ecosystems are calculated online using the MEGAN model v2.04 (Guenther et al., 2006)(Guenther et al., 2006). Further details on the MPIM WRF-chem model settings can be found in (Bouarar et al., 2019)(Bouarar et al., 2019).

Con formato: Subíndice

Con formato: Subíndice

The WRF-Chem run by USP (version 3.9.1) uses similar characteristics as previously described , d version 3.9.1, with the samea horizontal resolution (~22 km) and 35 vertical layers. Some Other differences from the MPIM WRF-Chem configuration are the version of global emissions CAMS-GLOB-ANT v5.3 (ECCAD, 2020)(ECCAD, 2020), the speciation of the chemical boundary condition from the CAM-Chem model (Buchholz et al., 2019; Emmons et al., 2010)(Buchholz et al., 2019; Emmons et al., 2010) (Buchholz et al., 2019; Emmons et al., 2019) and the speciation of FINN v1.5 emissions (Barth et al., 2015) which are suitable for simulation over São Paulo. For this exercise, WRF-Chem did not include Mexico City in the modeling domain.

CHIMERE, IFS, EMEP, WRF-Chem, LOTOS-EUROS and SILAM models were are used in an ensemble mode to configure the MarcoPolo-Panda prediction system in Asia (Brasseur et al., 2019; Petersen et al., 2019)(Brasseur et al., 2019; Petersen et al., 2019). It has been observed that, under specific circumstances, a model ensemble can outperform individual models, demonstrating the potential benefits of this approach. With the desire to replicate the experience in Latin America, the selected models were applied in a common domain, defined by the south-eastern corner at 119°54'W 59°54'S, and the north-eastern corner at 28°6'W 29°54'N. The models were run at a spatial resolution of ~0.2° x 0.2° (~20x20km). Input meteorology and emissions were up to the modeling group (Table 1). The simulation period covers January (southern hemisphere summer) and July (southern hemisphere winter) of 2015.

2.2. Model evaluation

The ~~models´~~ performance of the models was assessed by comparing the simulated concentrations with the average of the observations for each available city, pollutant, and considered period. ~~For every city and pollutant, the simulated concentration was estimated as the weighted average of the modeled grid cells that intersected with a city's polygon that encompasses the geographical boundaries. The weights were based on the area of the modeled grid cell that overlapped with the city's polygon.~~ The observation's average was constructed by computing the arithmetic mean of all air quality stations available in the network within the city's polygon. On the other hand, the simulated concentrations for the models were ~~as~~ estimated as the average of the models' closest grid point to the location of each station that is within the city's polygon for every city and pollutant considered in this study. This results in a weighted average of the model where the weight is given by the number ~~amount~~ of stations that measure the pollutant closest to each grid point, resulting in the same geographical sampling for the observations and the models, thus reducing any potential station's sampling bias to the best of our abilities. This approach was chosen with ~~given~~ the objective of ~~to~~ assessing the model performance in cities, rather than for each air quality station separately. It´s outside the scope of this work to conduct an intra-urban variability study of the model performance given the chosen resolution of 0.2 degrees. ~~The~~ model evaluation was focused on nitrogen dioxide (NO_2), ozone (O_3), carbon monoxide (CO), ~~sulphur~~sulphur dioxide (SO_2), and particulate matter less than 2.5 ~~microns~~ micrometers ($PM_{2.5}$) and less than 10 micrometers ~~and less than 10 microns~~ (PM_{10}).

Con formato: Resaltar

Con formato: Sin Resaltar

Con formato: Sin Resaltar

For each period, pollutant and city, the model evaluation included the following metrics: Model/Observations ratio, mean bias (BIAS), modified normalized bias (MNBIAS), root mean square error (RMSE), fractional gross error (FGE) and correlation coefficient (R). The formulas were replicated from the MarcoPolo-Panda project (Petersen et al., 2019) and are presented in Table A1. These evaluation metrics were computed for all models and the ensemble.

2.3. Air quality monitoring networks in Latin America

Several air quality monitoring networks (AQMN) are available throughout Latin America, especially in major cities. However, worldwide access to the datasets can be difficult due to language barriers and the lack of a centralized platform, which is lacking in some countries. A comprehensive list of AQMN in Latin America was assembled for the PAPILA project (https://papila-h2020.eu/observations). For the year 2015, we collected air quality data for 12 cities in México, Colombia, Ecuador, Perú, Chile, Brazil, and Uruguay. Only stations with a minimum of ~~For all AQMN, a filter ensuring~~ 75% data completeness ~~of the air quality database~~were considered when ~~was applied before selecting a site and~~ calculating the city average of the observations, resulting in eight cities with enough data to use for this study. This data completeness requirement considers a minimum of 75% of days available for each period, as well as a minimum of 75% of hourly data to construct their daily average. We focus in this study on the four major cities (from North to South): México City, Bogotá, São Paulo and Santiago (Fig. 1). However, data of all available cities were used in the model evaluation (Tables B1 through B8).

Con formato: Sin Resaltar

Con formato: Sin Resaltar

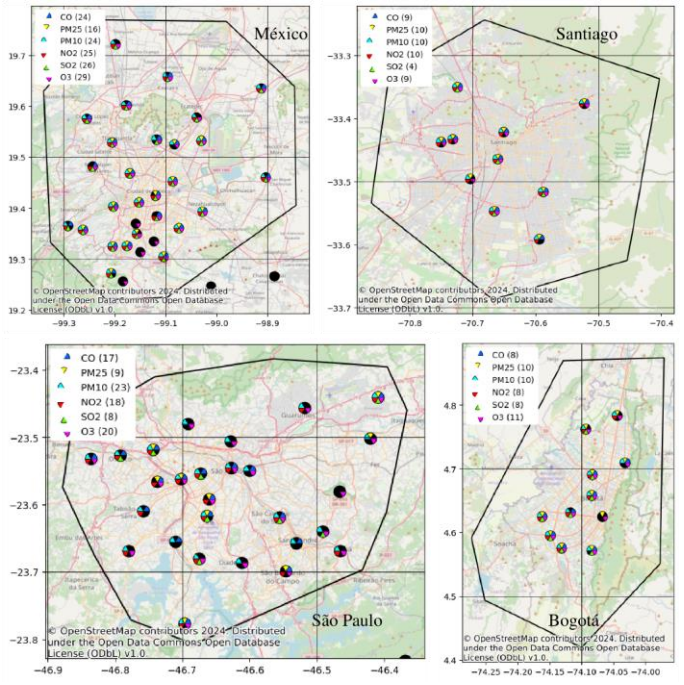

Figure 1. Location of air quality stations in major Latin American cities (Santiago, Bogotá, México City, São Paulo) alongside the city's polygon for computing the city average. The number of sites per pollutant is available as a color layer for every city. ~~© OpenStreetMap contributors 2024. Distributed under the Open Data Commons Open Database License (ODbL) v1.0.~~

3. Results

Simulated concentrations of all pollutants from all models were compared against observations from every city and for both periods (January and July) in 2015. In this section, we present results from the model evaluation, the ensemble performance, the spatial and temporal variability of ~~simulated~~simulated fields and the impact of large versus small urban areas in the model ~~intercomparison~~inter-comparison.

3.1 Model evaluation

The following results are presented for every pollutant: analysis of observations from AQMN, simulated concentrations by the models, comparison of evaluation metrics, discussion of model performance including the ensemble and ~~and~~ analysis of model ~~inter-variability~~variation.~~.~~

Con formato: Centrado

Con formato: Sin Resaltar

Con formato: Sin Resaltar

3.1.1 Nitrogen dioxide - NO_2

Observations

The number of stations per city recording NO_2 during January and July of 2015 varies between 7 in Bogotá and 24 in Mexico City is available in (Appendix B). ~~In all cities the data availability was 100%.~~ The highest daily average concentration of NO_2 is observed in Santiago during winter at around ~~40~~ 38 ppb (Fig. ~~1~~2). This can be attributed to adverse meteorological conditions and emissions from transportation and residential combustion in the surrounding municipalities (Mazzeo et al., 2018; Saide et al., 2016)~~(Mazzeo et al., 2018; Saide et al., 2016)~~, whereas in the summer NO_2 levels fall to 11 ppb. The second largest values are shown ~~in México City and São Paulo~~ in México City (~27 ppb) and São Paulo (~20 ppb)~~with a daily average NO_2 levels of 24 and 20 ppb respectively~~, due to the heavy use of fossil fuels in transportation and power generation. The lowest levels of NO_2 are measured in Bogotá with ~~15~~ 16.4 ppb on average.

Model performance

In Bogotá and Santiago, the NO_2 mean is mostly underestimated by the ensemble members ~~models~~ (Fig. 2~~1~~). In Santiago, the mean of the models is ~~7.3~~10.3 ppb in summer and ~~17.7~~22.1 ppb in winter, ~~much~~ lower than the mean of the observations. Similarly, in Bogotá the mean of the modeled values is ~~5~~6.6~~5~~ ppb, much lower than observations~~.~~. In contrast, in São Paulo and Mexico City, the models ~~fields~~ both over and underpredict ~~are above and below~~ the ~~observed~~ ambient concentrations and the average of the modeled fields~~values~~ (~~19.5~~23.6 ppb and ~~27~~ 30.3 ppb respectively) are in the same order of magnitude of observations.

Con formato: Resaltar

Table 1. Description of the models included in the ensemble

Institution and model	Type of model	Vertical resolution	Grid cells (lat / lon)	Projection	Initial and Boundary conditionsC and BC	Chemical mechanism/ Aerosol model	Meteorology	Emissions
FMI-SILAM	Global/ and regional offline v5.–7	25 layers of varying depth up to 5.25 Pa ? Lowest level~ 20m	590 x 526	lat/lon	Global modelBC CAMS-Global IFS, IC for meteorology from the ECMWF´s operational analysis and for chemistry from the previous forecastIC . BC CAMS-Global IFS.	gas-phase chemical mechanism CBM-IV4Gery et al., 1989)	C-IFS ECMWF	Anthropogenic CAMS-REG-AP_v3.1/2016, TNO-MACC, CAMS-GLOB-ANT-v2.1 IS4FIRES v1.0, Biogenic MEGAN 2.1
ECMWF - CAMS	Global	60 levels up to 0.1 hPa (65km). ?Lowest level~ 20m	450 x 460	lat/lonNot defined	Global modelIC for meteorology from the ECMWF´s operational analysis and for chemistry from the previous forecast.	chemistry: CB05 aerosol: AER bulk scheme (Morcrette et al., 2009)	C-IFS	Anthropogenic CAMS-REG-AP_v3.1/2016 provided by CAMS_81. MACCITY, MEGAN 2.1, GFAS v1.2 Biogenic MEGAN 2.1
CHIMERE /LMD-UCL	Regional offline V2017r4 .2	Variable, 8 levels from the surface up to 500 hPa. 7 levels below 2 km	450 x 455	Lambert - conformal	BC CAMS-Global IFS, IC previous day forecast. LMDz-INCA (gas, aerosols) and GOCART (mineral dust)	Chemistry: SAPRC-07-A Aerosol: 10 bins and 15 species LMDz-INCA (gas, aerosols) GOCART (mineral dust)	C-IFS	Anthropogenic Offline EDGAR-HTAP Biogenic , online MEGAN 2.1, mineral dust, online sea-salt, online NOx by lightning.
EMEP/UCL	RGlobal/ regional offline	20 layers up to 100 hPa with approximately 10 in the Planetary Boundary layer	450 x 460	lat/lon	BC CAMS-Global IFS, IC previous day forecast. Global CAMS	EMEP scheme MARS (Binkowski and Shankar, 1995)CBMZ (Zaveri and Peters, 1999, Gery et al. ,1989)	C-IFS ECMWF	Anthropogenic EDGAR-HTAP FINN 1.0 Biogenic Included internal calculation of biogenic emissions, FINN 1.0
MPIM-WRF-Chem	Regional online vV4.1.2 3.6.1	376 vertical levels up to 50 hPa Lowest level~ 50mLower level?	455 x 450	Mercator	BC and IC for meteorology from GFS, -for Chemistry from (meteorology), CAM-Chem (Chemistry)	MOZART-4/GOCART	WRF	Anthropogenic CAMS-GLOB-ANT v4.2CAMS 4.2 , FINN 1.5 Biogenic -MEGAN 2.1, FINN 1.5

Con formato
Tabla con formato
Con formato
Con formato
Con formato
Con formato
Con formato
Con formato
Con formato
Con formato
Con formato
Con formato
Con formato
Con formato
Con formato
Con formato
Con formato
Comentado [PQJE2]: https://doi.org/10.1029/2008JD
Con formato
Con formato
Con formato
Con formato
Con formato
Con formato
Con formato
Con formato
Con formato
Con formato
Con formato
Con formato
Con formato
Con formato
Con formato
Con formato
Con formato
Con formato
Con formato
Con formato
Con formato
Con formato
Con formato
Con formato
Con formato
Con formato
Con formato

USP-WRF-Chem	Regional online WRF-Chem v3.9.1	35 vertical levels up to 50 hPa? Lowest level~ 50m Lower level?	455 x 450	Mercator	BC and IC for meteorology from GFS,- for Chemistry from CAM-Chem GFS 0.25	MOZART/GOCART	WRF	Anthropogenic CAMS-GLOB-ANT v5.3 CAMS FINN v1.5 Biogenic MEGAN 2.1 FINN v1.5

Abbreviations: FMI – Finnish Meteorological Institute, ECMWF – European Center for Weather and Modeling Forecast, LMD – Laboratoire de Météorologie Dynamique, MPIM – Max Planck Institute for Meteorology, UCL – University of Chile, USP – University of São Paulo

Con formato: Fuente: (Predeterminada) Times New Roman

Con formato: Fuente: 9 pto

Con formato: Centrado

Con formato: Izquierda

Con formato: Izquierda

Con formato: Izquierda

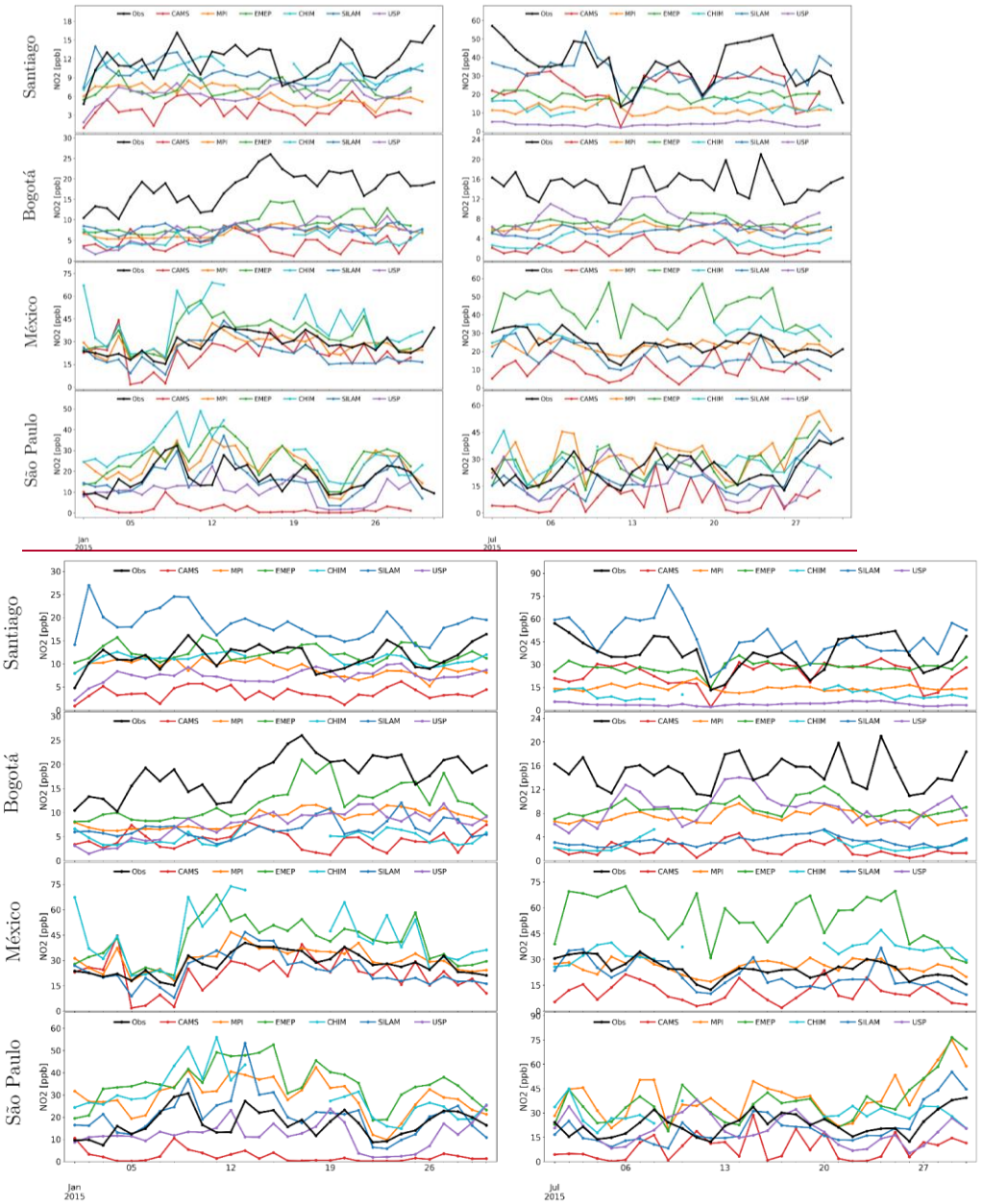
Obs
CAMS
MPI
EMEP
CHIM
SILAM
USP
Santiago
Bogotá
México
São Paulo
NO2 [ppb]
Jan
2015
Jul
2015

Figure ~~1~~2. Observed (~~orange~~black) and simulated NO_2 daily mean concentrations in Santiago, (top) Bogotá, México City, São Paulo (bottom) for January (left) and July (right) 2015.

~~In~~ São Paulo and México City ~~, the Model/Observations ratios for NO_2 varied from 0.13 to 1.7, indicating that some models overestimate the observations while others show underestimations. These cities~~ exhibit the lowest MNBIAS and FGE ~~, FGE and RMSE values~~ (Table A2) ~~with some models achieving benchmarks (MNBIAS < ±30%, FGE < 55%, Zhai).~~ ~~,~~ The correlation between ~~the~~ models and observations hovers around 0.7, which is larger than the goal benchmark proposed for this pollutant ($r \geq 0.6$) (Zhai et al., 2024)~~(Zhai et al., 2024)~~. ~~The adequate performance in São Paulo and México City may be attributed to an accurate portrayal of the temporal and spatial variability that is achieved in large urban areas like these (>3500 km²) which encompass at least nine model cells (20 kmx20 km).~~

~~I~~In Santiago, ~~Model/Observations ratios range from 0.1 to 0.9. T~~the MNBIAS is mostly ~~consistently~~ negative during both seasons except ~~with the exception of~~ the SILAM and EMEP models that resulted in a positive bias. T ~~for all models; however, t~~he degree of which the models are underestimating the observations is notably higher in ~~the~~ winter than in summer and with a larger FGE~~error~~ (Table A2). The correlation between ~~the median of the~~ models and observations in Santiago is larger in ~~ranges from 0.5~~ summer than ~~to 0.7~~in winter, with some models achieving the criteria benchmark ($r > 0.5$, Zhai et al., 2024Zhai). ~~.~~

Con formato: Resaltar

In Bogotá, ~~the Model/Observations ratios ranged between 0.1 and 0.5, indicating that only 50% of the NO_2 is reproduced by the models. T~~the MNBIAS ~~values a~~are large and consistently negative and the FGE varies between ~~63~~50% and ~~161~~156% (Table A2). Despite these lower scores, the correlation between observations and models are moderate around 0.6 in January ~~from 0.45 in July to 0.70 in January,~~ meeting criteria benchmark~~goal~~s Haga clic o pulse aquí para escribir texto. ~~-~~and demonstrate that certain models can successfully replicate the temporal variations but not the magnitude of the pollutant. This result suggests that the correlation is related to meteorology and the magnitude to emissions.

The adequate performance in São Paulo and México City may be attributed to an accurate portrayal of the temporal and spatial variability that is achieved in large urban areas like these (>3500 km²) which encompass at least nine model cells (20 kmx20 km).

The lower simulated NO_2 levels in Bogotá likely stems from an underestimation of emissions. A study by (Rojas et al., 2023)~~(Rojas et al., 2023)~~ utilized local data to estimate on-road emissions in Colombia and revealed substantial underestimation of NOx emissions by global inventories such as EDGAR 6.1, CAMS, and the Community Emissions Data System (CEDS). Their findings recommend adjustments to the emission factors used for NOx, particularly for heavy-duty and passenger vehicles, followed by a recalculation of the resulting emissions. The underestimation of NO_2 can also be noted in other cities such as Medellin, Guadalajara, Lima, and Quito (Fig. ~~8~~7). These cities, along with Bogotá, possess urban areas ranging from 235 to 890 km² and are confined within one or two cells of the models (20km x 20km). It is possible that the average of observations is heavily influenced by local sources, in which case a finer modeling resolution is required to accurately capture the spatial variability of air pollution.

Model ~~intercomparison~~inter-comparison

For NO_2, ~~both~~ CAMS ~~and SILAM~~ underestimates the observations in the four cities whereas SILAM underestimates this pollutant in Bogotá, Mexico City and São Paulo (only in July) and overestimates the observations in Santiago and in San Paulo (in January). ~~, with~~ CAMS displayed ~~ing~~ larger MNBIAS and FGE than SILAM. In general, SILAM reproduces at least 80% of the NO_2 levels, with the exception in Bogotá where only ~~40~~30% is simulated. The correlation coefficient is better for SILAM (R ~0.6) than for CAMS (R ~0.3). ~~The results from global models suggest that SILAM has a better performance for NO_2 in LAC than CAMS.~~

The results from regional models are very diverse. In general, WRF-MPI, CHIMERE and EMEP have lower values of MNBIAS and FGE for NO_2 in ~~Sao Paulo~~São Paulo and Mexico City (Table A2). In São Paulo, except for WRF-USP, regional models tend to overestimate NO_2 with MNBIAS between 20% and ~~50~~70%. WRF-USP reproduces about ~~60~~76% of NO_2 concentrations. In México City, the tendency of regional models is also to overestimate ~~the~~ NO_2 ~~levels~~ (MNBIAS: ~~20~~ 10 to ~~50~~75%). In Santiago, CHIMERE achieves the lowest MNBIAS (~~8~~ 2%) in January but not in July (~~-99~~119%). In ~~Bogota~~Bogotá, the MNBIAS in regional models remains consistently negative.

From Figure 2~~1~~ is visible the model variation~~intervariability as the dispersion between models~~. In Santiago in winter the range of NO_2 values is ~~30~~ 48 ppb, which corresponds to a coefficient of variation (C.V.) of ~~57~~71% (Table A8), this contrasts with the range in summer of ~~6.3~~14.9 ppb (C.V.=~~33~~49%). Other large variations are ~~dispersion is~~ observed in México City in July (range 54 ppb, C.V. 57%) and São Paulo ~~in January~~ (range ~~26~~ 32 ppb, C.V. ~~56~~46 to 58%) ~~and. México City in July (range 31 ppb, C.V. 47%). On the other hand, lower dispersion is found in January in Bogotá and México City (C.V. 24 and 31% respectively).~~ It's interesting to note the case of Bogotá where all models consistently underestimate NO_2, but the ~~dispersion~~ model variation ~~in the models~~ is the lowest (8ppm with C.V. 39 and 56%).

Median ensemble performance

The median ensemble underestimates NO_2 concentrations in Bogotá and in a lesser extent in Santiago. This is consistent with the underestimation trend by most of the models. The ensemble in these two cities has some of the lowest ~~achieve some benchmarks for~~ MNBIAS, ~~,~~FGE and R, but not always better than ~~As it was previously described, NO_2 is underestimated by all models in Santiago and Bogotá. Therefore, the median ensemble also underestimates NO_2 concentration and does not represent any improvement in the evaluation metrics~~individual models (Table A2). On the contrary, in Mexico City and São Paulo, the ensemble median outperforms the ~~individual~~ models for NO_2. In ~~both~~ summer and winter, the ensemble ~~median~~ presents the lowest ~~RMSE~~ and FGE ~~meeting the goal benchmark (FGE < 40%, Zhai)~~ in both cities. The~~, with a Model/Observations ratio close to 1.0, a~~ correlation coefficient range between ~~R=0~~0.~~7~~5 and 0.8 within the criteria benchmark (R>0.5. Zhai et al., 2024~~Zhai~~). The MNBIAS are also the lowest (-2.9 to 17.7%) ~~.observing the goal benchmark (MNBIAS < ± 20%, Zhai). , and MNBIAS between -3% (summer) to -12% (winter). The median ensemble also provided adequate statistics in a higher resolution modeling domain in São Paulo~~ Haga clic o pulse aquí para escribir texto.~~ In México City, the ensemble adequately simulates NO_2 (Model/Observations ~0.9) with lower error and bias than most of the individual models. In January, the correlation coefficient meets the goal benchmark for this pollutant (R>0.6) in all cities, whereas in July the goal benchmark is achieved for Sao Paulo and the criteria target (R>0.5) for Santiago and Mexico City.~~

Con formato: Fuente: Cursiva

Con formato: Resaltar

Con formato: Resaltar

Con formato: Resaltar

3.1.2 Ozone - O_3

Observations

The number of stations per city recording O_3 during January and July of 2015 varies between 9 in Santiago and 29 in Mexico City (Appendix B). The number of stations per city recording O3 is available in Appendix B. In January in Mexico City, data availability was 97%. The rest of the cities were 100%. The highest observed ozone concentration was in Ozone pollution is particularly significant in México City in during the July with an average concentration of 321 ppb. However, this value is significantly lower than the surface ozone concentrations reported in the MAM (March-April-May) season with values larger than 70 ppb The warm and dry weather creates the ideal conditions for ozone formation, leading to this period being referred to as the "ozone season" (Barrett and Raga, 2016; Silva-Quiroz et al., 2019)(Silva-Quiroz et al., 2019)(Barrett and Raga, 2016).

The second largest ozone value occurs in São Paulo during January with daily averages of 21 24 ppb. This is probably due to an abundance of ozone precursors, in particular, volatile organic compounds (VOC) from the use of biofuels in the transportation sector (Andrade et al., 2017; Gavidia-Calderón et al., 2024)(Andrade et al., 2017; Gavidia-Calderón et al., 2024) and biogenic VOCS (refs)(Martins et al., 2006). Santiago experiences displays a marked a strong seasonal cycle pattern of ozone concentrations, with summer values of approximately 22 ppb and winter concentrations around 3.3 6 ppb. This seasonal difference has been observed in other studies (Seguel et al., 2024).(Seguel, 2024). In Bogotá, ozone concentrations are the lowest and below 13 ppb.

Model performance

In the four cities, simulations of O_3 are mainly overestimated with the except ion offor Santiago in January and São Paulo in July (Fig. 23). In the summer in São Paulo and México City, simulations can reach up to 120 100 ppb, which is significantly above the observations. In Santiago in the winter, the mean of models (~ 20 ppb) is significantly larger than observations, indicating that the models have difficulty reproducing low values of this secondary pollutant. In the summer, ozone estimates are much closer to observations. Similarly, In Bogotá, models estimate an average of 17 ppb with maximum values of 30 ppb.which is in the same order of magnitude as the observations.

Con formato: Resaltar

Con formato: Color de fuente: Negro

Con formato: Resaltar

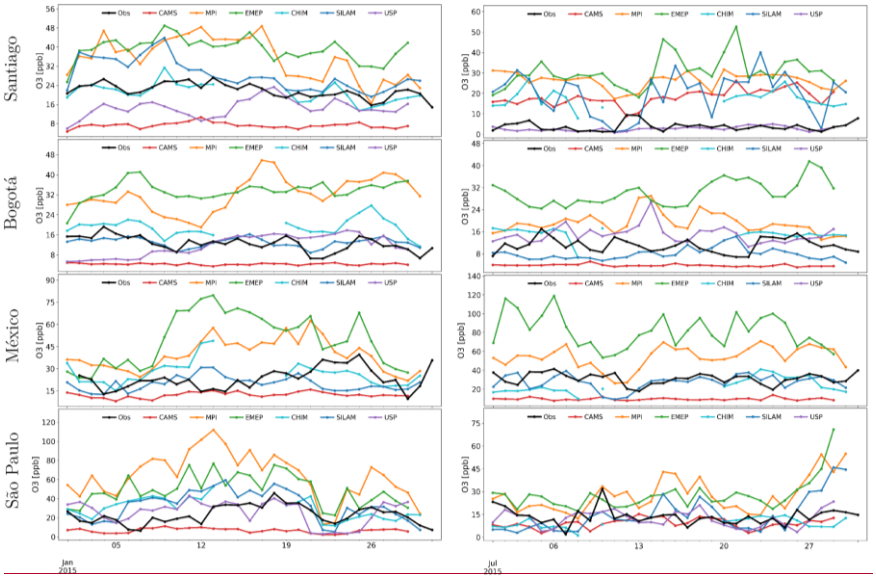
Santiago
Bogotá
México
São Paulo
Obs
CAMS
MPI
EMEP
CHIM
SILAM
USP
O3 [ppb]
Jan
2015
Jul
2015

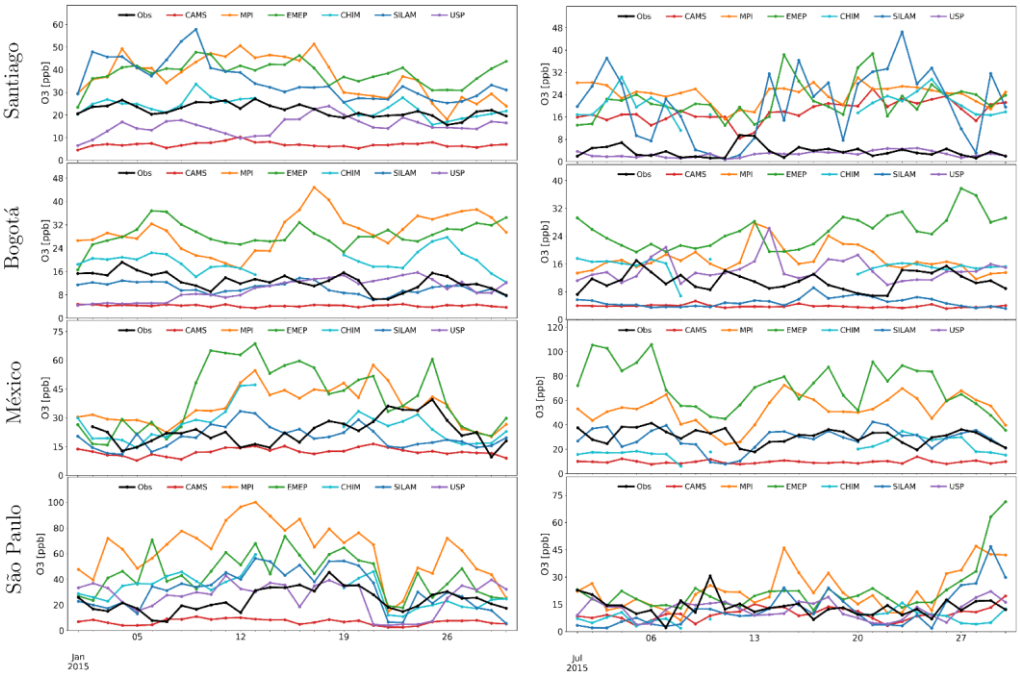
Santiago
Bogotá
México
São Paulo
Obs
CAMS
MPI
EMEP
CHIM
SILAM
USP
O3 [ppb]
Jan
2015
Jul
2015

400

Figure 23. Observed (blackorange) and simulated O_3 daily mean concentrations in Santiago, (top) Bogotá, México City, São Paulo (bottom) for January (left) and July (right) 2015.

For O_3, the Model/Observations ratios vary between 0.3 and 2.8, except in Santiago in July where Model/Observations ratio can be almost 10 (Table A3) and MNBIAS and FGE for most models are larger than 100%. The overestimation of O_3 in Santiago might be related to the underestimation of NO_2 previously described and the inadequate titration of ozone. Ozone formation in Santiago has been found VOC-limited (Seguel et al., 2020) (Seguel, 2020). This situation is also observed in BogotaBogotá where most models overestimate O_3 with MNBIAS between +4025% and +9380% (Table A3). In contrast, in Mexico and São Paulo, the models that overestimate NO_2 are also overestimating O_3. This complex situation is explained by the non-linearities in the formation of ozone (ref) (Grewe, 2004). In general, correlation coefficients for O_3 are very low ($R < 0.3$), especially in São Paulo and México City, indicating the challenge to adequately reproduce the spatial and time variability of this pollutant. Only in Santiago in January, the criteria benchmark for O_3 ($R > 0.5$) is achieved by some models (Emery et al., 2017)(Emery et al., 2017).

Model intercomparisoninter-comparison

In the case of global models, CAMS generally underestimates O_3 in the four cities except in Santiago during winter, where the Model/Observations ratio reaches about 6.0. Additionally, CAMS tends to have low correlation levels along with large bias and errors (Table A3). On the other hand, SILAM's O_3 displaysestimates show more variability, ranging between Model/Observations ratios of 0.7 and 1.4 while also maintaining lower bias and errors compared to CAMS. However, just like with CAMS, SILAM significantly overestimates O_3 levels in Santiago during the winter, with a Model/Observations ratio reaching around 7.0. In Bogotá, SILAM underestimates O_3 into a lesser extent than CAMS, with a larger FGE in July (74%) than in January (22%).

accurately simulates ozone levels with Model/Observations ratios ranging from 0.7 to 1.0 and presenting the lowest MNBIAS and RMSE.

In São Paulo, daytime concentrations of ozone are generally overestimated by most models (except for CAMS). The largest overprediction of O_3 (MNBIAS from 30 to 90%) is associated with overestimation of NO_2, especially for MPI, EMEP and CHIMERE models. For the models with NO_2 levels in reasonable agreement with observations (SILAM, USP) the ozone overprediction is lower (MNBIAS <25%). Among the regional models, EMEP and WRF-MPI consistently overestimate O_3 levels in all cities, with relatively high MNBIAS and FGE. In contrast, WRF-USP proves particularly suitable for São Paulo, achieving a Model/Observations ratio of approximately 1 some of the lowest FGE.0. CHIMERE also performs well in Santiago in the summer, , with a Model/Observations ratio of around 0.9, likely owing to local adjustments and parameterizations tailored to these specific cities.

Figure 32 shows a relatively large model variation intervariability for ozone. The largest ozone variation dispersion is shown in México City in summertime with a range of 74 62 ppb and a C.V. of 72% (Table A8). This wide variability is caused by the simulation of the EMEP model (84 71 ppb) and CAMS (9.8 6 ppb), that represent the extreme cases of over and underestimation. In a similar manner, in Bogotá, São Paulo and Santiago, the C.V. are approximately 6261%, 5749% and 5047% respectively, explained by the strong underestimation of CAMS and severe overestimation by EMEP and WRF-MPI.

Con formato: Resaltar
Con formato: Subíndice
Con formato: Subíndice
Con formato: Resaltar
Con formato: Subíndice
Con formato: Subíndice

Median ensemble performance

In Santiago in January, the median ensemble showed one of the lowest ~~biases (~~MNBIAS~~)~~ and ~~errors (~~FGE~~, RMSE)~~, surpassed only by CHIMERE~~only one model~~ (Table A3), and achieved the goal benchmark for this pollutant (R>0.75) (Emery et al., 2017)~~(Emery et al., 2017)~~. In July, the overestimation of ozone by most models impacts the performance of the ensemble, which also overestimates O_3 concentrations. In Bogotá, the ensemble has some of the best scores for ~~the second lowest~~ NM~~M~~BIAS and FGE~~, both in January and Jul~~ ~~y,~~ and represents an intermediate value between all models. In São Paulo, in wintertime, the ensemble has superior metrics ~~(Model/Observations ratio ~1.0,~~ MNBIAS ~-2%) compared to any individual model, while in the summer the ensemble overestimates the observations ~~(Model/Observations ratio ~1.5)~~ as most models do. In México City, the ensemble median performs better than all individual models with MNBIAS between ~~7~~4% (summer) and 13% (winter) and FGE less than 3~~2~~0%. Similar to the individual models, for most of the cases, the correlation coefficient for the ensemble does not meet any of the benchmarks (Emery et al., 2017)~~(Emery et al., 2017)~~.

3.1.3 Carbon monoxide - CO

Observations

The number of stations per city recording CO during January and July of 2015 varies between 7 in Bogotá and 24 in Mexico City (Appendix B).~~The number of stations per city recording CO is available in Appendix B.~~ ~~In January in Mexico City, data availability was 97%. The rest of the cities were 100%.~~ CO levels are generally ~~generally low in Latin America and daily averages are~~ below 1.~~5~~0 ppm for all cities (Fig. 4). However, in Santiago during winter ~~during July there are a few instances where~~some values surpass ~~the~~ 1.5 ppm ~~mark in Santiago~~ due to a combination of adverse meteorological conditions and emissions from the transportation sector and residential combustion, commonly employed for heating in neighboring municipalities (Gallardo et al., 2012; Saide et al., 2016)~~(Gallardo et al., 2012; Saide et al., 2016)~~.

There is a slight increase of CO in São Paulo in July with respect to January, due to the atmospheric conditions where lower winds and lower boundary layer increased primary pollutant concentration during winter. Additionally, biomass burning from wildfires which begin in July and peak in August and September for the southern part of the Amazon rainforest can bring more CO (Marlier et al., 2020)~~(Marlier et al., 2020)~~. Likewise, larger CO concentrations in Bogotá in January are part of the wildfire season in northern South America lasting from the end of December until April (Mendez-Espinosa et al., 2019)~~(Mendez-Espinosa et al., 2019)~~.

Model performance

~~México City~~Santiago records the largest simulated value ~~ion~~ of CO in winter with ~~a mean of 1.0 ppm and p~~peak ~~values~~ of ~~3~~5.0 ppm (Fig. ~~3~~4). The second largest values are observed in Mexico City with values around 3.0 ppm. In both cases, model estimates severely overestimate the observations with some NMBIAS larger than 100% (Table A4). ~~. Similarly, Santiago during July shows an average of 0.88 ppm and peak values over 3.0 ppm. During the summer in Santiago, CO is about 0.2 ppm, overestimated by~~

Con formato: Resaltar

Con formato: Sin Resaltar

most models. São Paulo displays intermediate values with an average CO of 0.5ppm, and Bogotá has the lowest modeled values with an average of 0.27 ppm. In general, simulations are underestimated, particularly in Bogotá where only 40% of the concentration is reproducible.

480

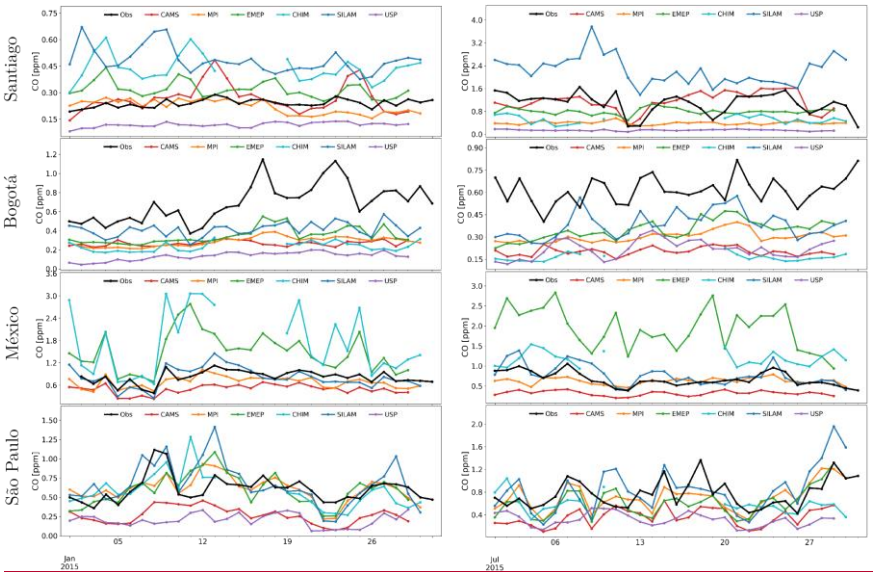
Santiago
Bogotá
México
São Paulo
Obs
CAMS
MPI
EMEP
CHIM
SILAM
USP
CO [ppm]
Jan
2015
Jul
2015

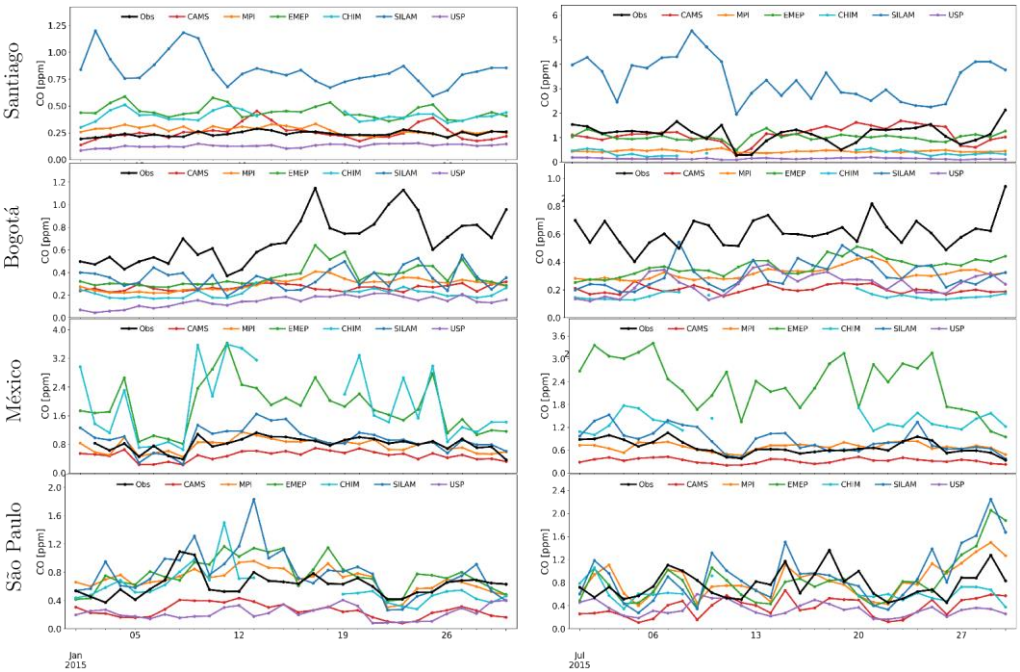
Santiago
Bogotá
México
São Paulo
Obs
CAMS
MPI
EMEP
CHIM
SILAM
USP
CO [ppm]
Jan
2015
Jul
2015

Figure 43. Observed (blackorange) and simulated CO daily mean concentrations in Santiago, (top) Bogotá, México City, São Paulo (bottom) for January (left) and July (right) 2015.

CO simulations in Santiago, São Paulo, and México City, are both over and underpredicting observationsabove and below the observations (Table A4Fig. 4). However, in Santiago in winter only the SILAM model overpredicts CO values (MNBIAS 98%), the other models underpredict (MNBIAS between -152 and -1%). This situation could be explained by emissions, synoptics or the models' simulation of the boundary layer (Mazzeo et al., 2018)(Mazzeo et al., 2018). In Bogotá, all models consistently underestimate the CO with MNBIAS between -50 and -131% (Table A4). In January correlation coefficients hover around 0.6, achieving benchmarks , with Model/Observations ratios ranging from 0.2 to 0.6. The correlation between models and observations for CO are within goal (R > 0.4) for this pollutant and criteria (R > 0.6) benchmarks (Zhai et al., 2024)(Zhai et al., 2024). This result in several cases, demonstrates ing the model's capability to reproduce the time variability of this pollutant in Bogotá, even if the levels are under or overestimated. The same situation is observed in Mexico City and São Paulo, where goal (R>0.6) and criteria (R>0.4) benchmarks are often achieved (Zhai et al., 2024).

In Santiago in winter, the MNBIAS ranges from -2 to -157% and the FGE vary from 20 to 157%, considerably more pronounced than in summer with bias from -67 to 69% and errors from 21 to 69%. This situation could be explained by emissions, synoptics or the models' simulation of the boundary layer (Mazzeo et al., 2018). In Bogotá, all models consistently underestimate the CO, with Model/Observations ratios ranging from 0.2 to 0.6. The correlation between models and observations for CO are within goal (R > 0.4) and criteria (R > 0.6) benchmarks (Zhai et al., 2024) in several cases, demonstrating the model's capability to reproduce the time variability of this pollutant, even if the levels are under or overestimated.

The underestimation in BogotaBogotá is similar to that observed for NO_2, which we attributed to a shortfall in emissions. According to the local inventory, CO emissions are predominantly attributed to mobile sources (99%), with motorcycles contributing to 45% of these emissions, automobiles accounting for 36%, and the remainder originating from other vehicles (SDA -Secretaria Distrital de Ambiente, 2018)(SDA -Secretaria Distrital de Ambiente, 2018). Notably, it has been identified that motorcycle emissions are underestimated in Colombia (Rojas et al., 2023)(Rojas et al., 2023). The significant rise in the number of motorcycles in the country and their declining condition is not accurately reflected in global emission inventories, such as EDGAR 6.1.

Observed CO mixing ratios are also underestimated in cities such as Medellin, Guadalajara, Quito, and Lima (Fig. 87), which might be explained by the coarse resolution of the model not capturing the local characteristics. It is possible that issues with CO emissions in global inventories or excess of OH radicals in the photochemistry also contribute to this trend. In addition, a major source of atmospheric CO is the oxidation of BVOCs (Worden et al., 2019), which are significantly underestimated in the Southern Hemisphere (Zeng et al., 2015).

In São Paulo, five out of six models slightly underestimate CO with a relatively high correlation coefficient. The simulated concentrations for daily values range from 0.1 to 2.0 ppm, similar to that found in other studies (Deroubaix et al., 2024)(Deroubaix et al., 2024). Nevertheless, concentrations exceeding 1.2 ppm are simulated only for certain days (Jan. 13 and July. 30) and are probably due to wood burning identified in hourly simulations (Fig. C1).

Model intercomparisoninter-comparison

Con formato: Inglés (Estados Unidos)
Con formato: Francés (Francia)
Con formato: Francés (Francia)
Con formato: Francés (Francia)
Con formato: Francés (Francia)
Con formato: Francés (Francia)
Con formato: Color de fuente: Negro

Global models, particularly CAMS, tend to underestimate CO levels in Bogotá, São Paulo, and México City with MNBIAS < -50%. ~~y, with Model/Observations ratios around 0.4.~~ In Santiago, CAMS ~~reproduces~~ adequately simulates CO levels ~~with a Model/Observations ratio of about 1.0,~~with ~~-~~MNBIAS (< ± ~~10~~2.5%) and FGE (<~~20~~25%). The correlation coefficient achieves the criteria benchmark (R > 0.4) proposed by (Zhai et al., 2024)~~(Zhai et al., 2024)~~. SILAM underestimates CO in Bogotá ~~(Model/Observations ~0.6)~~ and overestimates it in Santiago ~~(Model/Observations ~2.0)~~, while it performs relatively well in São Paulo and México City (~~Model/Observations ~1.1~~MNBIAS < 22%) with ~~and~~ correlation coefficients meeting the criteria and goal benchmarks (R > 0.~~6~~4 and R>0.6) proposed by (Zhai et al., 2024)~~(Zhai et al., 2024)~~.

When it comes to regional models, WRF-USP consistently underestimates CO levels with ~~Model/Observations ratios ranging from 0.1 to 0.5 with~~ large bias (MNBIAS < -60%) and errors (FGE > 60%). WRF-MPI has ~~a~~ better performance especially in São Paulo and Mexico City (MNBIAS < ± 15%) and ~~consistently underestimates CO in all cities, with Model/Observations ratios from 0.3 to 0.8 relative to observations, and 1.0 for São Paulo for both periods with~~ correlation coefficients within the goal benchmark (Zhai et al., 2024)~~(Zhai et al., 2024)~~. EMEP and CHIMERE ~~both~~ largely overestimate observations in México City ~~with values between 4.0 and 6.0ppm,~~ while in São Paulo they closely match observations ~~with ratios around 0.9 and low MNBIAS and FGE~~. In Santiago, these models tend to overpredict CO in the summer and underpredict it during the winter.

The largest model variation ~~bility~~ is observed in Santiago during wintertime with a range of ~~2.1~~3.2 ppm and C.V. of ~~86~~106% (Table A8). México City also shows large variation in summer (C.V. ~~of 54~~72%) and winter (C.V. ~~(January) and 65~~63%) ~~(July)~~. Bogotá and São Paulo present ~~more consistency~~less variation between model results ~~with C.V. between 33% and 42%.~~

Ensemble performance

~~In the summer in Santiago, the median ensemble outperforms individual models for CO, with MNBIAS of 3.6% and FGE of 0.1%, less than any other model (Table A4).~~ In winter in Santiago and Bogotá in both periods the ensemble follows the underestimation pattern of all models (Table A4). In São Paulo ~~o, t~~there are models with better performance than the ensemble, but the ensemble results are reasonable with ~~Model/Observations ratio ~0.7,~~ MNBIAS close to ~~-~~-30~~15~~% and R approximately ~~-~~0.7. In México City, the overestimation of CO by the EMEP and CHIMERE models (MNBIAS > ~~45~~60%) is reduced in the ensemble (MNBIAS ~ -~~15% in January and of 3% in July~~).

3.1.4 Sulfur dioxide - SO_2

Observations

The number of stations per city recording SO_2 during January and July of 2015 varies between 4 in Santiago and 26 in Mexico City (Appendix B).~~The number of stations per city recording SO_2 is available in Appendix B.~~ ~~In January in Mexico City, data availability was 97%. The rest of the cities were 100%.~~ The largest concentration of SO_2 is observed in México City with values between 3.0 ppb (Januar~~ulyy~~) and 4.~~6~~4 ppb (Jul~~anuary~~) due to volcanic emissions (de Foy et al., 2009)~~(de Foy et al., 2009)~~ and the heavy consumption of coal in power generation and cement production, especially in the proximity of the "Tula-Vito-Apasco"

Con formato: Fuente: Cursiva

Con formato: Resaltar

industrial area (SEMARNAT and INECC, 2020)~~(SEMARNAT and INECC, 2020)~~. On the other hand, SO_2 in Bogotá, Santiago and São Paulo are lower with concentrations ranging from 1.0 to 1.8 ppb (Fig. 5).

Model performance

The largest simulated SO_2 value ~~ion~~ is shown in México City with an average of ~~10~~ 45 ppb ~~SO_2~~, followed by São Paulo, with a mean concentration of ~~6.0~~8.5 ppb. In Santiago, the average SO_2 value is 8.5~~winter values are around 4.5~~ ppb ~~and summer values around 3.6 ppb~~. The lowest modeled values are found in Bogotá with an average of ~~0.76~~0.97ppb (Table A5).

Con formato: Fuente: (Predeterminada) Times New Roman, 10 pto, Color de fuente: Negro

Con formato: Subíndice

Con formato: Subíndice

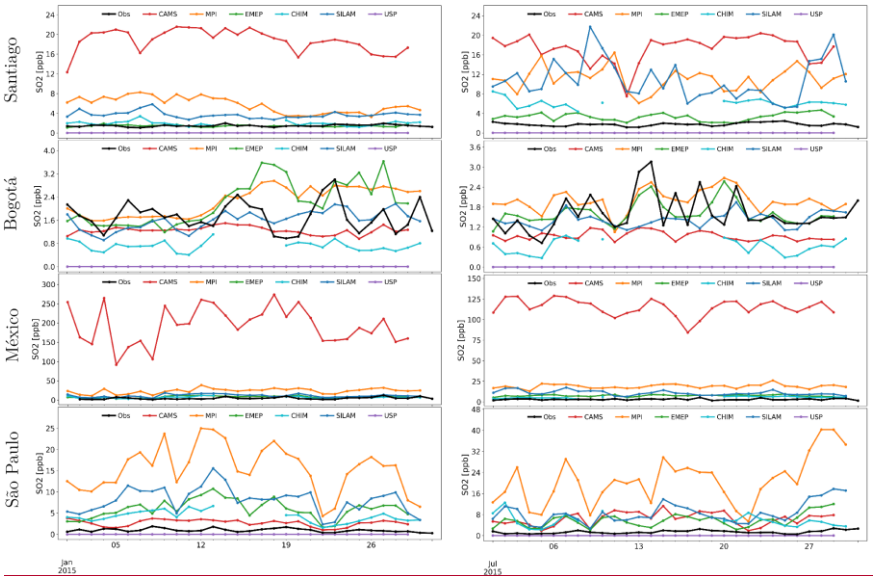
Santiago
Bogotá
México
São Paulo
Obs
CAMS
MPI
EMEP
CHIM
SILAM
USP
SO2 [ppb]
Jan
2015
Jul
2015

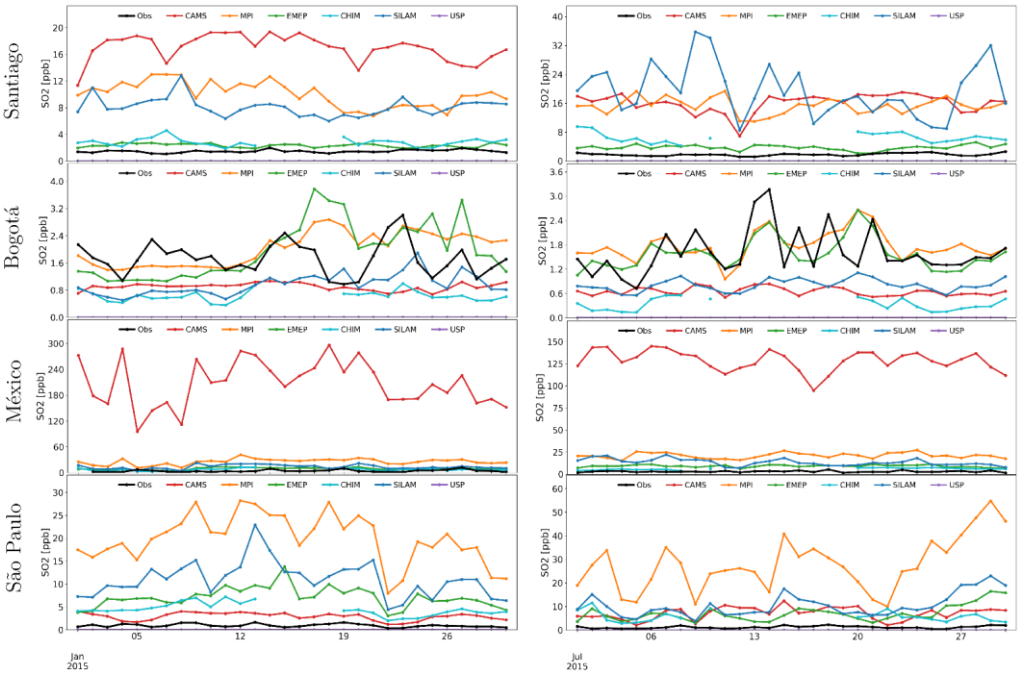
Santiago
Bogotá
México
São Paulo
Obs
CAMS
MPI
EMEP
CHIM
SILAM
USP
SO2 [ppb]
Jan
2015
Jul
2015

Figure 45. Observed (blackorange) and simulated SO_2 daily mean concentrations in Santiago, (top) Bogotá, México City, São Paulo (bottom) for January (left) and July (right) 2015

The models' simulated SO_2 exhibits significant discrepancies when compared to the observations, with severe overestimations in Santiago, México City, and São Paulo (Fig. 45), with MNBIAS reaching up to 190% and FGE errors up to 200% (Table A5). On the contrary, for Bogotá the predicted SO_2 values are in reasonable alignment with the observations (Model/Observations ratio around 0.9), except for the WRF-Chem USP simulation, which drastically underestimates SO_2 (MNBIAS -200%) (Table A5).

The overestimation of SO_2 levels could stem from issues within global emission inventories. In fact, an overestimation of SO_2 emissions in CAMS was observed for Buenos Aires and Santiago when compared to the PAPILA inventory (Castesana et al., 2022)(Castesana et al., 2022). These emissions primarily originate from the energy and industrial sectors, where the sulfur content in coal appears to be significantly contributing to this overestimation.

The good performance in Bogotá might be related to less SO_2 emissions apportioned in the city. In fact, the vast majority of SO_2 emissions (~90%) in Colombia originate from the industrial and energy production sectors (IDEAM, 2020)(IDEAM, 2020). However, these facilities are typically located outside major urban areas. Bogotá contributes only 1.5% of the total national SO_2 emissions (SDA -Secretaria Distrital de Ambiente, 2018)(SDA -Secretaria Distrital de Ambiente, 2018).

Model intercomparisoninter-comparison

With respect to global models, CAMS and SILAM severely overestimates SO_2 in México City, São Paulo and Santiago with MNBIAS and FGE larger than 1060%. In São Paulo, the bias and errors are lower but still significant (from 90 to 125%). Similarly, SILAM overestimation for these three cities is also large, with MNBIAS and FGE between 86% and 154%.In For Bogotá, both global models underestimate SO_2 concentrations (MNBIAS from -56 to -80%) but with lower FGE (< 80%) than CAMS. In January, SILAM demonstrates good performance in the simulation of SO_2 with MNBIAS between -5% (January) and 4% (July), FGE between 14% and 27% and correlation coefficients that meet the criteria benchmark (R > 0.35) suggested by (Zhai et al., 2024)(Zhai et al., 2024).

Con formato: Subíndice

The performance of regional models for SO_2 is quite diverse. WRF-USP severely underestimates SO_2 in all cities (MNBIAS close to -200%). In Santiago, México City and São Paulo the models overestimate SO_2 in a similar fashion than global models. In Bogotá, EMEP and WRF-MPI shows one of the lowest MNBIAS (< 16from 10 to 17%).

The largest model variation bility ffor SO_2 is found in México City where the range of models is reach 180200 ppb, and the C.V. is larger than 150% (Table A8). In Santiago and São Paulo, the model variation is close to C.V. 95%. In Bogotá, the variation is the lowest (C.V. ~75%). in January the C.V. is 130%. São Paulo and Bogotá present intermediate values of the C.V. between 64% and 88%.

Ensemble performance

In México City, Santiago and São Paulo, SO_2 is overestimated by all models, except USP. Therefore, the median ensemble also overestimates SO_2 concentration and does not represent any improvement in the evaluation metrics (Table A5). In Bogotá, the ensemble tends to underestimate the concentrations (MNBIAS ~ -55%) toin a lesser extent than individual models.
~~does not display the best metrics, but MNBIAS and FGE are relatively low.~~

3.1.5 Fine particulate matter - $PM_{2.5}$

Observations

The number of stations per city recording $PM_{2.5}$ during January and July of 2015 varies between 9 in Bogotá and 16 in Mexico City (Appendix B).~~The number of stations per city recording $PM_{2.5}$ is available in Appendix B. In January in Mexico City, data availability was 97%. The rest of the cities were 100%.~~ The largest $PM_{2.5}$ concentrations are found in Santiago during the southern hemispheric winter with daily values around ~~60~~ 56 ug/m^3. This can be attributed to adverse meteorological conditions and emissions from transportation and residential combustion in the surrounding municipalities (Mazzeo et al., 2018; Saide et al., 2016)~~(Mazzeo et al., 2018; Saide et al., 2016)~~. The second largest values are shown in México City with an average of 23~~1~~ ug/m^3 due to local emission sources. In São Paulo, $PM_{2.5}$ levels are slightly larger in July (18~~9~~ ug/m^3) than January (~~15~~ 16 ug/m^3), due to the impact of wildfires from the Amazon basis and sugarcane burning (Andrade et al., 2017). In Bogotá, $PM_{2.5}$ concentrations are the lowest in July (13 ug/m^3) due to the influence of the trade winds (Pachón et al., 2018) but with larger values in January (~~18~~ 19 ug/m^3) due to biomass burning events and frequent thermal inversions (Ramírez et al., 2018).

Model performance

In Santiago in wintertime, the mean of the models is larger than ~~close to the o~~observation whereas in summer the simulations are mostly below observations. ~~, but with a large standard deviation (62.6 ± 85 ug/m^3). In January, the simulation mean is 65% the observation.~~ In ~~São Paulo~~Mexico City, simulated values are approximately double the observations. In São Paulo, $PM_{2.5}$ is under and overpredicted by the models. ~~In México City, simulated values are above and below the observation.~~ In Bogotá, most of the simulations are below the observations (Fig. ~~5~~6).

Con formato: Resaltar

Con formato: Subíndice

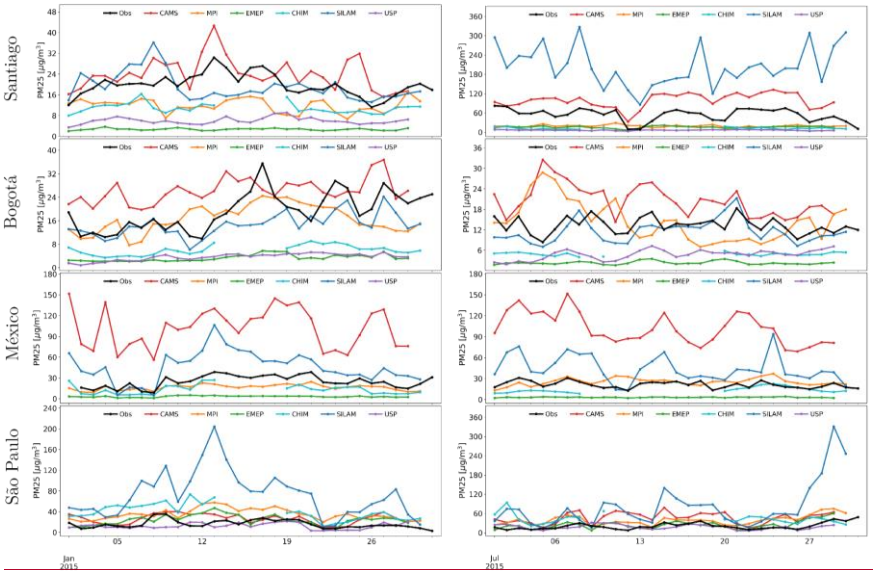
Santiago
Bogotá
México
São Paulo
Obs
CAMS
MPI
EMEP
CHIM
SILAM
USP
PM25 [μg/m³]
Jan 2015
Jul 2015

630

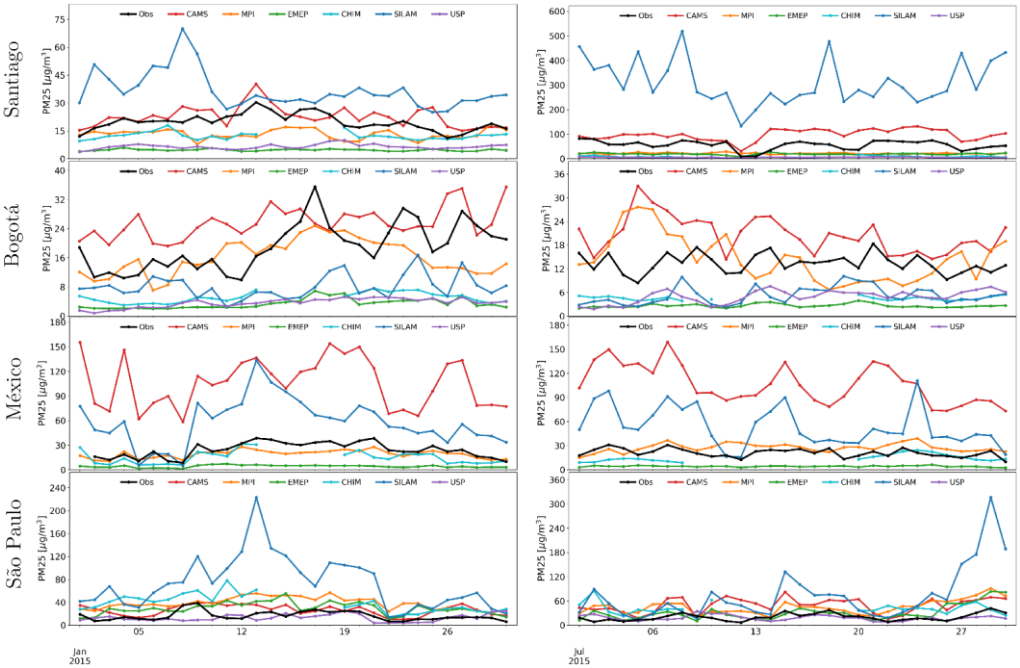
Santiago
Bogotá
México
São Paulo
Obs
CAMS
MPI
EMEP
CHIM
SILAM
USP
PM25 [μg/m³]
Jan 2015
Jul 2015

Figure 56. Observed (blackorange) and simulated $PM_{2.5}$ daily mean concentrations in Santiago, (top) Bogotá, México City, São Paulo (bottom) for January (left) and July (right) 2015.

In Santiago, Bogotá, and México City, some models over and underpredict overestimate and others underestimate $PM_{2.5}$ with large MNBIAS and FGE (Table A6). The MNBIAS and FGE are, in general, within the goal or criteria benchmarks suggested by (Boylan and Russell, 2006).. In São Paulo, overestimation is observed in all models with exception WRF-USP and may be linked to an excess of fire emissions, as suggested by other studies (Deroubaix et al., 2024). The Model/Observations ratios range from 1.3 to 4.5. The , and MNBIAS values vary from 2539% to 117120% except for WRF-USP, whose MNBIAS is negative 0.8% (Table A6). The correlation coefficients for $PM_{2.5}$ are in some cases larger than the goal (R > 0.7) or criteria (R > 0.4) benchmarks proposed by (Emery et al., 2017). It's worth noting the case of Mexico City in January and Sao PauloSão Paulo in July, where most models achieve the goal metric for R. In smaller urban areas like Medellin, Lima, and Quito (Fig. 78), most models tend to underestimate observations, potentially due to the coarse resolution of the models.

Hourly simulations of $PM_{2.5}$ are useful to understand the discrepancies between model and observations. In Fig. C2, we show the hourly data and model outputs. In São Paulo, the highest $PM_{2.5}$ concentrations are simulated by SILAM in January 13 (> 320 ug/m^3) and July 30 (> 400 ug/m^3), which corresponds to days with high simulated CO values as well (Fig. C1) and may indicate an overestimation of biomass burning by the IS4FIRES module in SILAM. From Jan 15 to 30 there is also an excess of $PM_{2.5}$ from SILAM.

In México City, the highest $PM_{2.5}$ concentrations are simulated by the CAMS model with about 250 ug/m^3 in January and 160 ug/m^3 in July (Fig. C3) which are severely overestimated. The large $PM_{2.5}$ values are distributed in the whole period rather than specific days and do not correspond with high CO concentrations to suspect the influence of fires. This situation might indicate a local and continuous source of $PM_{2.5}$

Model intercomparisoninter-comparison

Both global models consistently overestimate $PM_{2.5}$ in Santiago, São Paulo and México City, but they behave differently in Bogotá. In Mexico City, CAMS generally has a greater overestimation than SILAM but in São Paulo and Santiago SILAM values are larger (Figure 6 throughout the cities, reaching Model/Observations values between 1.5 to 5 while SILAM ranges between 2 to 4 (Table A6). In For Bogotá, CAMS overestimates PM2.5 (MNBIAS ~ 37%) whereas SILAM underestimates it (MNBIAS ~ -85%)(Boylan and Russell, 2006)(Boylan and Russell, 2006)(Boylan and Russell, 2006)(Boylan and Russell, 2006)(Boylan and Russell, 2006). SILAM CAMS displays an overestimation of around 1.5 times the observed values with a poor correlation coefficient, while SILAM slightly underestimates with a Model/Observations ratio of 0.8 but with a correlation coefficient that meets the criteria benchmark suggested by (Emery et al., 2017).

Among the regional models, EMEP shows the largest underestimation (MNBIAS < -110%) in all cites, except in São Paulo where the model overestimates PM2.5 (MNBIAS < 60%), but -within the criteria benchmark (Boylan) (MNBIAS < ±60%, Boylan and Russell, 2006) and typically shows Model/Observations ratios below 0.2, except for São Paulo where it overestimates by 1.5 times wwith a correlation coefficient (R >0.4) that meets the criteria goal benchmark by (Emery et al., 2017) in July (Table A6). WRF-

Con formato: Resaltar

USP heavily underestimates in Bogotá and Santiago, ~~at 0.3 times the observations,~~ but performs well in São Paulo with the lowest errors. This difference in behavior might be explained by a good adaptation of the model's inputs to the city. The WRF-MPI model meets goal benchmarks for MNBIAS and FGE in ~~Bogota~~Bogotá and Mexico City.

~~In general, global models achieve more benchmarks (goal or criteria) for $PM_{2.5}$ than regional models.~~

The largest model variation ~~intervariability~~ is observed in México City and Santiago during wintertime with a C.V. greater than 100% (Table A~~8~~8). Santiago in summer and Bogotá present intermediate values (C.V. ~~65~~ 70 to ~~78~~80%), whereas São Paulo shows the least variation ~~dispersion bb~~etween models (C.V.< ~~50~~56% ~~to 59%)~~).

Ensemble performance

Considering the large underestimation of most models in Bogotá and Santiago the ensemble displays less bias and errors than some of the individual models (Table A6). In Mexico City, the ensemble outperforms models with a MNBIAS of -5% in January and +30% in July, achieving the goal benchmark suggested by (Boylan and Russell, 2006), as well as the correlation coefficient (R>0.8) in January. ~~The median ensemble for Bogotá and Santiago does not represent any improvement in the evaluation metrics (Table A6). F~~For São Paulo, all models tend to overestimate $PM_{2.5}$, so it follows that the ensemble presents the same behavior with ~~Model/Observations ~ 1.9 and~~ MNBIAS ~ 647%. ~~However, t~~The correlation coefficient meets the criteria ~~goal~~ benchmark (R>0.74) in both periods (Emery et al., 2017).~~July and the criteria target (R>0.4) in January. In México City the severe overestimation of $PM_{2.5}$ by CAMS (MNBIAS > 125%) and SILAM (MNBIAS > 50%) is softened by the construction of the ensemble, resulting in a MNBIAS of -30% and 6% in January and July, respectively. The correlation coefficient meets the goal benchmark (R>0.7) in January.~~

~~**3.2 Median ensemble**~~

~~In this section, we present the results of the model ensemble based on the median value for every pollutant.~~

Con formato: Fuente: 9 pto, Cursiva

Con formato: Fuente: 10 pto, Cursiva

3.2.1 Nitrogen dioxide - NO_2

As it was previously described, NO_2 is underestimated by all models in Santiago and Bogotá. Therefore, the median ensemble also underestimates NO_2 concentration and does not represent any improvement in the evaluation metrics (Table A2). On the contrary, in São Paulo, the ensemble median outperforms individual models for NO_2. In both summer and winter, the ensemble median presents the lowest RMSE and FGE, with a Model/Observations ratio close to 1.0, a correlation coefficient R=0.7, and MNBIAS between -3% (summer) to -12% (winter). The median ensemble also provided adequate statistics in a higher resolution modeling domain in São Paulo. In México City, the ensemble adequately simulates NO_2 (Model/Observations ~0.9) with lower error and bias than most of the individual models. In January, the correlation coefficient meets the goal benchmark for this pollutant (R>0.6) in all cities, whereas in July the goal benchmark is achieved for Sao Paulo and the criteria target (R>0.5) for Santiago and Mexico City.

3.2.2 Ozone - O_3

In Santiago in January, the median ensemble showed one of the lowest biases (MNBIAS) and errors (FGE, RMSE), surpassed by only one model (Table A3), and achieved the goal benchmark for this pollutant (R>0.75) . In July, the overestimation of ozone by most models impacts the performance of the ensemble, which also overestimates O_3 concentrations. In Bogotá, the ensemble has the second lowest MBIAS and FGE, both in January and July, and represents an intermediate value between all models. In São Paulo, in wintertime, the ensemble has superior metrics (Model/Observations ratio ~1.0, MNBIAS ~-2%) compared to any individual model, while in the summer the ensemble overestimates the observations (Model/Observations ratio ~1.5) as most models do. In México City, the ensemble median performs better than all individual models with MNBIAS between 7% (summer) and 13% (winter) and FGE less than 30%. Similar to the individual models, for most of the cases, the correlation coefficient for the ensemble does not meet any of the benchmarks .

3.2.3 Carbon monoxide - CO

In the summer in Santiago, the median ensemble outperforms individual models for CO, with MNBIAS of 3.6% and FGE of 0.1%, less than any other model (Table A4). In winter in Santiago and Bogotá in both periods the ensemble follows the underestimation pattern of all models. In São Paulo, there are models with better performance than the ensemble, but the ensemble results are reasonable with Model/Observations ratio ~0.7, MNBIAS ~ -30% and R ~ 0.7. In México City, the overestimation of CO by the EMEP and CHIMERE models (MNBIAS > 45%) is reduced in the ensemble (MNBIAS -5% in January and of 3% in July).

3.2.4 Sulfur dioxide - SO_2

In México City, Santiago and São Paulo, SO_2 is overestimated by all models, except USP. Therefore, the median ensemble also overestimates SO_2 concentration and does not represent any improvement in the evaluation metrics (Table A5). In Bogotá, the ensemble does not display the best metrics, but MNBIAS and FGE are relatively low.

3.2.5 Particulate matter - $PM_{2.5}$

The median ensemble for Bogotá and Santiago does not represent any improvement in the evaluation metrics (Table A6). For São Paulo, all models tend to overestimate $PM_{2.5}$, so it follows that the ensemble presents the same behavior with Model/Observations ~ 1.9 and MNBIAS 64%. However, the correlation coefficient meets the goal benchmark (R>0.7) in July and the criteria target (R>0.4) in January. In México City the severe overestimation of $PM_{2.5}$ by CAMS (MNBIAS > 125%) and SILAM (MNBIAS > 50%) is softened by the construction of the ensemble, resulting in a MNBIAS of -30% and 6% in January and July, respectively. The correlation coefficient meets the goal benchmark (R>0.7) in January.

Con formato: Español (Colombia)
Con formato: Título 2, Izquierda, Interlineado: sencillo
Con formato: Español (Colombia)
Con formato: Título 2
Con formato: Fuente: Sin Negrita
Con formato: Español (Colombia)
Con formato: Título 2, Izquierda, Interlineado: sencillo
Con formato: Español (Colombia)
Con formato: Neerlandés (Países Bajos)
Con formato: Título 2
Con formato: Fuente: Sin Negrita
Con formato: Título 2, Izquierda, Interlineado: sencillo
Con formato: Título 2
Con formato: Fuente: Sin Negrita
Con formato: Título 2, Izquierda, Interlineado: sencillo
Con formato: Título 2
Con formato: Fuente: Sin Negrita
Con formato: Título 2, Izquierda, Interlineado: sencillo

3.32. Spatial seasonal variability of predictions

Con formato: Fuente: Sin Negrita

For all pollutants, models and periods, maps of mean concentrations were constructed to visualize the spatial differences (Appendix D). In order to summarize the results, other spatial plots were also prepared: median ensemble (Fig. 67), median absolute deviation (Fig. E1), mean standard deviation (Fig. E2). In Figure 76, pollution hot spots ~~pollution hot spots~~ are clearly visible around major urban areas, in particular, São Paulo in the southeastern coast and México City in the northwestern part of the continent. São Paulo and México City each cover a significant ~~area,~~area of approximately 3600 km^2, spanning at least nine modeling cells (400 km^2 each). This extensive coverage offers some spatial representation of the physical and chemical atmospheric processes. Other regions highlighted ~~e~~in the maps include Lima and Santiago on the Pacific coast, Buenos Aires along the southern shore of the Río de la Plata, and cities in the northern part of South America like Quito, Bogotá, Medellín, and Caracas. However, most of these cities are encompassed by six ~~three~~ or fewer modeling cells, limiting the potential for significant spatial variation.

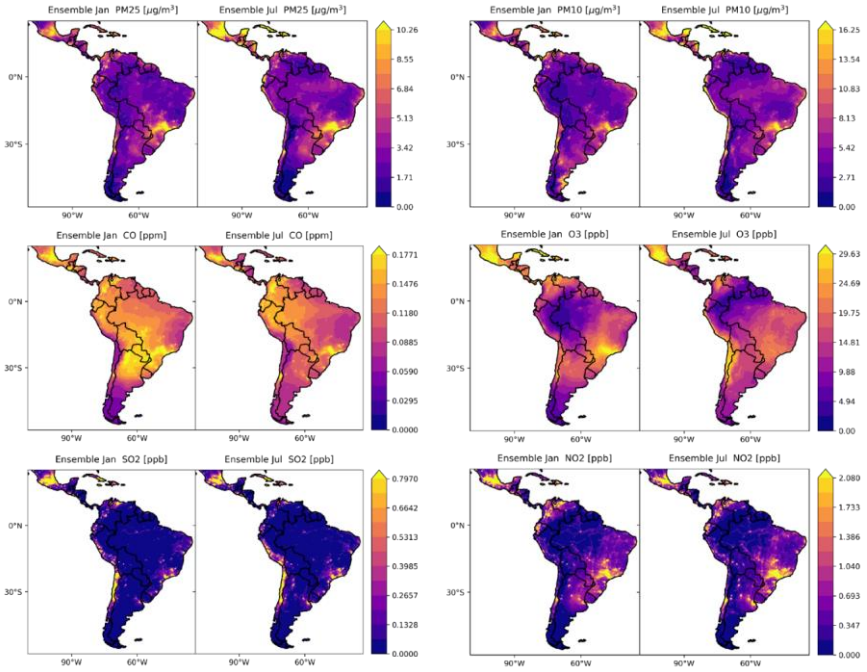

Figure 67. Spatial variability of simulated PM_{10}, $PM_{2.5}$, O_3, CO in LAC for January and July 2015 (based on the median of the models)

The temporal seasonality can also be observed in Figure ~~6~~7. The left and right panels show results for January and July, corresponding to the southern hemisphere summer and winter respectively. For SO_2, major hot spots appear in México City, São Paulo and surrounding areas, and the Pacific coast in Chile. The SO_2 concentrations are associated with volcanic emissions and the use of coal ~~use~~ in power generation, cement production and copper smelting that are active in both summer and winter (Huneeus et al., 2006; SEMARNAT and INECC, 2020). Similarly, NO_2 hotspots are common in major urban areas due to transportation ~~the major~~ emissions ~~source being transportation~~.

In January, the median ensemble shows high concentrations of PM_{10} in several areas. In the south of Argentina, the concentrations are primarily due to dust from the Patagonia desertic areas (Gassó and Torres, 2019). In the north of Brazil and the Guianas, increased PM_{10} levels are most likely associated with fires in the Orinoco basin during the dry season (Hernandez et al., 2019). In a similar manner, $PM_{2.5}$ concentrations ~~across LAC show similar behavior than PM_{10}, with~~ show an increase in the northern part of Brazil due to biomass burning~~wildfires~~. Large concentrations of $PM_{2.5}$ in São Paulo in both January and July are probably caused by overestimation of fires, as previously discussed.

During the austral summer, the southeastern part of ~~Brasil~~Brazil (including São Paulo) ~~displays presents~~ large concentrations of ozone that were simulated mainly by the regional models WRF-Chem, ~~, WRF-MPI and~~ EMEP and the global SILAM (Fig. D3). Several studies have shown the influence of urban plumes of NO_2 into the Amazon rainforest, rich in BVOCs, with the consequent generation of ozone (Abou Rafee et al., 2017; Nascimento et al., 2022). In January, simulated O3 concentrations are also large in Mexico City during winter, a situation that has been observed in other studies (Barrett and Raga, 2016)~~(Barret and Raga)~~. T~~t~~here is a maximum of CO in the area between north of Argentina, south of Bolivia, Paraguay and south of Brazil, probably related to fires and the abundance of BVOCs.~~.~~

In July, during the austral winter, concentrations of CO, $PM_{2.5}$ and PM_{10} are significant in Santiago due to transportation and residential heating emissions under adverse meteorological conditions ~~in the austral winter~~. PM_{10} concentrations are large in the Caribbean and central México, primarily due to the transport of Saharan dust into these urban areas (Kramer and Kirtman, 2021; Ramírez-Romero et al., 2021). Similarly, along the Pacific coast between Chile and Peru, increased PM_{10} is probably explained by anthropogenic emissions of copper smelters in connection with strong eastern wind events (Huneeus et al., 2006). Large concentrations of O_3 are visible in México City associated with~~to~~ clear skies under high-pressure atmospheric conditions (Barrett and Raga, 2016)~~(Barrett y Raga)~~. Elevated O_3 values in ~~and in~~ the Andes mountains between northern Chile and central Peru might be explained by the abundance of VOCs from metropolitan regions and industrial zones (Seguel et al., 2024)~~(Seguel, 2024)~~. ~~Ozone is also large in the São Paulo metropolitan area in January.~~

The median absolute deviation maps (Fig. E1) and the standard deviation maps (Fig. E2), display spatial differences between model simulations. In particular, for particulate matter (PM_{10} and $PM_{2.5}$) notorious dissimilarity is observed in northern Brazil in January, Venezuela in July, and the south of Argentina in both periods. The reason for this deviation ~~disagreement~~ is the simulation of the WRF-MPI model, which contributes with significant PM mass in the mentioned zones, probably due to an overestimation of fires in the northern part of the continent and dust in the southern areas. In July, CO showed large differences in the Colombian and Peruvian Amazon, mostly driven by the EMEP model. This situation might be related to an incorrect estimation of BVOCs

Con formato: Subíndice

Con formato: Resaltar

Con formato: Resaltar

Con formato: Subíndice

Con formato: Fuente: (Predeterminada) Times New Roman, 10 pto, Color de fuente: Negro

Con formato: Resaltar

emissions as precursors of CO in forested areas. The inadequate simulation of NO_2 by the CAMS model, explained in section 3.1.1, is the cause of the large standard deviation of model results for this pollutant

3.34 Large versus small urban areas

The coarse resolution used in the modeling systems (0.2° x 0.2°) poses challenges in adequately representing the intricate topography and diverse meteorological conditions of the different cities in LAC. Capturing these physical phenomena can be very difficult and requires a finer scale with much greater computational demand. In the last years, emission inventories for LAC at high spatial and temporal resolution have been constructed (Álamos et al., 2022; Castesana et al., 2022; Puliafito et al., 2015, 2017; Rojas et al., 2023)~~(Castesana et al., 2022; Álamos et al., 2022; Puliafito et al., 2015, 2017; Rojas et al., 2023)~~ and it's expected they will complement existing global emission inventories at coarse resolution.

We observe that, in large urban areas (> 3500 km^2) the models tend in general to have lower and positive MNBIAS compared to medium size (600 < area < 3600 km^2) or small (area <600 km^2) cities (Fig. ~~7~~8). For example, for México City and São Paulo, the two largest cities in LAC, the mean of the ~~models~~ models show the lowest MNBIAS ~~and FGE~~ for CO (-27% to 29%) and NO_2 (-6% to 6%), while in other cities they display larger and negative MNBIAS and FGE (Table A2 and A~~S~~4). ~~This trend suggests that models typically underpredict CO and NO_2 in medium and small urban areas.~~ The discrepancies in NO_2 have a corresponding impact in the overestimation of O_3. For particulate matter, a similar pattern is observed, with positive MNBIAS for large~~r~~ urban areas and negative MNBIAS for medium and small cities. High-resolution simulations are necessary to resolve the spatial variation, but unfortunately global models at high performance are scarce in the Southern Hemisphere (Zhang et al., 2023)~~(Zhang et al., 2023).~~

Although the size of cities can influence the performance of the models at coarse resolution, other challenging features for models exist. For instance, ~~Bogota~~Bogotá and Santiago have several challenges in terms of topography and meteorology (Mazzeo et al., 2018; Nedbor-Gross et al., 2017; Reboredo et al., 2015) and local emissions not always accounted in global inventories (Castesana et al., 2022; Huneeus et al., 2020; Osses et al., 2022; Rojas et al., 2023). Ideally, we would have access to more cities of various sizes to make this determination with more certainty, unfortunately, local measured data was only available for the cities we considered.

Con formato: Subíndice

Con formato: Fuente: (Predeterminada) Times New Roman, 10 pto, Color de fuente: Negro

Con formato: Fuente: (Predeterminada) Times New Roman, 10 pto, Color de fuente: Negro

Con formato: Fuente: (Predeterminada) Times New Roman, 10 pto, Color de fuente: Negro

Con formato: Fuente: (Predeterminada) Times New Roman, 10 pto, Color de fuente: Negro

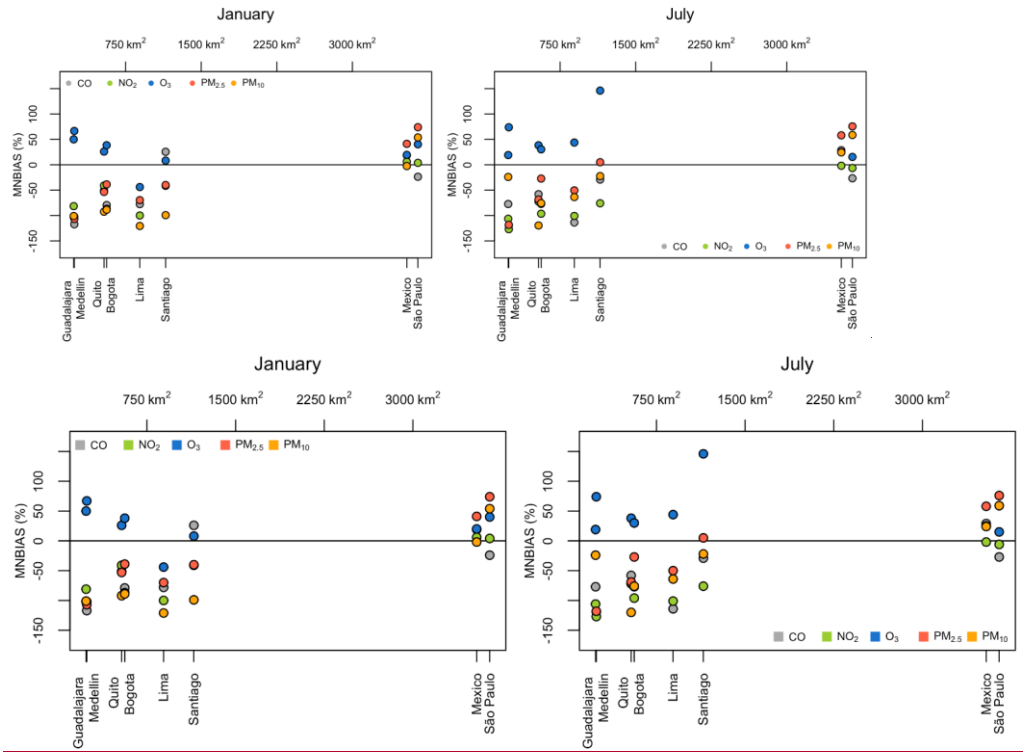

Figure ~~7~~8 MNBIAS estimated for large and small urban areas

~~4~~. Conclusions and future developments

This study performed the first ~~intercomparison~~inter-comparison and model evaluation effort in Latin America with the idea to develop an AQF ~~air quality analysis and forecasting~~ system that can inform the public about air pollution episodes and support

Con formato: Fuente: (Predeterminada) Times New Roman, 10 pto

Con formato: Normal, Justificado, Interlineado: 1.5 líneas

policy actions. Despite the limitations of air quality and emissions data, as well as computing resources, the scientific community in Latin America, with international support, has achieved significant progress in air quality modeling and in understanding the fate and transport of pollutants in the region. For instance, the impact of Saharan dust, biomass burning from the Orinoco and the Amazon basis, biogenic VOCs of the Amazon rainforest, are becoming better understood through modeling.

Several challenges still exist. In addition to the intricate topography and diverse meteorological conditions, limitations are found in anthropogenic, volcanic and biogenic emissions, spatial and temporal profiles, land use and vegetation types, as well as other data that are relevant for the calculation of wildfire emissions. This last source is crucial in the region under a climate change scenario, for which adequate parametrization of biomass burning is necessary. The boundary conditions of the models can be improved, which are especially important for long-lived species. The experience of local researchers who have been implementing air quality models for several years can greatly benefit international efforts such as global emissions inventories and the recently-launched WMO GAFIS initiative.

At this first stage of development, interesting and insightful findings were identified for the region. Despite the fact that some of the models were still in an early phase for regional implementation, most models could adequately reproduce air quality observations with the best performance observed for nitrogen dioxide in México City and São Paulo. These enormous urban areas (> 3500 km^2) outperformed Bogotá and Santiago, which are cities between 500 and 1000 km^2. This suggests an accurate portrayal of the temporal and spatial variability in large cities with the current model resolution (0.2° x 0.2°) and the need for a finer model domain ~~resolution~~ in smaller cities that could capture circulation and emission features. At the moment, high-resolution global simulations in the Global South remain rare.~~.~~

~~Several challenges were faced and partially overcome~~overcome~~. In addition to the intricate topography and diverse meteorological conditions in LAC, of cities in LAC, some of the individual models were still in an early phase of regional modeling. L~~l~~imitations in model inputs exist in on anthropogenic and biogenic emissions, spatial and temporal profiles, land use and vegetation types, as well as other data that is relevant for the calculation of biogenic fluxes and wildfire emissions~~.~~ The latter emission source is is crucial in the region for the region, and more relevant under a climate change scenario, for which an adequate parametrization of biomass burning is necessary. The models´ boundary conditions of the models can be improved, which are particularly important may be relevant for longer-lived species such as CO and ozone. The experience of local researches that have been implementing air quality models for several years can greatly benefit international efforts such as global emissions inventories and the recent-launched WMO GAFIS initiative.

The ensemble median was evaluated on its potential to outperform individual models. In certain periods and cities, the ensemble performed better than any individual models, for example, when the errors of the models compensate for each other, but not when the errors are recurring in all the models. The results varied per city, pollutant and period. ~~NO_2 and O_3 in São Paulo and Mexico City. In the latter, the ensemble also softened large overestimations of $PM_{2.5}$ by global models. However, certain individual models outperformed the ensemble for specific pollutants and cities.~~ Before defining whether the ensemble is the correct approximation for an AQF ~~a forecasting~~ system, more research is necessary~~, for which a similar exercise of inter-comparison of models is currently~~

Con formato: Punto de tabulación: 2.12", Izquierda

being carried out for a more recent year. This work only looked at two months (one in summer and one in winter), a thorough analysis of one entire annual cycle with sufficient spin-up time should be conducted. More observations should also be included for model calibration and evaluation. For 2015, only eight cities in LAC had data that complied with quality and completeness criteria. In recent years, more AQ networks have been implemented and data is more publicly available.

Despite the above limitations and the coarse resolution (0.2° x 0.2°) adopted in this work, most models could reproduce air quality observations with the best performance observed for nitrogen dioxide in México City and São Paulo. These enormous urban areas (> 3500 km²) outperformed Bogotá and Santiago, cities between 500 and 1000 km². This suggests an accurate portrayal of the temporal and spatial variability in large cities and the need for a finer resolution in smaller cities. During wintertime simulations in Santiago, some pollutants displayed large discrepancies with observations, especially for NO_2, O_3 and $PM_{2.5}$. In Bogotá, all models systematically underestimate CO and NO_2. The discrepancies in NO_2 had a corresponding impact in the overestimation of O_3. Most models overestimate SO_2 concentrations in all cities, except Bogotá, due to the high sulfur content in solid and liquid fuels attributed to the region.

Global and regional models provided different results. The SILAM model showed a better performance for NO_2 than CAMS. In Bogotá, SILAM presents low bias for ozone concentrations, while CAMS severely underestimated this pollutant. This underestimation was also observed in São Paulo and Santiago. Regional models that have been previously implemented in the cities showed lower bias, such as CHIMERE in Santiago for NO_2 and WRF-Chem in São Paulo for NO_2 and O_3. Global models show an overestimation of biomass burning emissions, which may explain the overprediction of $PM_{2.5}$ in São Paulo.

The ensemble median was evaluated on its potential to outperform individual models. offered a promising avenue for establishing a regional analysis and forecasting system.In certain periods and cities, the ensemble performed better than any individual model, for example, NO_2 and O_3 in Sao Paulo and Mexico City. In the latter, the ensemble also softened large overestimations of $PM_{2.5}$ by global models. However, While certain individual models outperformed the ensemble for specific pollutants and cities. , Before defining whether the ensemble is the correct approximation for a forecasting system, more research is necessary, for which a similar exercise of intercomparison of models is currently being carried out for a more recent year. This work only looked at two months (one in summer and one in winter), , a thorough analysis of one entire annual cycle with sufficient spin-up time should be conducted.the ensemble provides a useful tool to mitigate the extreme over or underestimation of certain models. In São Paulo, the ensemble median performed better than any model for NO_2. In México City, the creation of the ensemble softened large overestimations of $PM_{2.5}$ by global models. In Santiago in the summer, the median ensemble shows one of the lowest biases (MNBIAS) and errors (FGE, RMSE). In México City, the ensemble median for O_3 performed better than all individual models. In the summer in Santiago, the median ensemble outperformed individual models for CO.

This study aimed to assemble a multi-scale ensemble chain as a first step towards an Air Quality forecasting system for Latin America. Before such a prototype can be operative, a thorough analysis of one entire annual cycle with sufficient spin-up time should be conducted. This work only looked at two months (one in summer and one in winter). More AQ observations should also

Con formato: Subíndice

Con formato: Subíndice

~~be included for model calibration and evaluation. For 2015, only eight cities in LAC had data that complied with quality and completeness criteria. In recent years, more AQ networks have been implemented and data is more publicly available.~~

Data availability

All model data analyzed in the inter-comparison is archived at https://zenodo.org/records/13151018. The tool to create the plots, MOSPAT, can be found in GitHub at https://github.com/NeoMOSPAT/NeoMOSPAT_PAPILA.git ~~All raw data can be provided by the corresponding authors upon request.~~

Con formato: Fuente de párrafo predeter., Fuente: (Predeterminada) Calibri, 11 pto

Author contribution

JE and MO performed the formal analysis of the data; PL, NH, IB, JF, ~~SM,~~ LM, CM, MG, MS, RK, JP, AU, MG, AD, ~~and~~ DS performed the model simulations; JE, MO, PL, NH, and IB prepared the manuscript with contributions from all co-authors; GB and LG provided the financial support for the project leading to this publication; LD, NR, NH, MA coordinated research activities; CL provided technical support; all co-authors reviewed and edited the manuscript.

Competing interests

The authors declare that they have no conflict of interest.

Acknowledgments

The PAPILA (Prediction of Air Pollutants in Latin America) project was funded by the European Commission under the MSCA action for research and innovation staff exchange, Grant agreement ID: 777544. Support of Academy of Finland HEATCOST and ACCC flagship projects (grants Nbr 334798 and 337552), and H2020 project AQ-Watch (grant Nbr 870301) is acknowledged. Support from the German Climate Computer Center (Deutsches Klimarechenzentrum, DKRZ) is acknowledged. Support from the Center for Climate and Resilience Research (FONDAP/ANID 1523A0002) is acknowledged.~~The PAPILA (Prediction of Air Pollutants in Latin America) project was funded by the European Commission under the MSCA action for research and innovation staff exchange, Grant agreement ID: 777544. Support of Academy of Finland HEATCOST and ACCC flagship projects (grants Nbr 334798 and 337552), and H2020 project AQ-Watch (grant Nbr 870301) is acknowledged.~~

~~**Financial support**~~

~~This work was supported by the European Commission under the MSCA action for research and innovation staff exchange, Grant agreement ID: 777544. Support of Academy of Finland HEATCOST and ACCC flagship projects (grants Nbr 334798 and 337552), and H2020 project AQ-Watch (grant Nbr 870301) is acknowledged.~~

Con formato: Inglés (Estados Unidos)

References

Abou Rafee, S. A., Martins, L. D., Kawashima, A. B., Almeida, D. S., Morais, M. V. B., Souza, R. V. A., Oliveira, M. B. L., Souza, R. A. F., Medeiros, A. S. S., Urbina, V., Freitas, E. D., Martin, S. T., and Martins, J. A.: Contributions of mobile, stationary and biogenic sources to air pollution in the Amazon rainforest: a numerical study with the WRF-Chem model, Atmos. Chem. Phys., 17, 7977–7995, https://doi.org/10.5194/acp-17-7977-2017, 2017.

Álamos, N., Huneeus, N., Opazo, M., Osses, M., Puja, S., Pantoja, N., Denier van der Gon, H., Schueftan, A., Reyes, R., and Calvo, R.: High-resolution inventory of atmospheric emissions from transport, industrial, energy, mining and residential activities in Chile, Earth Syst. Sci. Data, 14, 361–379, https://doi.org/10.5194/essd-14-361-2022, 2022.

Albuquerque, T. T., West, J., de F. Andrade, M., Ynoue, R. Y., Andreão, W. L., dos Santos, F. S., Maciel, F. M., Pedruzzi, R., de O. Mateus, V., Martins, J. A., Martins, L. D., Nascimento, E. G. S., and Moreira, D. M.: Analysis of PM2.5 concentrations under pollutant emission control strategies in the metropolitan area of São Paulo, Brazil, Environmental Science and Pollution Research, 26, 33216–33227, https://doi.org/10.1007/s11356-019-06447-6, 2019.

Alfaro, S. C. and Gomes, L.: Modeling mineral aerosol production by wind erosion: Emission intensities and aerosol size distributions in source areas, Journal of Geophysical Research: Atmospheres, 106, 18075–18084, https://doi.org/https://doi.org/10.1029/2000JD900339, 2001.

Andersson, C., Bergström, R., Bennet, C., Robertson, L., Thomas, M., Korhonen, H., Lehtinen, K. E. J., and Kokkola, H.: MATCH-SALSA – Multi-scale Atmospheric Transport and CHemistry model coupled to the SALSA aerosol microphysics model – Part 1: Model description and evaluation, Geosci Model Dev, 8, 171–189, https://doi.org/10.5194/gmd-8-171-2015, 2015.

Andersson-Sköld, Y. and Simpson, D.: Comparison of the chemical schemes of the EMEP MSC-W and IVL photochemical trajectory models, Atmos Environ, 33, 1111–1129, https://doi.org/https://doi.org/10.1016/S1352-2310(98)00296-9, 1999.

Andrade, M. de F., Kumar, P., de Freitas, E. D., Ynoue, R. Y., Martins, J., Martins, L. D., Nogueira, T., Perez-Martinez, P., de Miranda, R. M., Albuquerque, T., Gonçalves, F. L. T., Oyama, B., and Zhang, Y.: Air quality in the megacity of São Paulo: Evolution over the last 30 years and future perspectives, Atmos Environ, 159, 66–82, https://doi.org/https://doi.org/10.1016/j.atmosenv.2017.03.051, 2017.

Con formato: Inglés (Estados Unidos)

Ballesteros-González, K., Sullivan, A. P., and Morales-Betancourt, R.: Estimating the air quality and health impacts of biomass burning in northern South America using a chemical transport model, Science of The Total Environment, 739, 139755, https://doi.org/https://doi.org/10.1016/j.scitotenv.2020.139755, 2020.

Ballesteros-González, K., Espitia-Cano, S. O., Rincón-Caro, M. A., Rincón-Riveros, J. M., Perez-Peña, M. P., Sullivan, A., and Morales Betancourt, R.: Understanding organic aerosols in Bogotá, Colombia: In-situ observations and regional-scale modeling, Atmos Environ, 284, 119161, https://doi.org/https://doi.org/10.1016/j.atmosenv.2022.119161, 2022.

Barrett, B. S. and Raga, G. B.: Variability of winter and summer surface ozone in Mexico City on the intraseasonal timescale, Atmos. Chem. Phys., 16, 15359–15370, https://doi.org/10.5194/acp-16-15359-2016, 2016.

Binkowski, F. S. and Shankar, U.: The Regional Particulate Matter Model: 1. Model description and preliminary results, Journal of Geophysical Research: Atmospheres, 100, 26191–26209, https://doi.org/https://doi.org/10.1029/95JD02093, 1995.

Blechschmidt, A.-M., Arteta, J., Coman, A., Curier, L., Eskes, H., Foret, G., Gielen, C., Hendrick, F., Marécal, V., Meleux, F., Parmentier, J., Peters, E., Pinardi, G., Piters, A. J. M., Plu, M., Richter, A., Segers, A., Sofiev, M., Valdebenito, Á. M., Van Roozendael, M., Vira, J., Vlemmix, T., and Burrows, J. P.: Comparison of tropospheric NO2 columns from MAX-DOAS retrievals and regional air quality model simulations, Atmos. Chem. Phys., 20, 2795–2823, https://doi.org/10.5194/acp-20-2795-2020, 2020.

Bouarar, I., Brasseur, G., Petersen, K., Granier, C., Fan, Q., Wang, X., Wang, L., Ji, D., Liu, Z., Xie, Y., Gao, W., and Elguindi, N.: Influence of anthropogenic emission inventories on simulations of air quality in China during winter and summer 2010, Atmos Environ, 198, 236–256, https://doi.org/https://doi.org/10.1016/j.atmosenv.2018.10.043, 2019.

Boylan, J. W. and Russell, A. G.: PM and light extinction model performance metrics, goals, and criteria for three-dimensional air quality models, Atmos Environ, 40, 4946–4959, https://doi.org/https://doi.org/10.1016/j.atmosenv.2005.09.087, 2006.

Brasseur, G. P., Xie, Y., Petersen, A. K., Bouarar, I., Flemming, J., Gauss, M., Jiang, F., Kouznetsov, R., Kranenburg, R., Mijling, B., Peuch, V.-H., Pommier, M., Segers, A., Sofiev, M., Timmermans, R., van der A, R., Walters, S., Xu, J., and Zhou, G.: Ensemble forecasts of air quality in eastern China – Part 1: Model description and implementation of the MarcoPolo–Panda prediction system, version 1, Geosci Model Dev, 12, 33–67, https://doi.org/10.5194/gmd-12-33-2019, 2019.

Buchholz, R. R., Emmons, L. K., Tilmes, S., and The CESM2 Development Team: CESM2.1/CAM-chem Instantaneous Output for Boundary Conditions, https://doi.org/10.5065/NMP7-EP60., 2019.

Busch, P., Cifuentes, L. A., and Cabrera, C.: Chronic exposure to fine particles (PM2.5) and mortality: Evidence from Chile, Environmental Epidemiology, 7, 2023.

Casallas, A., Castillo-Camacho, M. P., Sanchez, E. R., González, Y., Celis, N., Mendez-Espinosa, J. F., Belalcazar, L. C., and Ferro, C.: Surface, satellite ozone variations in Northern South America during low anthropogenic emission conditions: a machine learning approach, Air Qual Atmos Health, 16, 745–764, https://doi.org/10.1007/s11869-023-01303-6, 2023.

Casallas, A., Cabrera, A., Guevara-Luna, M.-A., Tompkins, A., González, Y., Aranda, J., Belalcazar, L. C., Mogollon-Sotelo, C., Celis, N., Lopez-Barrera, E., Peña-Rincon, C. A., and Ferro, C.: Air pollution analysis in Northwestern South America: A new Lagrangian framework, Science of The Total Environment, 906, 167350, https://doi.org/https://doi.org/10.1016/j.scitotenv.2023.167350, 2024.

Castesana, P., Diaz Resquin, M., Huneeus, N., Puliafito, E., Darras, S., Gómez, D., Granier, C., Osses Alvarado, M., Rojas, N., and Dawidowski, L.: PAPILA dataset: a regional emission inventory of reactive gases for South America based on the combination of local and global information, Earth Syst Sci Data, 14, 271–293, https://doi.org/10.5194/essd-14-271-2022, 2022.

Chin, M., Ginoux, P., Kinne, S., Torres, O., Holben, B. N., Duncan, B. N., Martin, R. V, Logan, J. A., Higurashi, A., and Nakajima, T.: Tropospheric Aerosol Optical Thickness from the GOCART Model and Comparisons with Satellite and Sun Photometer Measurements, J Atmos Sci, 59, 461–483, https://doi.org/https://doi.org/10.1175/1520-0469(2002)059<0461:TAOTFT>2.0.CO;2, 2002.

Colette, A., Collin, G., and Barré, J.: Update on European Regional Air Quality Forecast in the Copernicus Atmosphere Monitoring Service (CAMS), in: EGU General Assembly Conference Abstracts, 3487, https://doi.org/10.5194/egusphere-egu2020-3487, 2020.

Deroubaix, A. M., Hoelzemann, J. J., Ynoue, R., Bouarar, I., de Souza Fernandes Duarte, E., Elbern, H., Lichtig, P., Martins, L. D., do Rosário, N. M. É., Brasseur, G. P., rafaela Cruz Alves, de Arruda Moreira, G., phiipp franke, de Fatima Andrade, M., Lange, A. C., Andreao, W. L., rizzieri Pedruzzi, de Almeida Albuquerque, T. T., and Lugon, L.: Intercomparison of air quality models in a megacity: Towards an operational ensemble forecasting system for São Paulo, JGR Atmospheres, 129, 1–27, https://doi.org/https://doi.org/10.1029/2022JD038179, 2024.

Diaz Resquin, M., Santágata, D., Gallardo, L., Gómez, D., Rössler, C., and Dawidowski, L.: Local and remote black carbon sources in the Metropolitan Area of Buenos Aires, Atmos Environ, 182, 105–114, https://doi.org/https://doi.org/10.1016/j.atmosenv.2018.03.018, 2018.

East, J., Montealegre, J. S., Pachon, J. E., and Garcia-Menendez, F.: Air quality modeling to inform pollution mitigation strategies in a Latin American megacity, Science of The Total Environment, 776, 145894, https://doi.org/https://doi.org/10.1016/j.scitotenv.2021.145894, 2021.

ECCAD: Global Anthropogenic Emissions (CAMS-GLOB-ANT) for the Copernicus Atmosphere Monitoring Service Simulations of Air Quality Forecasts and Reanalyses, 2020.

ECCAD: Global Biogenic VOC emissions CAMS-GLOB-BIO v3.0 Snapshot, 2021.

Emery, C., Liu, Z., Russell, A. G., Odman, M. T., Yarwood, G., and Kumar, N.: Recommendations on statistics and benchmarks to assess photochemical model performance, J Air Waste Manage Assoc, 67, 582–598, https://doi.org/10.1080/10962247.2016.1265027, 2017.

Emmons, L. K., Walters, S., Hess, P. G., Lamarque, J.-F., Pfister, G. G., Fillmore, D., Granier, C., Guenther, A., Kinnison, D., Laepple, T., Orlando, J., Tie, X., Tyndall, G., Wiedinmyer, C., Baughcum, S. L., and Kloster, S.: Description and evaluation of the Model for Ozone and Related chemical Tracers, version 4 (MOZART-4), Geosci Model Dev, 3, 43–67, https://doi.org/10.5194/gmd-3-43-2010, 2010.

Fast, J. D., Gustafson Jr., W. I., Easter, R. C., Zaveri, R. A., Barnard, J. C., Chapman, E. G., Grell, G. A., and Peckham, S. E.: Evolution of ozone, particulates, and aerosol direct radiative forcing in the vicinity of Houston using a fully coupled meteorology-chemistry-aerosol model, Journal of Geophysical Research: Atmospheres, 111, https://doi.org/https://doi.org/10.1029/2005JD006721, 2006.

Flemming, J., Huijnen, V., Arteta, J., Bechtold, P., Beljaars, A., Blechschmidt, A.-M., Diamantakis, M., Engelen, R. J., Gaudel, A., Inness, A., Jones, L., Josse, B., Katragkou, E., Marecal, V., Peuch, V.-H., Richter, A., Schultz, M. G., Stein, O., and Tsikerdekis, A.: Tropospheric chemistry in the Integrated Forecasting System of ECMWF, Geosci Model Dev, 8, 975–1003, https://doi.org/10.5194/gmd-8-975-2015, 2015.

Flemming, J., Benedetti, A., Inness, A., Engelen, R. J., Jones, L., Huijnen, V., Remy, S., Parrington, M., Suttie, M., Bozzo, A., Peuch, V.-H., Akritidis, D., and Katragkou, E.: The CAMS interim Reanalysis of Carbon Monoxide, Ozone and Aerosol for 2003–2015, Atmos Chem Phys, 17, 1945–1983, https://doi.org/10.5194/acp-17-1945-2017, 2017.

de Foy, B., Krotkov, N. A., Bei, N., Herndon, S. C., Huey, L. G., Martínez, A.-P., Ruiz-Suárez, L. G., Wood, E. C., Zavala, M., and Molina, L. T.: Hit from both sides: tracking industrial and volcanic plumes in Mexico City with surface measurements and OMI SO_2 retrievals during the MILAGRO field campaign, Atmos. Chem. Phys., 9, 9599–9617, https://doi.org/10.5194/acp-9-9599-2009, 2009.

Franco, J. F., Gidhagen, L., Morales, R., and Behrentz, E.: Towards a better understanding of urban air quality management capabilities in Latin America, Environ Sci Policy, 102, 43–53, https://doi.org/https://doi.org/10.1016/j.envsci.2019.09.011, 2019.

Freitas, S. R., Longo, K. M., Alonso, M. F., Pirre, M., Marecal, V., Grell, G., Stockler, R., Mello, R. F., and Sánchez Gácita, M.: PREP-CHEM-SRC – 1.0: a preprocessor of trace gas and aerosol emission fields for regional and global atmospheric chemistry models, Geosci. Model Dev., 4, 419–433, https://doi.org/10.5194/gmd-4-419-2011, 2011.

Gallardo, L., Olivares, G., Langner, J., and Aarhus, B.: Coastal lows and sulfur air pollution in Central Chile, Atmos Environ, 36, 3829–3841, https://doi.org/https://doi.org/10.1016/S1352-2310(02)00285-6, 2002.

Gallardo, L., Escribano, J., Dawidowski, L., Rojas, N., de Fátima Andrade, M., and Osses, M.: Evaluation of vehicle emission inventories for carbon monoxide and nitrogen oxides for Bogotá, Buenos Aires, Santiago, and São Paulo, Atmos Environ, 47, 12–19, https://doi.org/https://doi.org/10.1016/j.atmosenv.2011.11.051, 2012.

Gassó, S. and Torres, O.: Temporal Characterization of Dust Activity in the Central Patagonia Desert (Years 1964–2017), Journal of Geophysical Research: Atmospheres, 124, 3417–3434, https://doi.org/https://doi.org/10.1029/2018JD030209, 2019.

Gavidia-Calderón, M., Schuch, D., Vara-Vela, A., Inoue, R., Freitas, E. D., Albuquerque, T. T. de A., Zhang, Y., Andrade, M. de F., and Bell, M. L.: Air quality modeling in the metropolitan area of São Paulo, Brazil: A review, Atmos Environ, 319, 120301, https://doi.org/https://doi.org/10.1016/j.atmosenv.2023.120301, 2024.

Gery, M. W., Whitten, G. Z., Killus, J. P., and Dodge, M. C.: A photochemical kinetics mechanism for urban and regional scale computer modeling, Journal of Geophysical Research: Atmospheres, 94, 12925–12956, https://doi.org/https://doi.org/10.1029/JD094iD10p12925, 1989.

Ginoux, P., Chin, M., Tegen, I., Prospero, J. M., Holben, B., Dubovik, O., and Lin, S.-J.: Sources and distributions of dust aerosols simulated with the GOCART model, Journal of Geophysical Research: Atmospheres, 106, 20255–20273, https://doi.org/https://doi.org/10.1029/2000JD000053, 2001.

González, C. M., Ynoue, R. Y., Vara-Vela, A., Rojas, N. Y., and Aristizábal, B. H.: High-resolution air quality modeling in a medium-sized city in the tropical Andes: Assessment of local and global emissions in understanding ozone and PM10 dynamics, Atmos Pollut Res, 9, 934–948, https://doi.org/10.1016/j.apr.2018.03.003, 2018.

Gouveia, N., Junger, W. L., Romieu, I., Cifuentes, L. A., de Leon, A. P., Vera, J., Strappa, V., Hurtado-Díaz, M., Miranda-Soberanis, V., Rojas-Bracho, L., Carbajal-Arroyo, L., and Tzintzun-Cervantes, G.: Effects of air pollution on infant and children respiratory mortality in four large Latin-American cities, Environmental Pollution, 232, 385–391, https://doi.org/https://doi.org/10.1016/j.envpol.2017.08.125, 2018.

Granier, C., Bessagnet, B., Bond, T., D'Angiola, A., Denier van der Gon, H., Frost, G. J., Heil, A., Kaiser, J. W., Kinne, S., Klimont, Z., Kloster, S., Lamarque, J.-F., Liousse, C., Masui, T., Meleux, F., Mieville, A., Ohara, T., Raut, J.-C., Riahi, K., Schultz, M. G., Smith, S. J., Thompson, A., van Aardenne, J., van der Werf, G. R., and van Vuuren, D. P.: Evolution of anthropogenic and biomass burning emissions of air pollutants at global and regional scales during the 1980–2010 period, Clim Change, 109, 163, https://doi.org/10.1007/s10584-011-0154-1, 2011.

Granier, C. , S. D. H. D. van der G. J. D. N. E. B. G. M. G. M. G. J.-P. J. J. K. C. L. B. Q. D. S. K. S.: The Copernicus Atmosphere Monitoring Service global and regional emissions, 2019.

Grell, G. A., Peckham, S. E., Schmitz, R., McKeen, S. A., Frost, G., Skamarock, W. C., and Eder, B.: Fully coupled "online" chemistry within the WRF model, Atmos Environ, 39, 6957–6975, https://doi.org/https://doi.org/10.1016/j.atmosenv.2005.04.027, 2005.

Grewe, V.: Technical Note: A diagnostic for ozone contributions of various NO_x emissions in multi-decadal chemistry-climate model simulations, Atmos. Chem. Phys., 4, 729–736, https://doi.org/10.5194/acp-4-729-2004, 2004.

Guenther, A., Karl, T., Harley, P., Wiedinmyer, C., Palmer, P. I., and Geron, C.: Estimates of global terrestrial isoprene emissions using MEGAN (Model of Emissions of Gases and Aerosols from Nature), Atmos Chem Phys, 6, 3181–3210, https://doi.org/10.5194/acp-6-3181-2006, 2006.

Hernandez, A. J., Morales-Rincon, L. A., Wu, D., Mallia, D., Lin, J. C., and Jimenez, R.: Transboundary transport of biomass burning aerosols and photochemical pollution in the Orinoco River Basin, Atmos Environ, 205, 1–8, https://doi.org/https://doi.org/10.1016/j.atmosenv.2019.01.051, 2019.

Huneeus, N., Gallardo, L., and Rutllant, J. A.: Offshore transport episodes of anthropogenic sulfur in northern Chile: Potential impact on the stratocumulus cloud deck, Geophys Res Lett, 33, https://doi.org/https://doi.org/10.1029/2006GL026921, 2006.

Huneeus, N., Denier van der Gon, H., Castesana, P., Menares, C., Granier, C., Granier, L., Alonso, M., de Fatima Andrade, M., Dawidowski, L., Gallardo, L., Gomez, D., Klimont, Z., Janssens-Maenhout, G., Osses, M., Puliafito, E., Rojas, N., Ccoyllo, O. S.-, Tolvett, S., and Ynoue, R. Y.: Evaluation of anthropogenic air pollutant emission inventories for South America at national and city scale, Atmos Environ, 117606, https://doi.org/https://doi.org/10.1016/j.atmosenv.2020.117606, 2020.

IDEAM: Primer inventario indicativo Nacional de emisiones de contaminantes criterio y carbono negro 2010-2014, Bogota, 93 pp., 2020.

Inness, A., Ades, M., Agustí-Panareda, A., Barré, J., Benedictow, A., Blechschmidt, A.-M., Dominguez, J. J., Engelen, R., Eskes, H., Flemming, J., Huijnen, V., Jones, L., Kipling, Z., Massart, S., Parrington, M., Peuch, V.-H., Razinger, M., Remy, S., Schulz, M., and Suttie, M.: The CAMS reanalysis of atmospheric composition, Atmos. Chem. Phys., 19, 3515–3556, https://doi.org/10.5194/acp-19-3515-2019, 2019.

Kaiser, J. W., Heil, A., Andreae, M. O., Benedetti, A., Chubarova, N., Jones, L., Morcrette, J.-J., Razinger, M., Schultz, M. G., Suttie, M., and van der Werf, G. R.: Biomass burning emissions estimated with a global fire assimilation system based on observed fire radiative power, Biogeosciences, 9, 527–554, https://doi.org/10.5194/bg-9-527-2012, 2012.

Kouznetsov, R. and Sofiev, M.: A methodology for evaluation of vertical dispersion and dry deposition of atmospheric aerosols, Journal of Geophysical Research: Atmospheres, 117, https://doi.org/https://doi.org/10.1029/2011JD016366, 2012.

Kramer, S. J. and Kirtman, B. P.: Saharan Dust Transport Predictability Utilizing a Subseasonal Experiment (SubX) Model, Journal of Geophysical Research: Atmospheres, 126, e2020JD033802, https://doi.org/https://doi.org/10.1029/2020JD033802, 2021.

Kukkonen, J., Olsson, T., Schultz, D. M., Baklanov, A., Klein, T., Miranda, A. I., Monteiro, A., Hirtl, M., Tarvainen, V., Boy, M., Peuch, V.-H., Poupkou, A., Kioutsioukis, I., Finardi, S., Sofiev, M., Sokhi, R., Lehtinen, K. E. J., Karatzas, K., San José, R., Astitha, M., Kallos, G., Schaap, M., Reimer, E., Jakobs, H., and Eben, K.: A review of operational, regional-scale, chemical weather forecasting models in Europe, Atmos. Chem. Phys., 12, 1–87, https://doi.org/10.5194/acp-12-1-2012, 2012.

de la Barrera, F., Barraza, F., Favier, P., Ruiz, V., and Quense, J.: Megafires in Chile 2017: Monitoring multiscale environmental impacts of burned ecosystems, Science of The Total Environment, 637–638, 1526–1536, https://doi.org/https://doi.org/10.1016/j.scitotenv.2018.05.119, 2018.

Con formato: Español (Colombia)

Con formato: Español (Colombia)

Lapere, R.: Modeling the Impacts of Future Emission Scenarios on Air Pollution in Santiago, Chile, Ecole Polytechnique, Santiago, 1–44 pp., 2018.

Lapere, R., Menut, L., Mailler, S., and Huneeus, N.: Seasonal variation in atmospheric pollutants transport in central Chile: dynamics and consequences, Atmos. Chem. Phys., 21, 6431–6454, https://doi.org/10.5194/acp-21-6431-2021, 2021.

Longo, K. M., Freitas, S. R., Pirre, M., Marécal, V., Rodrigues, L. F., Panetta, J., Alonso, M. F., Rosário, N. E., Moreira, D. S., Gácita, M. S., Arteta, J., Fonseca, R., Stockler, R., Katsurayama, D. M., Fazenda, A., and Bela, M.: The Chemistry CATT-BRAMS model (CCATT-BRAMS 4.5): a regional atmospheric model system for integrated air quality and weather forecasting and research, Geosci. Model Dev., 6, 1389–1405, https://doi.org/10.5194/gmd-6-1389-2013, 2013.

Mailler, S., Menut, L., Khvorostyanov, D., Valari, M., Couvidat, F., Siour, G., Turquety, S., Briant, R., Tuccella, P., Bessagnet, B., Colette, A., Létinois, L., Markakis, K., and Meleux, F.: CHIMERE-2017: from urban to hemispheric chemistry-transport modeling, Geosci. Model Dev., 10, 2397–2423, https://doi.org/10.5194/gmd-10-2397-2017, 2017.

Marécal, V., Peuch, V.-H., Andersson, C., Andersson, S., Arteta, J., Beekmann, M., Benedictow, A., Bergström, R., Bessagnet, B., Cansado, A., Chéroux, F., Colette, A., Coman, A., Curier, R. L., Denier van der Gon, H. A. C., Drouin, A., Elbern, H., Emili, E., Engelen, R. J., Eskes, H. J., Foret, G., Friese, E., Gauss, M., Giannaros, C., Guth, J., Joly, M., Jaumouillé, E., Josse, B., Kadygrov, N., Kaiser, J. W., Krajsek, K., Kuenen, J., Kumar, U., Liora, N., Lopez, E., Malherbe, L., Martinez, I., Melas, D., Meleux, F., Menut, L., Moinat, P., Morales, T., Parmentier, J., Piacentini, A., Plu, M., Poupkou, A., Queguiner, S., Robertson, L., Rouïl, L., Schaap, M., Segers, A., Sofiev, M., Tarasson, L., Thomas, M., Timmermans, R., Valdebenito, Á., van Velthoven, P., van Versendaal, R., Vira, J., and Ung, A.: A regional air quality forecasting system over Europe: the MACC-II daily ensemble production, Geosci. Model Dev., 8, 2777–2813, https://doi.org/10.5194/gmd-8-2777-2015, 2015.

Marlier, M. E., Bonilla, E. X., and Mickley, L. J.: How Do Brazilian Fires Affect Air Pollution and Public Health?, Geohealth, 4, e2020GH000331, https://doi.org/https://doi.org/10.1029/2020GH000331, 2020.

Martins, L. D., Vasconcellos, P. de C., Carvalho, L. R. F. de, and Andrade, M. de F.: Estimated impact of biogenic hydrocarbon emissions on photochemical oxidant formation en São Paulo during two periods of the winters of 1999-2000, Revista Brasileira de Meteorologia, 21, 190–200, 2006.

Mazzeo, A., Huneeus, N., Ordoñez, C., Orfanoz-Cheuquelaf, A., Menut, L., Mailler, S., Valari, M., Denier van der Gon, H., Gallardo, L., Muñoz, R., Donoso, R., Galleguillos, M., Osses, M., and Tolvett, S.: Impact of residential combustion and transport emissions on air pollution in Santiago during winter, Atmos Environ, 190, 195–208, https://doi.org/https://doi.org/10.1016/j.atmosenv.2018.06.043, 2018.

Mendez-Espinosa, J. F., Belalcazar, L. C., and Morales Betancourt, R.: Regional air quality impact of northern South America biomass burning emissions, Atmos Environ, 203, 131–140, https://doi.org/https://doi.org/10.1016/j.atmosenv.2019.01.042, 2019.

Mendez-Espinosa, J. F., Rojas, N. Y., Vargas, J., Pachón, J. E., Belalcazar, L. C., and Ramírez, O.: Air quality variations in Northern South America during the COVID-19 lockdown, Science of The Total Environment, 141621, https://doi.org/https://doi.org/10.1016/j.scitotenv.2020.141621, 2020.

Menut, L., Bessagnet, B., Khvorostyanov, D., Beekmann, M., Blond, N., Colette, A., Coll, I., Curci, G., Foret, G., Hodzic, A., Mailler, S., Meleux, F., Monge, J.-L., Pison, I., Siour, G., Turquety, S., Valari, M., Vautard, R., and Vivanco, M. G.: CHIMERE 2013: a model for regional atmospheric composition modelling, Geosci. Model Dev., 6, 981–1028, https://doi.org/10.5194/gmd-6-981-2013, 2013.

Menut, L., Bessagnet, B., Mailler, S., Pennel, R., and Siour, G.: Impact of Lightning NOx Emissions on Atmospheric Composition and Meteorology in Africa and Europe, Atmosphere (Basel), 11, https://doi.org/10.3390/atmos11101128, 2020.

Menut, L., Bessagnet, B., Briant, R., Cholakian, A., Couvidat, F., Mailler, S., Pennel, R., Siour, G., Tuccella, P., Turquety, S., and Valari, M.: The CHIMERE v2020r1 online chemistry-transport model, Geosci Model Dev, 14, 6781–6811, https://doi.org/10.5194/gmd-14-6781-2021, 2021.

METEO-FRANCE: CAMS Regional air quality production systems, 1–81 pp., 2020.

Molina, L. T., Gallardo, L., Andrade, M., Baumgardner, D., Borbor-Córdova, M., Bórquez, R., Casassa, G., Cereceda-Balic, F., Dawidowski, L., Garreaud, R., Huneeus, N., Lambert, F., McCarty, J. L., Mc Phee, J., Mena-Carrasco, M., Raga, G. B., Schmitt, C., and Schwarz, J. P.: Pollution and its Impacts on the South American Cryosphere, Earths Future, 3, 345–369, https://doi.org/https://doi.org/10.1002/2015EF000311, 2015.

Monahan, E. C.: The Ocean as a Source for Atmospheric Particles, in: The Role of Air-Sea Exchange in Geochemical Cycling, edited by: Buat-Ménard, P., Springer Netherlands, Dordrecht, 129–163, https://doi.org/10.1007/978-94-009-4738-2_6, 1986.

Morcrette, J.-J., Boucher, O., Jones, L., Salmond, D., Bechtold, P., Beljaars, A., Benedetti, A., Bonet, A., Kaiser, J. W., Razinger, M., Schulz, M., Serrar, S., Simmons, A. J., Sofiev, M., Suttie, M., Tompkins, A. M., and Untch, A.: Aerosol analysis and forecast in the European Centre for Medium-Range Weather Forecasts Integrated Forecast System: Forward modeling, Journal of Geophysical Research: Atmospheres, 114, https://doi.org/https://doi.org/10.1029/2008JD011235, 2009.

Nascimento, J. P., Barbosa, H. M. J., Banducci, A. L., Rizzo, L. V, Vara-Vela, A. L., Meller, B. B., Gomes, H., Cezar, A., Franco, M. A., Ponczek, M., Wolff, S., Bela, M. M., and Artaxo, P.: Major Regional-Scale Production of O3 and Secondary Organic Aerosol in Remote Amazon Regions from the Dynamics and Photochemistry of Urban and Forest Emissions, Environ Sci Technol, 56, 9924–9935, https://doi.org/10.1021/acs.est.2c01358, 2022.

Nedbor-Gross, R., Henderson, B. H., Davis, J. R., Pachón, J. E., Rincón, A., Guerrero, O. J., and Grajales, F.: Comparing Standard to Feature-Based Meteorological Model Evaluation Techniques in Bogotá, Colombia, J Appl Meteorol Climatol, https://doi.org/10.1175/jamc-d-16-0058.1, 2017.

Nedbor-Gross, R., Henderson, B., Perez-Peña, M., and Pachon, J. E.: Air quality modeling in Bogotá, Colombia using local emissions and natural mitigation factor adjustment for re-suspended particulate matter, Atmos Pollut Res, 9, 95–104, https://doi.org/http://dx.doi.org/10.1016/j.apr.2017.07.004, 2018.

Osses, M., Rojas, N., Ibarra, C., Valdebenito, V., Laengle, I., Pantoja, N., Osses, D., Basoa, K., Tolvett, S., Huneeus, N., Gallardo, L., and Gómez, B.: High-resolution spatial-distribution maps of road transport exhaust emissions in Chile, 1990--2020, Earth Syst Sci Data, 14, 1359–1376, https://doi.org/10.5194/essd-14-1359-2022, 2022.

Pachón, J. E., Galvis, B., Lombana, O., Carmona, L. G., Fajardo, S., Rincón, A., Meneses, S., Chaparro, R., Nedbor-Gross, R., and Henderson, B.: Development and evaluation of a comprehensive atmospheric emission inventory for air quality modeling in the megacity of Bogotá, Atmosphere (Basel), 9, https://doi.org/10.3390/atmos9020049, 2018.

Pereira, G., Shimabukuro, Y. E., Moraes, E. C., Freitas, S. R., Cardozo, F. S., and Longo, K. M.: Monitoring the transport of biomass burning emission in South America, Atmos Pollut Res, 2, 247–254, https://doi.org/https://doi.org/10.5094/APR.2011.031, 2011.

Pérez-Peña, M. P., Henderson, B. H., Nedbor-Gross, R., and Pachón, J. E.: Natural mitigation factor adjustment for re-suspended particulate matter emissions inventory for Bogotá, Colombia, Atmos Pollut Res, 8, https://doi.org/10.1016/j.apr.2016.07.006, 2017.

Petersen, A. K., Brasseur, G. P., Bouarar, I., Flemming, J., Gauss, M., Jiang, F., Kouznetsov, R., Kranenburg, R., Mijling, B., Peuch, V.-H., Pommier, M., Segers, A., Sofiev, M., Timmermans, R., van der A, R., Walters, S., Xie, Y., Xu, J., and Zhou, G.: Ensemble forecasts of air quality in eastern China – Part 2: Evaluation of the MarcoPolo–Panda prediction system, version 1, Geosci Model Dev, 12, 1241–1266, https://doi.org/10.5194/gmd-12-1241-2019, 2019.

Puliafito, S. E., Allende, D., Pinto, S., and Castesana, P.: High resolution inventory of GHG emissions of the road transport sector in Argentina, Atmos Environ, 101, 303–311, https://doi.org/https://doi.org/10.1016/j.atmosenv.2014.11.040, 2015.

Puliafito, S. E., Allende, D. G., Castesana, P. S., and Ruggeri, M. F.: High-resolution atmospheric emission inventory of the argentine energy sector. Comparison with edgar global emission database, Heliyon, 3, e00489, https://doi.org/https://doi.org/10.1016/j.heliyon.2017.e00489, 2017.

Ramírez, O., Sánchez de la Campa, A. M., Amato, F., Catacolí, R. A., Rojas, N. Y., and de la Rosa, J.: Chemical composition and source apportionment of PM10 at an urban background site in a high–altitude Latin American megacity (Bogota, Colombia), Environmental Pollution, 233, 142–155, https://doi.org/https://doi.org/10.1016/j.envpol.2017.10.045, 2018.

Ramírez-Romero, C., Jaramillo, A., Córdoba, M. F., Raga, G. B., Miranda, J., Alvarez-Ospina, H., Rosas, D., Amador, T., Kim, J. S., Yakobi-Hancock, J., Baumgardner, D., and Ladino, L. A.: African dust particles over the western Caribbean – Part I: Impact on air quality over the Yucatán Peninsula, Atmos. Chem. Phys., 21, 239–253, https://doi.org/10.5194/acp-21-239-2021, 2021.

Reboredo, B., Arasa, R., and Codina, B.: Evaluating Sensitivity to Different Options and Parameterizations of a Coupled Air Quality Modelling System over Bogotá, Colombia. Part I: WRF Model Configuration, Open Journal of Air Pollution, 4, 47–64, https://doi.org/10.4236/ojap.2015.42006., 2015.

Rodríguez-Villamizar, A. L., Rojas-Roa, Y. N., Blanco-Becerra, C. L., Herrera-Galindo, M. V., and Fernández-Niño, A. J.: Short-Term Effects of Air Pollution on Respiratory and Circulatory Morbidity in Colombia 2011–2014: A Multi-City, Time-Series Analysis, https://doi.org/10.3390/ijerph15081610, 2018.

Rojas, N. Y., Mangones, S. C., Osses, M., Granier, C., Laengle, I., Alfonso A., J. V, and Mendez, J. A.: Road transport exhaust emissions in Colombia. 1990–2020 trends and spatial disaggregation, Transp Res D Transp Environ, 121, 103780, https://doi.org/https://doi.org/10.1016/j.trd.2023.103780, 2023.

Romieu, I., Gouveia, N., Cifuentes, L., De Leon, A., Junger, W., Vera, J., Strappa, V., Hurtado-Díaz, M., and Miranda-Soberanis, V Rojas-Bracho L , Carbajal-Arroyo L, T.-C. G.: Multicity study of air pollution and mortality in Latin America (the ESCALA study), Washington D.C., 2012.

Saide, P. E., Mena-Carrasco, M., Tolvett, S., Hernandez, P., and Carmichael, G. R.: Air quality forecasting for winter-time PM2.5 episodes occurring in multiple cities in central and southern Chile, Journal of Geophysical Research: Atmospheres, 121, 558–575, https://doi.org/https://doi.org/10.1002/2015JD023949, 2016.

Sarricolea, P., Serrano-Notivoli, R., Fuentealba, M., Hernández-Mora, M., de la Barrera, F., Smith, P., and Meseguer-Ruiz, Ó.: Recent wildfires in Central Chile: Detecting links between burned areas and population exposure in the wildland urban interface, Science of The Total Environment, 706, 135894, https://doi.org/https://doi.org/10.1016/j.scitotenv.2019.135894, 2020.

SDA -Secretaria Distrital de Ambiente: Inventario de emisiones de Bogotá, Contaminantes atmosféricos año 2018, Bogota, 1–75 pp., 2018.

Seguel, R. J., Gallardo, L., Fleming, Z. L., and Landeros, S.: Two decades of ozone standard exceedances in Santiago de Chile, Air Qual Atmos Health, 13, 593–605, https://doi.org/10.1007/s11869-020-00822-w, 2020.

Seguel, R. J., Castillo, L., Opazo, C., Rojas, N. Y., Nogueira, T., Cazorla, M., Gavidia-Calderón, M., Gallardo, L., Garreaud, R., Carrasco-Escaff, T., and Elshorbany, Y.: Changes in South American surface ozone trends: exploring the influences of precursors and extreme events, Atmos. Chem. Phys., 24, 8225–8242, https://doi.org/10.5194/acp-24-8225-2024, 2024.

SEMARNAT and INECC: Calidad del Aire en la Cuenca Atmosférica de Tula, Mexico City, 1–27 pp., 2020.

Silva-Quiroz, R., Rivera, A. L., Ordoñez, P., Gay-Garcia, C., and Frank, A.: Atmospheric blockages as trigger of environmental contingencies in Mexico City, Heliyon, 5, e02099, https://doi.org/https://doi.org/10.1016/j.heliyon.2019.e02099, 2019.

Simpson, D., Benedictow, A., Berge, H., Bergström, R., Emberson, L. D., Fagerli, H., Flechard, C. R., Hayman, G. D., Gauss, M., Jonson, J. E., Jenkin, M. E., Nyíri, A., Richter, C., Semeena, V. S., Tsyro, S., Tuovinen, J.-P., Valdebenito, Á., and Wind, P.: The EMEP MSC-W chemical transport model – technical description, Atmos. Chem. Phys., 12, 7825–7865, https://doi.org/10.5194/acp-12-7825-2012, 2012.

Con formato: Español (Colombia)

Con formato: Español (Colombia)

Soares, J. and Sofiev, M.: A Global Wildfire Emission and Atmospheric Composition: Refinement of the Integrated System for Wild-Land Fires IS4FIRES, in: Air Pollution Modeling and its Application XXIII, 253–258, 2014.

Sofiev, M.: Extended resistance analogy for construction of the vertical diffusion scheme for dispersion models, Journal of Geophysical Research: Atmospheres, 107, ACH 10-1-ACH 10-8, https://doi.org/https://doi.org/10.1029/2001JD001233, 2002.

Sofiev, M., Siljamo, P., Valkama, I., Ilvonen, M., and Kukkonen, J.: A dispersion modelling system SILAM and its evaluation against ETEX data, Atmos Environ, 40, 674–685, https://doi.org/https://doi.org/10.1016/j.atmosenv.2005.09.069, 2006.

Sofiev, M., Vankevich, R., Lotjonen, M., Prank, M., Petukhov, V., Ermakova, T., Koskinen, J., and Kukkonen, J.: An operational system for the assimilation of the satellite information on wild-land fires for the needs of air quality modelling and forecasting, Atmos. Chem. Phys., 9, 6833–6847, https://doi.org/10.5194/acp-9-6833-2009, 2009.

Sofiev, M., Genikhovich, E., Keronen, P., and Vesala, T.: Diagnosing the Surface Layer Parameters for Dispersion Models within the Meteorological-to-Dispersion Modeling Interface, J Appl Meteorol Climatol, 49, 221–233, https://doi.org/https://doi.org/10.1175/2009JAMC2210.1, 2010.

Sofiev, M., Vira, J., Kouznetsov, R., Prank, M., Soares, J., and Genikhovich, E.: Construction of the SILAM Eulerian atmospheric dispersion model based on the advection algorithm of Michael Galperin, Geosci Model Dev, 8, 3497–3522, https://doi.org/10.5194/gmd-8-3497-2015, 2015.

United Nations: The World's Cities in 2018—Data Booklet , 1–34 pp., 2018.

Wiedinmyer, C., Akagi, S. K., Yokelson, R. J., Emmons, L. K., Al-Saadi, J. A., Orlando, J. J., and Soja, A. J.: The Fire INventory from NCAR (FINN): a high resolution global model to estimate the emissions from open burning, Geosci. Model Dev., 4, 625–641, https://doi.org/10.5194/gmd-4-625-2011, 2011.

WMO: Global Air Quality Forecasting and Information System (GAFIS), Geneva, 2022.

Worden, H. M., Bloom, A. A., Worden, J. R., Jiang, Z., Marais, E. A., Stavrakou, T., Gaubert, B., and Lacey, F.: New constraints on biogenic emissions using satellite-based estimates of carbon monoxide fluxes, Atmos. Chem. Phys., 19, 13569–13579, https://doi.org/10.5194/acp-19-13569-2019, 2019.

Zaveri, R. A. and Peters, L. K.: A new lumped structure photochemical mechanism for large-scale applications, Journal of Geophysical Research: Atmospheres, 104, 30387–30415, https://doi.org/https://doi.org/10.1029/1999JD900876, 1999.

Zeng, G., Williams, J. E., Fisher, J. A., Emmons, L. K., Jones, N. B., Morgenstern, O., Robinson, J., Smale, D., Paton-Walsh, C., and Griffith, D. W. T.: Multi-model simulation of CO and HCHO in the Southern Hemisphere: comparison with observations and impact of biogenic emissions, Atmos. Chem. Phys., 15, 7217–7245, https://doi.org/10.5194/acp-15-7217-2015, 2015.

Zhai, H., Huang, L., Emery, C., Zhang, X., Wang, Y., Yarwood, G., Fu, J. S., and Li, L.: Recommendations on benchmarks for photochemical air quality model applications in China — NO2, SO2, CO and PM10, Atmos Environ, 319, 120290, https://doi.org/https://doi.org/10.1016/j.atmosenv.2023.120290, 2024.

Zhang, D., Martin, R. V, Bindle, L., Li, C., Eastham, S. D., van Donkelaar, A., and Gallardo, L.: Advances in Simulating the Global Spatial Heterogeneity of Air Quality and Source Sector Contributions: Insights into the Global South, Environ Sci Technol, 57, 6955–6964, https://doi.org/10.1021/acs.est.2c07253, 2023.

Zhang, Y., Bocquet, M., Mallet, V., Seigneur, C., and Baklanov, A.: Real-time air quality forecasting, part I: History, techniques, and current status, Atmos Environ, 60, 632–655, https://doi.org/https://doi.org/10.1016/j.atmosenv.2012.06.031, 2012.

Zimmerman, P. R., Greenberg, J. P., and Westberg, C. E.: Measurements of atmospheric hydrocarbons and biogenic emission fluxes in the Amazon Boundary layer, Journal of Geophysical Research: Atmospheres, 93, 1407–1416, https://doi.org/https://doi.org/10.1029/JD093iD02p01407, 1988.

Appendix A. Evaluation scores

Table A1. Metrics used for model evaluation.

Metric Obs - Model	**Formula for each city, model and month**
Model/Observations ratio	$ratio = \frac{\underline{m}}{\underline{o}} = \frac{\frac{1}{N}\sum_d \; m_d}{\frac{1}{N}\sum_d \; o_d}$
Mean Bias	$BIAS = \frac{1}{N}\sum_d \; (m_d - o_d)$
Modified normalized Bias	$MNBIAS = \frac{2}{N}\sum_d \; \frac{(m_d - o_d)}{(m_d + o_d)}$
Fractional gross error	$FGE = \frac{2}{N}\sum_d \; \left\lvert\frac{m_d - o_d}{m_d + o_d}\right\rvert$
Root mean square error	$RMSE = \sqrt{\frac{1}{N}\sum_d \; (m_d - o_d)^2}$
Correlation coefficient	$R = \frac{1}{N}\frac{\sum_d \; (m_d - \underline{m})(o_d - \underline{o})}{\sigma_m \sigma_o}$
Coefficient of Variation	$CV = \frac{\sigma_m \underline{m}}{\sigma_m \underline{m}}$ or $CV = \frac{\sigma_o \underline{o}}{\sigma_o \underline{o}}$
Metric	**Formula for each pixel and day**
Median of Models (Ensemble)	$MED = Median(\{ m_i \;\; \lvert i \in N, \quad 1 \leq i \leq 6\})$
Metric	**Formula for each pixel**
Median Absolute Deviation	$MAD = Median(\{\lvert m_{i,d} - MED_d \rvert\})$ $i \in N, 1 \leq i \leq 6 \quad and \quad d \in N, 1 \leq d \leq 31$
Metric	**Formula for each city, day and model**
Observation	$\boldsymbol{o_d} = \sum_{i,j} \; g_{A_{i,j}} M_{i,j} \; con \; \sum_{i,j} \; g_{A_{i,j}} = 1$ $i,j \in N \mid representing\ a\ specific\ pixel$ $g_{A_{i,j}} \; represents\ how\ much\ the \in N, 1 \leq d \leq 31$

m_d and o_d the modeled value and the observation value for each day. $\underline{m}$ is the mean of the models for each month and $\underline{o}$ of the observations of each city. σ_m is the standard deviation of each model. N is the number of model-observation pairs available for each month.

Tabla con formato

Table A2. NO_2 model evaluation scores (January / July)

		ENSEMBLE		Mean		CAMS		MPI		EMEP		CHIM		SILAM		USP	
NO_2	City	Jan	Jul	Jan	Jul	Jan	Jul	Jan	Jul	Jan	Jul	Jan	Jul	Jan	Jul	Jan	Jul
Model/Observations	Santiago	0.55	0.38	0.61	0.48	0.33	0.67	0.54	0.33	0.61	0.53	0.88	0.37	0.82	0.86	0.54	0.10
	Bogotá	0.37	0.34	0.38	0.37	0.24	0.13	0.39	0.41	0.52	0.49	0.30	0.21	0.42	0.36	0.39	0.53
	México	0.92	0.84	1.03	1.00	0.78	0.44	0.99	0.95	1.25	1.80	1.44	1.29	0.78	0.71		
	São Paulo	0.96	0.88	1.03	0.92	0.13	0.33	1.39	1.39	1.53	1.17	1.65	1.16	0.96	0.78	0.63	0.76
MNBIAS [%]	Santiago	−55.2	−87.8	−44.5	−66.6	−100	−44.0	−58.0	−97.4	−44.4	−57.8	−8.6	−98.1	−16.2	−14.5	−56.3	−161
	Bogotá	−91.2	−97.3	−87.5	−91.9	−120	−155	−85.7	−82.2	−63.3	−67.2	−102	−129	−78.9	−92.6	−90.0	−61.5
	México	−8.0	−17.3	3.2	1.4	−34.3	−84.6	0.5	−3.7	21.5	55.0	37.7	19.7	−27.0	−36.4		
	São Paulo	−4.3	−9.9	3.0	−4.9	−159	−112	31.2	33.2	40.4	18.3	48.9	21.1	−9.1	−25.6	−52.9	−31.2
RMSE [ppb]	Santiago	5.58	25.37	4.85	21.64	7.79	16.35	5.85	27.44	5.06	20.94	2.41	28.14	2.83	11.22	5.56	35.08
	Bogotá	11.78	10.04	11.50	9.67	14.31	13.06	11.32	9.04	9.19	7.98	12.07	11.83	10.90	9.71	11.39	7.55
	México	4.91	5.64	5.38	3.94	10.24	15.27	4.62	5.19	10.52	20.92	18.38	8.81	7.64	8.13		
	São Paulo	4.59	6.54	4.65	5.99	16.16	16.20	8.63	12.66	10.60	9.92	13.41	11.09	4.86	7.92	9.17	10.65
FGE	Santiago	0.55	0.88	0.44	0.67	1.01	0.45	0.59	0.97	0.46	0.61	0.18	0.98	0.23	0.24	0.57	1.61
	Bogotá	0.91	0.97	0.88	0.92	1.20	1.56	0.86	0.82	0.63	0.67	1.02	1.29	0.79	0.93	0.90	0.62
	México	0.16	0.20	0.15	0.13	0.42	0.85	0.13	0.17	0.22	0.55	0.39	0.28	0.30	0.37		
	São Paulo	0.24	0.24	0.23	0.22	1.60	1.14	0.34	0.38	0.42	0.34	0.52	0.36	0.29	0.35	0.61	0.50
R	Santiago	0.52	0.54	0.56	0.65	0.62	0.46	0.25	−0.01	0.11	0.12	0.50	0.36	0.51	0.47	0.39	0.63
	Bogotá	0.72	0.37	0.73	0.38	−0.12	0.52	0.74	0.41	0.66	0.20	0.23	0.11	0.54	0.42	0.62	0.19
	México	0.77	0.71	0.74	0.70	0.55	0.35	0.71	0.42	0.68	0.36	0.65	−0.20	0.78	0.77		
	São Paulo	0.68	0.49	0.66	0.55	0.34	0.43	0.60	0.60	0.56	0.33	0.58	−0.13	0.74	0.62	0.36	0.19

		ENSEMBLE		Mean		CAMS		MPI		EMEP		CHIM		SILAM		USP	
NO_2	City	Jan	Jul	Jan	Jul	Jan	Jul	Jan	Jul	Jan	Jul	Jan	Jul	Jan	Jul	Jan	Jul
Model/Observations	Santiago	0.81	0.44	0.89	0.58	0.31	0.63	0.78	0.39	1.06	0.75	0.94	0.27	1.60	1.26	0.63	0.10
	Bogotá	0.40	0.34	0.42	0.38	0.24	0.13	0.48	0.49	0.68	0.60	0.26	0.18	0.37	0.22	0.42	0.59
	México	1.04	0.97	1.15	1.18	0.78	0.44	1.11	1.06	1.46	2.21	1.57	1.44	0.87	0.85		
	São Paulo	1.18	1.06	1.24	1.11	0.14	0.37	1.69	1.72	2.04	1.61	1.72	1.28	1.20	0.92	0.71	0.83
MNBIAS [%]	Santiago	−18.8	−73.5	−9.7	−47.9	−106	−46.7	−22.6	−83.3	7.2	−24.5	−2.2	−118	47.0	24.6	−44.6	−160
	Bogotá	−85.8	−97.8	−81.6	−88.7	−121	−156	−68.7	−67.0	−39.2	−49.6	−111	−138	−92.1	−128	−84.5	−52.2
	México	1.7	−2.9	12.0	17.0	−35.0	−83.7	10.4	7.3	35.5	74.0	44.0	30.8	−18.2	−20.3		
	São Paulo	17.7	6.8	22.8	10.8	−157	−107	51.2	51.1	69.1	44.3	54.0	28.3	14.1	−14.7	−40.6	−24.2
RMSE [ppb]	Santiago	3.11	23.64	2.45	18.36	8.23	17.17	3.58	25.67	3.07	14.65	2.27	32.10	7.53	15.15	4.88	35.30
	Bogotá	11.22	10.16	10.89	9.55	14.41	13.22	9.73	7.98	6.60	6.63	12.85	12.44	11.83	11.92	10.81	6.92
	México	5.06	3.97	7.13	5.81	10.26	14.93	5.22	5.23	15.87	31.52	21.45	12.25	6.48	6.01		
	São Paulo	5.90	7.03	6.59	6.94	15.92	16.31	13.74	19.38	19.57	18.07	15.56	12.38	7.70	8.82	8.70	10.81
FGE	Santiago	0.24	0.74	0.18	0.48	1.06	0.48	0.27	0.84	0.21	0.36	0.16	1.19	0.47	0.30	0.46	1.60
	Bogotá	0.86	0.98	0.82	0.89	1.22	1.56	0.69	0.67	0.39	0.50	1.12	1.39	0.92	1.28	0.84	0.52
	México	0.14	0.13	0.18	0.19	0.43	0.84	0.14	0.17	0.36	0.74	0.45	0.36	0.24	0.26		
	São Paulo	0.24	0.23	0.26	0.24	1.58	1.09	0.51	0.52	0.69	0.47	0.56	0.41	0.29	0.34	0.56	0.45
R	Santiago	0.57	0.26	0.64	0.53	0.65	0.44	0.32	0.02	0.08	0.11	0.55	0.24	0.51	0.52	0.44	0.57
	Bogotá	0.74	0.25	0.76	0.31	−0.12	0.44	0.74	0.34	0.66	0.15	0.14	0.15	0.56	0.43	0.65	0.17
	México	0.80	0.73	0.78	0.73	0.58	0.40	0.80	0.48	0.69	0.52	0.68	−0.21	0.81	0.80		
	São Paulo	0.63	0.49	0.62	0.60	0.36	0.47	0.54	0.62	0.48	0.52	0.49	−0.20	0.67	0.64	0.29	0.18

*ENSEMBLE: ~~Median: ensemble~~ based on the median value of the models; MEAN: arithmetic mean of the models; CAMS: Copernicus Atmosphere Monitoring Service's (CAMS); MPI: WRF-Chem executed by MPIM; EMEP: European Monitoring and Evaluation Programme; CHIM: CHIMERE transport model; SILAM: System for Integrated modeling of Atmospheric composition; USP: WRF-Chem executed by University of São Paulo.

Table A3. O_3 model evaluation scores (January / July)

		ENSEMBLE		Mean		CAMS		MPI		EMEP		CHIM		SILAM		USP	
O_3	City	Jan	Jul	Jan	Jul	Jan	Jul	Jan	Jul	Jan	Jul	Jan	Jul	Jan	Jul	Jan	Jul
Model/Observations	Santiago	1.13	4.84	1.12	5.07	0.33	4.76	1.62	6.96	1.79	8.04	0.96	4.58	1.30	5.21	0.67	0.72
	Bogotá	1.38	1.36	1.52	1.38	0.34	0.34	2.56	1.74	2.68	2.74	1.51	1.37	1.03	0.72	0.94	1.36
	México	1.20	1.09	1.27	1.28	0.53	0.31	1.69	1.73	2.09	2.58	1.16	0.77	0.86	0.88		
	São Paulo	1.46	1.14	1.52	1.28	0.29	0.67	2.77	2.00	2.13	2.00	1.31	0.67	1.41	1.05	1.14	0.89
MNBIAS [%]	Santiago	10.3	133	10.0	136	−101	132	43.4	151	55.5	155	−5.0	137	23.1	121	−42.6	−19.2
	Bogotá	33.4	31.5	42.3	33.2	−96.0	−95.4	86.0	52.7	89.8	91.8	41.9	30.6	4.9	−32.8	−11.6	29.6
	México	21.8	8.7	26.8	25.0	−56.2	−103	52.9	52.5	68.2	86.8	14.6	−30.6	−11.2	−13.6		
	São Paulo	32.8	12.9	38.3	25.9	−106	−35.2	86.9	64.6	67.7	68.2	32.0	−36.3	22.9	−11.7	−0.8	−12.5
RMSE [ppb]	Santiago	3.73	15.52	3.40	16.24	15.10	15.27	14.85	23.21	17.41	28.14	2.85	14.62	8.05	18.95	9.03	2.56
	Bogotá	5.48	5.26	7.48	5.44	8.95	7.81	20.85	9.47	21.36	19.91	7.14	5.42	2.49	4.91	6.16	5.97
	México	10.57	9.94	12.05	12.96	12.83	22.25	19.56	26.13	31.91	52.61	11.37	13.24	10.17	9.97		
	São Paulo	14.69	7.43	15.70	8.11	19.42	7.52	45.58	17.33	28.80	16.97	15.52	9.11	15.24	11.14	13.28	6.41
FGE	Santiago	0.13	1.35	0.12	1.37	1.01	1.33	0.43	1.52	0.56	1.56	0.11	1.37	0.23	1.34	0.44	0.52
	Bogotá	0.34	0.34	0.43	0.35	0.96	0.95	0.86	0.53	0.90	0.92	0.42	0.38	0.17	0.44	0.41	0.36
	México	0.33	0.25	0.35	0.30	0.57	1.04	0.53	0.55	0.69	0.87	0.31	0.43	0.36	0.28		
	São Paulo	0.44	0.42	0.46	0.42	1.09	0.53	0.89	0.67	0.68	0.70	0.47	0.61	0.45	0.58	0.56	0.42
R	Santiago	0.64	−0.23	0.70	−0.15	0.42	−0.38	0.72	−0.22	0.63	−0.30	0.69	0.31	0.59	0.08	−0.14	−0.06
	Bogotá	0.39	−0.27	−0.01	−0.49	0.03	−0.11	−0.02	−0.27	−0.13	−0.27	0.60	−0.10	0.59	−0.31	−0.46	−0.30
	México	0.07	−0.08	0.09	−0.02	0.20	−0.01	0.34	0.08	0.07	−0.01	0.00	−0.26	−0.28	0.03		
	São Paulo	0.48	0.24	0.47	0.27	0.10	0.00	0.40	0.36	0.45	0.24	0.07	−0.28	0.55	0.23	0.24	0.30

		ENSEMBLE		Mean		CAMS		MPI		EMEP		CHIM		SILAM		USP	
O_3	City	Jan	Jul	Jan	Jul	Jan	Jul	Jan	Jul	Jan	Jul	Jan	Jul	Jan	Jul	Jan	Jul
Model/Observations	Santiago	1.21	4.51	1.19	4.95	0.32	5.01	1.67	6.78	1.75	6.12	1.06	5.72	1.60	5.76	0.69	0.74
	Bogotá	1.24	1.20	1.35	1.22	0.34	0.35	2.36	1.57	2.27	2.30	1.54	1.38	0.82	0.45	0.78	1.29
	México	1.12	1.05	1.19	1.23	0.54	0.31	1.58	1.70	1.76	2.33	1.12	0.68	0.87	0.93		
	São Paulo	1.39	0.97	1.44	1.11	0.29	0.72	2.65	1.71	1.84	1.67	1.30	0.58	1.34	0.90	1.13	0.89
MNBIAS [%]	Santiago	18.8	127	16.8	133	−104	133	47.7	149	54.2	142	6.1	147	44.0	118	−38.0	−20.8
	Bogotá	23.5	19.9	31.4	21.3	−95.2	−94.0	79.7	43.8	77.7	78.0	43.6	32.3	−18.7	−73.9	−25.9	24.8
	México	12.6	4.1	17.5	20.0	−56.1	−102	45.3	50.2	49.3	77.0	9.1	−42.1	−12.4	−10.3		
	São Paulo	30.0	−3.4	35.1	11.0	−104	−29.6	86.4	46.8	56.8	45.6	32.3	−50.8	19.6	−30.3	4.5	−13.0
RMSE [ppb]	Santiago	5.62	13.44	4.84	14.88	15.29	15.17	16.39	21.13	17.01	19.66	3.23	17.76	14.85	20.92	8.52	2.55
	Bogotá	4.08	4.05	5.63	4.08	8.84	7.70	18.57	8.12	16.87	15.43	7.53	5.63	3.16	6.77	6.28	5.69
	México	9.62	9.38	10.78	11.45	12.62	21.93	16.81	24.96	24.98	44.77	11.24	14.21	10.60	10.19		
	São Paulo	13.90	7.06	14.58	7.45	19.00	7.30	43.50	14.24	24.62	16.06	16.30	9.90	14.31	10.84	12.89	6.24
FGE	Santiago	0.19	1.30	0.17	1.34	1.04	1.34	0.48	1.49	0.54	1.42	0.11	1.48	0.44	1.32	0.40	0.51
	Bogotá	0.25	0.27	0.33	0.28	0.95	0.94	0.80	0.45	0.78	0.78	0.44	0.40	0.22	0.74	0.46	0.34
	México	0.31	0.23	0.34	0.27	0.57	1.02	0.45	0.53	0.56	0.77	0.31	0.50	0.39	0.29		
	São Paulo	0.43	0.41	0.43	0.39	1.06	0.50	0.88	0.58	0.57	0.52	0.49	0.71	0.47	0.65	0.52	0.43
R	Santiago	0.68	−0.22	0.76	−0.06	0.42	−0.40	0.76	−0.20	0.59	−0.19	0.74	0.33	0.64	0.17	−0.20	−0.06
	Bogotá	0.42	−0.19	0.05	−0.36	0.15	−0.12	0.02	−0.29	−0.16	−0.12	0.56	−0.13	0.69	−0.09	−0.53	−0.23
	México	0.07	0.02	0.09	0.09	0.26	−0.00	0.32	0.14	0.08	0.13	0.04	−0.19	−0.26	0.11		
	São Paulo	0.52	0.16	0.48	0.18	0.16	−0.01	0.40	0.29	0.39	0.13	0.08	−0.33	0.61	0.16	0.26	0.28

*ENSEMBLE: based on the median value of the models; MEAN: arithmetic mean of the models; CAMS: Copernicus Atmosphere Monitoring Service's (CAMS); MPI: WRF-Chem executed by MPIM; EMEP: European Monitoring and Evaluation Programme; CHIM: CHIMERE transport model; SILAM: System for Integrated modeling of Atmospheric composition; USP: WRF-Chem executed by University of São Paulo.

~~*Median: ensemble based on the median value of the models; CAMS: Copernicus Atmosphere Monitoring Service's (CAMS); MPI: WRF-Chem executed by MPIM; EMEP: European Monitoring and Evaluation Programme; CHIM: CHIMERE transport model; SILAM: System for Integrated modeling of Atmospheric composition; USP: WRF-Chem executed by University of São Paulo.~~

Table A4. CO model evaluation scores (January / July)

		ENSEMBLE		Mean		CAMS		MPI		EMEP		CHIM		SILAM		USP	
CO	City	Jan	Jul	Jan	Jul	Jan	Jul	Jan	Jul	Jan	Jul	Jan	Jul	Jan	Jul	Jan	Jul
Model/Observations	Santiago	1.03	0.54	1.26	0.82	1.11	1.06	0.92	0.36	1.32	0.74	1.83	0.47	2.01	2.07	0.49	0.13
	Bogotá	0.38	0.41	0.41	0.45	0.39	0.33	0.41	0.49	0.50	0.56	0.34	0.26	0.60	0.63	0.19	0.36
	México	0.98	1.06	1.23	1.40	0.60	0.48	0.84	0.94	1.82	2.92	2.09	1.76	0.99	1.15		
	São Paulo	0.76	0.67	0.78	0.72	0.43	0.45	0.99	0.90	0.97	0.76	0.91	0.74	1.08	1.03	0.33	0.40
MNBIAS [%]	Santiago	3.6	−55.2	23.1	−15.4	7.2	4.0	−9.4	−88.7	26.9	−26.8	58.6	−80.1	66.4	69.0	−67.9	−150
	Bogotá	−86.0	−81.5	−80.8	−74.2	−83.3	−99.2	−80.2	−66.7	−63.6	−54.2	−93.6	−114	−47.4	−45.5	−134	−94.4
	México	−5.3	5.4	16.3	33.7	−51.6	−71.1	−18.5	−5.7	53.2	94.4	59.6	46.0	−6.9	10.7		
	São Paulo	−29.5	−37.7	−26.3	−31.8	−83.1	−76.3	−3.1	−10.8	−6.0	−26.5	−10.7	−23.8	1.7	−2.8	−102	−84.1
RMSE [ppm]	Santiago	0.03	0.60	0.07	0.36	0.07	0.34	0.05	0.79	0.09	0.48	0.21	0.74	0.26	1.24	0.12	1.03
	Bogotá	0.46	0.36	0.44	0.34	0.46	0.41	0.44	0.32	0.37	0.27	0.47	0.45	0.33	0.24	0.58	0.40
	México	0.12	0.09	0.28	0.28	0.35	0.39	0.19	0.16	0.80	1.34	1.10	0.50	0.15	0.18		
	São Paulo	0.20	0.32	0.20	0.30	0.38	0.45	0.15	0.24	0.19	0.31	0.21	0.33	0.21	0.32	0.45	0.52
FGE	Santiago	0.10	0.60	0.23	0.32	0.19	0.24	0.19	0.90	0.27	0.43	0.59	0.80	0.66	0.69	0.68	1.50
	Bogotá	0.86	0.82	0.81	0.74	0.83	0.99	0.80	0.67	0.64	0.54	0.94	1.14	0.47	0.46	1.34	0.94
	México	0.12	0.12	0.19	0.34	0.52	0.71	0.22	0.17	0.53	0.94	0.60	0.46	0.17	0.18		
	São Paulo	0.33	0.41	0.31	0.37	0.83	0.77	0.19	0.27	0.25	0.38	0.27	0.36	0.26	0.37	1.02	0.84
R	Santiago	0.28	0.52	0.25	0.53	0.56	0.47	0.06	0.30	0.01	0.07	0.24	0.15	−0.09	0.30	0.49	0.19
	Bogotá	0.75	0.33	0.78	0.37	0.01	0.31	0.78	0.40	0.68	0.26	0.49	0.15	0.59	0.37	0.66	0.14
	México	0.85	0.83	0.74	0.79	0.79	0.63	0.71	0.46	0.58	0.51	0.76	−0.05	0.86	0.78		
	São Paulo	0.59	0.56	0.58	0.55	0.60	0.63	0.56	0.56	0.42	0.41	0.49	0.00	0.63	0.53	0.13	0.20

		ENSEMBLE		Mean		CAMS		MPI		EMEP		CHIM		SILAM		USP	
CO	City	Jan	Jul	Jan	Jul	Jan	Jul	Jan	Jul	Jan	Jul	Jan	Jul	Jan	Jul	Jan	Jul
Model/Observations	Santiago	1.31	0.55	1.62	0.98	1.05	0.97	1.14	0.38	1.86	0.89	1.70	0.32	3.47	2.94	0.54	0.12
	Bogotá	0.36	0.41	0.40	0.45	0.38	0.33	0.42	0.52	0.52	0.60	0.31	0.25	0.51	0.50	0.21	0.40
	México	1.14	1.18	1.45	1.61	0.60	0.48	0.94	1.01	2.28	3.48	2.40	1.99	1.16	1.28		
	São Paulo	0.87	0.80	0.89	0.85	0.42	0.48	1.11	1.08	1.23	1.08	0.94	0.81	1.26	1.19	0.36	0.44
MNBIAS [%]	Santiago	26.5	−51.4	47.6	3.4	2.2	−0.8	12.6	−81.4	59.4	−6.1	52.4	−108	109	98.5	−60.3	−151
	Bogotá	−90.0	−83.3	−83.1	−76.1	−84.8	−99.9	−78.0	−62.8	−60.2	−49.6	−99.7	−118	−63.0	−68.3	−130	−87.3
	México	10.4	17.8	32.6	48.2	−49.8	−69.0	−5.8	3.9	73.9	108	72.3	59.0	9.8	21.6		
	São Paulo	−15.0	−22.8	−12.7	−17.2	−84.7	−73.3	10.4	6.1	18.9	1.8	−8.1	−15.3	17.2	8.9	−94.2	−76.2
RMSE [ppm]	Santiago	0.08	0.64	0.15	0.38	0.06	0.40	0.05	0.80	0.22	0.40	0.18	0.96	0.61	2.38	0.11	1.08
	Bogotá	0.47	0.38	0.45	0.36	0.47	0.43	0.43	0.31	0.37	0.27	0.49	0.48	0.39	0.33	0.58	0.39
	México	0.18	0.15	0.45	0.43	0.34	0.38	0.14	0.16	1.20	1.77	1.40	0.67	0.23	0.26		
	São Paulo	0.17	0.27	0.17	0.26	0.39	0.44	0.18	0.28	0.27	0.38	0.25	0.29	0.31	0.43	0.43	0.50
FGE	Santiago	0.26	0.59	0.48	0.30	0.18	0.27	0.15	0.85	0.59	0.32	0.52	1.08	1.09	0.98	0.60	1.52
	Bogotá	0.90	0.83	0.83	0.76	0.85	1.00	0.78	0.63	0.60	0.50	1.00	1.19	0.63	0.69	1.31	0.87
	México	0.16	0.19	0.34	0.48	0.50	0.69	0.16	0.19	0.74	1.09	0.72	0.59	0.21	0.24		
	São Paulo	0.26	0.32	0.24	0.31	0.85	0.74	0.23	0.30	0.28	0.36	0.27	0.30	0.30	0.41	0.94	0.76
R	Santiago	0.36	0.20	0.22	0.28	0.54	0.38	0.17	0.32	−0.04	0.21	0.30	−0.00	−0.16	0.24	0.50	0.02
	Bogotá	0.72	0.27	0.71	0.28	0.07	0.18	0.77	0.36	0.60	0.32	0.42	0.22	0.29	0.19	0.67	0.11
	México	0.85	0.87	0.73	0.85	0.78	0.68	0.75	0.49	0.59	0.65	0.74	−0.04	0.85	0.82		
	São Paulo	0.50	0.48	0.49	0.48	0.57	0.62	0.46	0.44	0.31	0.37	0.36	0.07	0.54	0.45	0.09	0.15

*ENSEMBLE: based on the median value of the models; MEAN: arithmetic mean of the models; CAMS: Copernicus Atmosphere Monitoring Service's (CAMS); MPI: WRF-Chem executed by MPIM; EMEP: European Monitoring and Evaluation Programme; CHIM: CHIMERE transport model; SILAM: System for Integrated modeling of Atmospheric composition; USP: WRF-Chem executed by University of São Paulo.

~~*Median: ensemble based on the median value of the models; CAMS: Copernicus Atmosphere Monitoring Service's (CAMS); MPI: WRF-Chem executed by MPIM; EMEP: European Monitoring and Evaluation Programme; CHIM: CHIMERE transport model; SILAM: System for Integrated modeling of Atmospheric composition; USP: WRF-Chem executed by University of São Paulo.~~

Table A5. SO_2 model evaluation scores (January / July)

		ENSEMBLE		Mean		CAMS		MPI		EMEP		CHIM		SILAM		USP	
SO_2	City	Jan	Jul	Jan	Jul	Jan	Jul	Jan	Jul	Jan	Jul	Jan	Jul	Jan	Jul	Jan	Jul
Model/Observations	Santiago	1.81	3.62	3.69	4.72	12.89	9.92	3.93	6.36	0.99	1.88	1.31	3.51	2.52	6.22	0.01	0.01
	Bogotá	0.77	0.68	0.79	0.70	0.72	0.58	1.30	1.23	1.27	1.00	0.41	0.38	0.92	0.88	0.00	0.00
	México	2.92	4.08	11.08	11.14	42.79	38.47	5.07	6.15	1.74	2.49	1.44	1.78	2.46	3.56		
	São Paulo	5.16	4.72	6.66	6.39	2.97	5.18	17.02	16.89	6.37	4.42	4.34	4.34	8.75	6.55	0.01	0.01
MNBIAS [%]	Santiago	56.3	112	113	129	170	162	114	143	−1.8	58.3	24.2	107	84.5	138	−197	−197
	Bogotá	−23.4	−33.0	−22.3	−30.0	−28.0	−47.8	25.8	25.0	21.1	3.9	−80.0	−81.3	−6.8	−7.2	−199	−199
	México	98.6	119	165	166	190	189	134	142	62.2	86.0	44.2	57.1	85.6	108		
	São Paulo	133	130	146	144	94.7	133	176	175	141	123	123	125	156	143	−197	−194
RMSE [ppb]	Santiago	1.28	4.62	3.97	6.53	17.46	15.76	4.56	9.61	0.30	1.72	0.74	4.38	2.32	10.00	1.47	1.78
	Bogotá	0.65	0.68	0.67	0.65	0.69	0.85	0.85	0.60	1.01	0.48	1.11	0.86	0.53	0.58	1.80	1.70
	México	10.16	9.82	48.69	31.49	198.74	116.27	19.96	16.11	4.88	4.76	3.98	2.72	8.02	8.48		
	São Paulo	4.03	4.99	5.49	7.31	1.92	5.80	15.55	21.96	5.28	4.93	3.26	4.96	7.63	7.88	1.02	1.30
FGE	Santiago	0.56	1.12	1.14	1.29	1.71	1.63	1.14	1.44	0.16	0.58	0.31	1.07	0.84	1.38	1.97	1.97
	Bogotá	0.33	0.35	0.35	0.32	0.33	0.50	0.32	0.31	0.37	0.21	0.80	0.81	0.27	0.21	1.99	1.99
	México	1.01	1.19	1.65	1.66	1.91	1.90	1.35	1.43	0.70	0.86	0.64	0.57	0.89	1.09		
	São Paulo	1.33	1.30	1.46	1.45	0.95	1.33	1.77	1.76	1.41	1.23	1.23	1.25	1.57	1.44	1.98	1.95
R	Santiago	−0.22	0.02	−0.19	0.21	−0.06	0.59	−0.32	0.16	−0.07	0.13	−0.45	0.22	−0.13	−0.24	0.12	0.49
	Bogotá	0.21	0.71	0.11	0.71	0.06	0.47	0.04	0.57	−0.02	0.55	0.32	0.39	0.28	0.20	0.11	0.47
	México	0.26	0.02	0.10	−0.04	0.08	−0.13	0.29	−0.14	0.24	0.11	0.19	0.06	0.14	−0.09		
	São Paulo	0.46	0.50	0.55	0.54	0.34	0.53	0.59	0.49	0.35	0.30	0.58	−0.02	0.53	0.47	0.28	0.11

		ENSEMBLE		Mean		CAMS		MPI		EMEP		CHIM		SILAM		USP	
SO_2	City	Jan	Jul	Jan	Jul	Jan	Jul	Jan	Jul	Jan	Jul	Jan	Jul	Jan	Jul	Jan	Jul
Model/Observations	Santiago	3.38	4.82	4.69	5.82	11.64	8.99	6.87	8.52	1.59	2.09	1.93	3.65	5.55	10.93	0.01	0.01
	Bogotá	0.58	0.50	0.64	0.56	0.52	0.40	1.17	1.10	1.13	0.98	0.36	0.20	0.56	0.50	0.00	0.00
	México	3.53	4.85	12.43	12.46	46.93	42.11	5.83	6.92	2.12	3.02	1.65	1.98	3.12	4.44		
	São Paulo	6.27	5.69	8.13	8.01	3.08	5.73	21.01	22.41	7.46	5.68	4.70	4.64	11.57	8.43	0.01	0.01
MNBIAS [%]	Santiago	107	130	129	140	168	159	147	157	45.4	69.3	61.2	109	138	162	−196	−197
	Bogotá	−50.2	−63.5	−42.4	−53.3	−58.8	−79.9	16.0	12.9	7.2	0.4	−89.2	−127	−55.8	−62.0	−199	−199
	México	111	131	169	170	191	190	141	149	76.2	101	57.0	69.8	102	124		
	São Paulo	144	139	156	153	101	136	181	181	151	134	129	128	167	154	−196	−193
RMSE [ppb]	Santiago	3.58	7.05	5.46	8.76	15.67	14.51	8.79	13.64	0.94	2.11	1.53	4.85	6.79	19.21	1.46	1.82
	Bogotá	0.87	0.93	0.83	0.84	0.96	1.09	0.75	0.49	0.97	0.48	1.15	1.15	0.93	0.95	1.79	1.70
	México	12.44	12.10	52.40	35.18	207.29	125.97	22.42	18.35	6.08	6.33	4.62	3.39	10.63	11.19		
	São Paulo	5.26	6.17	7.04	9.28	2.11	6.34	19.66	28.76	6.49	6.66	3.71	5.16	10.68	10.32	1.01	1.33
FGE	Santiago	1.08	1.30	1.29	1.41	1.68	1.60	1.48	1.58	0.45	0.69	0.61	1.09	1.38	1.62	1.96	1.97
	Bogotá	0.52	0.64	0.49	0.53	0.59	0.80	0.31	0.24	0.38	0.21	0.89	1.28	0.60	0.62	1.99	1.99
	México	1.14	1.31	1.69	1.70	1.91	1.91	1.42	1.49	0.82	1.01	0.73	0.70	1.06	1.24		
	São Paulo	1.44	1.39	1.56	1.54	1.01	1.37	1.82	1.81	1.52	1.34	1.30	1.29	1.67	1.54	1.97	1.94
R	Santiago	−0.09	−0.17	−0.13	0.02	0.00	0.54	−0.23	0.16	−0.26	0.00	−0.43	0.25	−0.06	−0.20	0.29	0.37
	Bogotá	0.24	0.70	0.07	0.68	0.03	0.42	−0.01	0.55	−0.01	0.52	0.37	0.37	0.17	0.44	0.10	0.48
	México	0.24	0.18	0.17	0.16	0.10	−0.03	0.20	−0.04	0.19	0.21	0.14	0.04	0.11	0.04		
	São Paulo	0.36	0.50	0.55	0.54	0.39	0.54	0.61	0.47	0.30	0.36	0.57	−0.06	0.56	0.46	0.11	0.05

*ENSEMBLE: based on the median value of the models; MEAN: arithmetic mean of the models; CAMS: Copernicus Atmosphere Monitoring Service's (CAMS); MPI: WRF-Chem executed by MPIM; EMEP: European Monitoring and Evaluation Programme; CHIM: CHIMERE transport model; SILAM: System for Integrated modeling of Atmospheric composition; USP: WRF-Chem executed by University of São Paulo.

~~*Median: ensemble based on the median value of the models; CAMS: Copernicus Atmosphere Monitoring Service's (CAMS); MPI: WRF-Chem executed by MPIM; EMEP: European Monitoring and Evaluation Programme; CHIM: CHIMERE transport model; SILAM: System for Integrated modeling of Atmospheric composition; USP: WRF-Chem executed by University of São Paulo.~~

Table A6. $PM_{2.5}$ model evaluation scores (January / July)

		ENSEMBLE		Mean		CAMS		MPI		EMEP		CHIM		SILAM		USP	
$PM_{2.5}$	City	Jan	Jul	Jan	Jul	Jan	Jul	Jan	Jul	Jan	Jul	Jan	Jul	Jan	Jul	Jan	Jul
Model/Observations	Santiago	0.50	0.38	0.63	1.15	1.21	1.83	0.60	0.36	0.14	0.29	0.55	0.22	0.96	3.79	0.30	0.12
	Bogotá	0.48	0.57	0.62	0.76	1.36	1.55	0.86	1.09	0.17	0.18	0.31	0.37	0.76	0.87	0.19	0.36
	México	0.84	1.22	1.51	1.87	4.16	4.91	0.66	1.20	0.13	0.15	0.52	0.65	1.85	2.06		
	São Paulo	1.78	1.62	2.13	1.94	1.64	2.22	2.16	1.84	1.44	1.10	2.37	1.99	4.41	3.63	0.76	0.83
MNBIAS [%]	Santiago	−65.7	−82.2	−44.1	17.8	18.3	58.7	−49.5	−87.1	−150	−103	−52.5	−128	−4.6	114	−105	−152
	Bogotá	−68.4	−54.6	−40.9	−26.8	35.8	41.4	−11.8	2.2	−139	−139	−96.7	−88.9	−24.1	−16.4	−134	−95.6
	México	−23.5	17.2	41.2	59.7	122	130	−35.1	17.6	−153	−147	−62.7	−44.1	48.1	60.8		
	São Paulo	56.7	53.6	70.8	66.8	44.9	79.0	74.8	64.0	31.4	12.1	84.2	73.9	114	96.7	−32.3	−11.2
RMSE $[\mu g/m^2]$	Santiago	10.69	39.84	8.26	18.31	6.68	46.91	9.22	40.96	17.68	44.27	8.72	49.58	6.48	160.50	14.46	53.10
	Bogotá	11.06	6.25	8.67	4.17	9.68	8.69	6.66	7.23	16.64	11.27	12.91	8.49	6.42	3.12	16.41	9.01
	México	7.12	8.71	13.77	19.17	80.13	84.48	10.06	7.99	23.03	18.92	11.56	10.38	25.96	27.52		
	São Paulo	14.68	16.64	20.80	24.48	13.05	30.84	20.43	22.09	11.48	11.19	26.31	29.61	66.31	82.01	9.86	10.01
FGE	Santiago	0.66	0.92	0.44	0.29	0.24	0.59	0.50	0.97	1.50	1.06	0.52	1.29	0.24	1.14	1.06	1.52
	Bogotá	0.68	0.55	0.42	0.30	0.40	0.41	0.30	0.40	1.39	1.40	0.97	0.89	0.26	0.22	1.34	0.96
	México	0.30	0.27	0.41	0.60	1.22	1.31	0.39	0.28	1.53	1.48	0.63	0.46	0.60	0.63		
	São Paulo	0.57	0.56	0.71	0.68	0.48	0.81	0.75	0.66	0.46	0.46	0.84	0.80	1.14	0.99	0.52	0.44
R	Santiago	0.51	0.05	0.58	0.42	0.56	0.52	0.20	0.02	0.24	0.28	0.39	0.07	0.10	0.30	0.32	0.36
	Bogotá	0.72	0.33	0.73	0.17	0.34	0.18	0.41	−0.42	0.80	0.40	0.51	0.12	0.71	0.63	0.60	0.18
	México	0.85	0.32	0.88	0.61	0.69	0.57	0.82	0.05	0.80	0.11	0.75	−0.22	0.85	0.59		
	São Paulo	0.52	0.57	0.54	0.61	0.46	0.47	0.48	0.52	0.34	0.44	0.48	−0.16	0.53	0.62	0.20	0.24

		ENSEMBLE		Mean		CAMS		MPI		EMEP		CHIM		SILAM		USP	
$PM_{2.5}$	City	Jan	Jul	Jan	Jul	Jan	Jul	Jan	Jul	Jan	Jul	Jan	Jul	Jan	Jul	Jan	Jul
Model/Observations	Santiago	0.61	0.40	0.78	1.45	1.15	1.74	0.66	0.39	0.20	0.34	0.62	0.17	1.66	5.55	0.34	0.10
	Bogotá	0.34	0.42	0.55	0.67	1.34	1.54	0.85	1.09	0.18	0.20	0.26	0.34	0.42	0.39	0.19	0.37
	México	1.02	1.38	1.72	2.06	4.35	5.06	0.79	1.30	0.18	0.20	0.62	0.70	2.38	2.56		
	São Paulo	1.90	1.88	2.23	2.14	1.60	2.46	2.33	2.23	1.79	1.54	2.33	2.11	4.44	3.63	0.79	0.90
MNBIAS [%]	Santiago	−46.9	−75.3	−23.1	41.4	14.0	57.5	−40.3	−78.9	−129	−89.5	−40.0	−144	48.0	138	−97.9	−156
	Bogotá	−95.8	−81.4	−53.2	−38.3	32.9	41.0	−15.0	1.8	−139	−133	−109	−95.8	−79.9	−90.8	−135	−93.6
	México	−5.0	29.8	53.4	69.5	125	133	−18.0	26.9	−138	−130	−46.6	−34.8	69.6	79.1		
	São Paulo	66.0	61.5	77.7	71.2	48.5	82.6	83.5	75.3	58.2	35.0	85.7	76.2	117	92.4	−23.4	−7.4
RMSE $[\mu g/m^2]$	Santiago	8.61	38.52	5.92	31.44	5.47	46.62	8.22	39.07	16.27	41.00	7.48	53.00	16.82	269.80	13.80	53.60
	Bogotá	13.64	8.02	9.98	5.17	9.25	8.64	6.84	7.28	16.60	10.97	13.77	8.83	12.42	8.50	16.47	8.87
	México	7.72	12.00	18.45	23.41	83.04	87.94	7.63	9.43	21.60	17.48	9.59	9.89	39.20	39.23		
	São Paulo	16.90	20.90	23.07	27.26	12.99	32.92	23.86	28.83	16.68	19.52	26.71	28.98	69.79	78.88	10.30	10.15
FGE	Santiago	0.47	0.87	0.25	0.42	0.20	0.57	0.41	0.90	1.30	0.94	0.40	1.44	0.48	1.38	0.98	1.57
	Bogotá	0.96	0.81	0.53	0.41	0.38	0.41	0.32	0.42	1.40	1.34	1.09	0.96	0.80	0.91	1.35	0.94
	México	0.23	0.36	0.53	0.70	1.25	1.34	0.28	0.34	1.39	1.31	0.47	0.43	0.79	0.80		
	São Paulo	0.66	0.63	0.78	0.72	0.50	0.84	0.84	0.76	0.65	0.55	0.86	0.80	1.17	0.94	0.51	0.40
R	Santiago	0.50	−0.15	0.43	0.42	0.60	0.51	0.20	0.05	0.13	0.25	0.26	0.00	0.02	0.37	0.21	0.33
	Bogotá	0.67	0.47	0.69	0.05	0.30	0.17	0.41	−0.42	0.77	0.38	0.44	0.37	0.43	0.43	0.61	0.16
	México	0.83	0.35	0.89	0.66	0.69	0.62	0.84	0.11	0.74	0.32	0.75	−0.19	0.83	0.63		
	São Paulo	0.53	0.59	0.54	0.63	0.51	0.56	0.45	0.49	0.37	0.50	0.45	−0.11	0.53	0.63	0.08	0.22

*ENSEMBLE: based on the median value of the models; MEAN: arithmetic mean of the models; CAMS: Copernicus Atmosphere Monitoring Service's (CAMS); MPI: WRF-Chem executed by MPIM; EMEP: European Monitoring and Evaluation Programme; CHIM: CHIMERE transport model; SILAM: System for Integrated modeling of Atmospheric composition; USP: WRF-Chem executed by University of São Paulo.

~~*Median: ensemble based on the median value of the models; CAMS: Copernicus Atmosphere Monitoring Service's (CAMS); MPI: WRF-Chem executed by MPIM; EMEP: European Monitoring and Evaluation Programme; CHIM: CHIMERE transport model; SILAM: System for Integrated modeling of Atmospheric composition; USP: WRF-Chem executed by University of São Paulo.~~

Table A7. PM_{10} model evaluation scores (January / July)

		ENSEMBLE		Mean		CAMS		MPI		EMEP		CHIM		SILAM		USP	
PM_{10}	City	Jan	Jul	Jan	Jul	Jan	Jul	Jan	Jul	Jan	Jul	Jan	Jul	Jan	Jul	Jan	Jul
Model/Observations	Santiago	0.25	0.34	0.32	0.88	0.60	1.51	0.29	0.23	0.21	0.37	0.23	0.17	0.47	2.69	0.11	0.07
	Bogotá	0.28	0.31	0.37	0.45	0.76	0.83	0.59	0.83	0.20	0.18	0.14	0.18	0.39	0.44	0.08	0.14
	México	0.52	0.83	1.01	1.25	2.79	3.19	0.38	0.88	0.36	0.44	0.26	0.34	1.08	1.10		
	São Paulo	1.38	1.34	1.71	1.64	1.32	1.87	1.45	1.34	1.72	1.37	1.55	1.55	3.70	3.10	0.43	0.50
MNBIAS [%]	Santiago	−119	−89.6	−101	−7.7	−49.0	42.6	−108	−116	−128	−87.2	−121	−143	−70.8	90.5	−159	−170
	Bogotá	−110	−104	−88.8	−74.2	−22.7	−18.3	−50.2	−27.4	−133	−138	−145	−137	−85.7	−77.8	−170	−149
	México	−68.5	−19.0	0.4	22.6	93.7	103	−85.1	−13.6	−96.3	−76.6	−117	−94.1	−2.3	4.1		
	São Paulo	31.1	32.6	49.6	48.7	22.0	60.9	36.0	30.0	44.8	23.5	44.3	48.9	104	87.6	−82.6	−62.0
RMSE $[\mu g/m^2]$	Santiago	43.56	72.44	39.53	33.12	24.59	54.51	41.34	81.91	45.50	70.55	42.96	92.60	32.16	166.82	50.95	95.38
	Bogotá	35.53	24.67	31.77	20.45	16.16	10.52	23.31	18.52	39.47	29.35	39.99	28.69	30.82	20.45	45.32	30.52
	México	26.65	12.02	10.84	15.73	98.60	104.79	34.17	13.64	34.21	27.20	36.93	29.98	18.30	19.14		
	São Paulo	15.21	19.11	23.97	30.66	15.34	38.42	19.56	24.10	26.44	32.33	23.00	32.13	90.06	105.60	20.61	20.91
FGE	Santiago	1.19	0.95	1.01	0.33	0.49	0.46	1.09	1.22	1.29	0.89	1.22	1.43	0.71	0.90	1.60	1.70
	Bogotá	1.10	1.04	0.89	0.74	0.30	0.27	0.54	0.52	1.34	1.38	1.46	1.38	0.86	0.78	1.70	1.49
	México	0.68	0.26	0.19	0.26	0.94	1.03	0.85	0.29	0.96	0.77	1.17	0.94	0.31	0.29		
	São Paulo	0.34	0.42	0.50	0.53	0.34	0.64	0.44	0.47	0.50	0.54	0.47	0.56	1.04	0.90	0.83	0.70
R	Santiago	0.36	−0.12	0.41	0.42	0.41	0.51	0.20	−0.35	0.04	0.13	0.15	0.14	0.07	0.38	0.13	0.45
	Bogotá	0.75	0.40	0.70	0.06	0.39	0.20	0.31	−0.17	0.74	0.14	0.52	0.28	0.66	0.43	0.66	0.02
	México	0.65	0.53	0.72	0.44	0.55	0.20	0.30	0.23	0.60	0.15	0.61	−0.23	0.73	0.42		
	São Paulo	0.48	0.46	0.54	0.54	0.39	0.48	0.10	0.14	0.38	0.37	0.46	−0.05	0.56	0.55	0.20	0.21

		ENSEMBLE		Mean		CAMS		MPI		EMEP		CHIM		SILAM		USP	
PM_{10}	City	Jan	Jul	Jan	Jul	Jan	Jul	Jan	Jul	Jan	Jul	Jan	Jul	Jan	Jul	Jan	Jul
Model/Observations	Santiago	0.31	0.35	0.41	1.08	0.57	1.43	0.31	0.24	0.29	0.39	0.27	0.13	0.88	3.89	0.12	0.06
	Bogotá	0.21	0.22	0.33	0.40	0.75	0.83	0.59	0.84	0.19	0.18	0.12	0.16	0.21	0.19	0.08	0.15
	México	0.57	0.87	1.10	1.31	2.96	3.30	0.42	0.91	0.41	0.51	0.28	0.35	1.21	1.16		
	São Paulo	1.46	1.53	1.76	1.80	1.28	2.02	1.52	1.54	2.04	1.93	1.54	1.66	3.61	3.08	0.45	0.54
MNBIAS [%]	Santiago	−102	−85.2	−81.6	13.9	−53.8	39.9	−103	−110	−108	−79.5	−111	−155	−13.1	118	−156	−173
	Bogotá	−130	−127	−98.4	−82.9	−25.6	−18.4	−52.3	−26.6	−136	−136	−153	−141	−130	−137	−170	−147
	México	−62.9	−15.4	6.2	27.0	96.5	105	−79.5	−11.0	−89.3	−65.6	−115	−92.6	4.2	7.2		
	São Paulo	39.4	42.1	54.9	53.8	24.2	64.1	42.6	40.4	64.8	45.6	46.4	53.8	104	84.1	−75.1	−57.0
RMSE $[\mu g/m^2]$	Santiago	39.65	72.46	34.40	32.08	25.86	53.34	39.82	81.63	41.21	67.84	40.52	99.01	16.89	295.63	50.28	97.44
	Bogotá	39.06	27.77	33.59	21.92	16.96	10.48	23.52	18.66	39.84	29.01	40.77	29.11	39.54	28.84	45.34	30.23
	México	25.44	12.05	12.80	18.74	105.46	110.21	32.93	13.46	32.46	25.05	36.82	29.92	24.00	22.35		
	São Paulo	17.51	24.28	26.48	35.41	15.11	40.68	21.35	28.36	36.89	55.94	23.75	33.12	91.62	102.20	20.03	20.42
FGE	Santiago	1.03	0.93	0.82	0.30	0.54	0.43	1.04	1.17	1.08	0.83	1.12	1.55	0.27	1.19	1.56	1.73
	Bogotá	1.31	1.27	0.98	0.83	0.31	0.27	0.56	0.53	1.37	1.36	1.54	1.42	1.31	1.38	1.71	1.48
	México	0.64	0.25	0.20	0.31	0.96	1.05	0.80	0.27	0.90	0.66	1.16	0.93	0.38	0.34		
	São Paulo	0.41	0.47	0.55	0.57	0.34	0.67	0.48	0.51	0.66	0.62	0.48	0.58	1.04	0.87	0.78	0.65
R	Santiago	0.30	−0.17	0.35	0.44	0.44	0.48	0.20	−0.33	−0.03	0.26	0.07	0.03	0.03	0.45	0.07	0.37
	Bogotá	0.72	0.37	0.65	−0.00	0.33	0.20	0.33	−0.17	0.74	0.05	0.45	0.42	0.32	0.24	0.65	−0.02
	México	0.69	0.46	0.77	0.37	0.58	0.14	0.36	0.20	0.64	0.08	0.66	−0.24	0.76	0.37		
	São Paulo	0.51	0.45	0.56	0.50	0.43	0.51	0.12	0.13	0.41	0.37	0.45	−0.01	0.58	0.52	0.11	0.19

*ENSEMBLE: based on the median value of the models; MEAN: arithmetic mean of the models; CAMS: Copernicus Atmosphere Monitoring Service's (CAMS); MPI: WRF-Chem executed by MPIM; EMEP: European Monitoring and Evaluation Programme; CHIM: CHIMERE transport model; SILAM: System for Integrated modeling of Atmospheric composition; USP: WRF-Chem executed by University of São Paulo.

~~*Median: ensemble based on the median value of the models; CAMS: Copernicus Atmosphere Monitoring Service's (CAMS); MPI: WRF-Chem executed by MPIM; EMEP: European Monitoring and Evaluation Programme; CHIM: CHIMERE transport model; SILAM: System for Integrated modeling of Atmospheric composition; USP: WRF-Chem executed by University of São Paulo.~~

Table A8 Coefficient of Variation (C.V.) per city during January and July

City	NO_2	O_3	CO	SO_2	$PM_{2.5}$
Santiago	33% / 57%	51% / 49%	45% / 86%	130% / 78%	65% / 136%

~~Bogota~~Bogotá	24% / 44%	62% / 63%	35% / 33%	64% / 67%	78% / 73%
São Paulo	56% / 46%	57% / 57%	42% / 38%	88% / 88%	59% / 50%
Mexico	31% / 47%	48% / 72%	54% / 63%	166% / 149%	111% / 105%

Appendix B. Air quality observations

Table B1. Stations availability and location for Mexico City

		Obs		ENSEMBLE		CAMS		MPI		EMEP		CHIM		SILAM		USP	
		Jan	Jul	Jan	Jul	Jan	Jul	Jan	Jul	Jan	Jul	Jan	Jul	Jan	Jul	Jan	Jul
CO																	
México	Number Stations	21	24	21	24	21	24	21	24	21	24	21	24	21	24		
	Availability [%]	96.67	100	100	100	100	100	100	100	100	100	83.33	66.67	100	100		
	CV	0.24	0.26	0.29	0.22	0.26	0.20	0.24	0.15	0.36	0.29	0.50	0.16	0.35	0.35		
NO_2																	
México	Number Stations	24	24	24	24	24	24	24	24	24	24	24	24	24	24		
	Availability [%]	100	100	100	100	100	100	100	100	100	100	83.33	66.67	100	100		
	CV	0.24	0.23	0.29	0.21	0.46	0.52	0.22	0.15	0.30	0.24	0.38	0.14	0.38	0.38		
O_3																	
México	Number Stations	21	29	28	29	28	29	28	29	28	29	28	29	28	29		
	Availability [%]	96.67	100	100	100	100	100	100	100	100	100	83.33	66.67	100	100		
	CV	0.31	0.20	0.25	0.22	0.17	0.14	0.27	0.23	0.41	0.26	0.32	0.33	0.28	0.30		
PM_{10}																	
México	Number Stations	17	24	17	24	17	24	17	24	17	24	17	24	17	24		
	Availability [%]	96.67	100	100	100	100	100	100	100	100	100	83.33	66.67	100	100		
	CV	0.27	0.20	0.55	0.27	0.28	0.23	0.24	0.26	0.48	0.31	0.52	0.25	0.48	0.43		
$PM_{2.5}$																	
México	Number Stations	14	16	14	16	14	16	14	16	14	16	14	16	14	16		
	Availability [%]	96.67	100	100	100	100	100	100	100	100	100	83.33	66.67	100	100		
	CV	0.37	0.24	0.52	0.32	0.28	0.22	0.25	0.19	0.34	0.19	0.52	0.30	0.48	0.46		
SO_2																	
México	Number Stations	23	26	23	26	23	26	23	26	23	26	23	26	23	26		
	Availability [%]	96.67	100	100	100	100	100	100	100	100	100	83.33	66.67	100	100		
	CV	0.60	0.30	0.35	0.20	0.25	0.09	0.26	0.15	0.30	0.14	0.38	0.18	0.35	0.28		

The observations availability refers to the percentage of days in each period when at least one station records enough data to construct their daily average (minimum of 18 hours). Additionally, only stations that maintain at least 75% of daily availability throughout the entire period are considered (at least 23 days with 18 hours minimum). The model availability refers to the percentage of days for which we have modeled data, being CHIMERE the only one with missing days, and USP missing information for México given their simulation domain did not include it. ~~Availability (%) for Observations refers to ……~~ ~~Availability (%) for the models refers to ……~~

Con formato: Interlineado: sencillo

Con formato: Resaltar

Table B2. Stations availability and location for Bogotá

		Obs		ENSEMBLE		CAMS		MPI		EMEP		CHIM		SILAM		USP	
		Jan	Jul	Jan	Jul	Jan	Jul	Jan	Jul	Jan	Jul	Jan	Jul	Jan	Jul	Jan	Jul
CO																	
Bogotá	Number Stations	7	8	7	8	7	8	7	8	7	8	7	8	7	8	7	8
	Availability [%]	100	100	100	100	100	100	100	100	100	100	83.33	66.67	100	100	100	100
	CV	0.29	0.17	0.16	0.17	0.10	0.13	0.18	0.14	0.26	0.17	0.18	0.14	0.25	0.31	0.33	0.30
NO_2																	
Bogotá	Number Stations	8	7	8	7	8	7	8	7	8	7	8	7	8	7	8	7
	Availability [%]	100	100	100	100	100	100	100	100	100	100	83.33	66.67	100	100	100	100
	CV	0.22	0.18	0.24	0.26	0.42	0.57	0.21	0.14	0.30	0.15	0.28	0.39	0.28	0.24	0.37	0.29
O_3																	
Bogotá	Number Stations	10	11	10	11	10	11	10	11	10	11	10	11	10	11	10	11
	Availability [%]	100	100	100	100	100	100	100	100	100	100	83.33	66.67	100	100	100	100
	CV	0.23	0.23	0.11	0.13	0.08	0.11	0.22	0.21	0.14	0.19	0.18	0.15	0.18	0.27	0.35	0.24
PM_{10}																	
Bogotá	Number Stations	10	10	10	10	10	10	10	10	10	10	10	10	10	10	10	10
	Availability [%]	100	100	100	100	100	100	100	100	100	100	83.33	66.67	100	100	100	100
	CV	0.27	0.22	0.31	0.19	0.16	0.21	0.33	0.52	0.37	0.17	0.26	0.14	0.37	0.40	0.33	0.34
$PM_{2.5}$																	
Bogotá	Number Stations	9	10	9	10	9	10	9	10	9	10	9	10	9	10	9	10
	Availability [%]	100	100	100	100	100	100	100	100	100	100	83.33	66.67	100	100	100	100
	CV	0.33	0.18	0.29	0.22	0.16	0.22	0.29	0.40	0.40	0.18	0.28	0.11	0.40	0.42	0.34	0.33
SO_2																	
Bogotá	Number Stations	7	6	7	6	7	6	7	6	7	6	7	6	7	6	7	6
	Availability [%]	100	100	100	100	100	100	100	100	100	100	83.33	66.67	100	100	100	100
	CV	0.28	0.34	0.22	0.20	0.12	0.15	0.24	0.20	0.41	0.24	0.24	0.45	0.32	0.18	0.30	0.37

The observations availability refers to the percentage of days in each period when at least one station records enough data to construct their daily average (minimum of 18 hours). Additionally, only stations that maintain at least 75% of daily availability throughout the entire period are considered (at least 23 days with 18 hours minimum). The model availability refers to the percentage of days for which we have modeled data, being CHIMERE the only one with missing days, and USP missing information for México given their simulation domain did not include it.

Table B3. Stations availability and location for Santiago

		Obs		ENSEMBLE		CAMS		MPI		EMEP		CHIM		SILAM		USP	
		Jan	Jul	Jan	Jul	Jan	Jul	Jan	Jul	Jan	Jul	Jan	Jul	Jan	Jul	Jan	Jul
CO																	
Santiago	Number Stations	8	9	8	9	8	9	8	9	8	9	8	9	8	9	8	9
	Availability [%]	100	100	100	100	100	100	100	100	100	100	83.33	66.67	100	100	100	100
	CV	0.10	0.33	0.10	0.19	0.27	0.29	0.13	0.10	0.13	0.16	0.12	0.29	0.17	0.25	0.13	0.20
NO_2																	
Santiago	Number Stations	9	9	10	10	10	10	10	10	10	10	10	10	10	10	10	10
	Availability [%]	100	100	100	100	100	100	100	100	100	100	83.33	66.67	100	100	100	100
	CV	0.22	0.29	0.11	0.16	0.36	0.32	0.17	0.14	0.14	0.13	0.11	0.28	0.17	0.26	0.21	0.27
O_3																	
Santiago	Number Stations	9	9	9	9	9	9	9	9	9	9	9	9	9	9	9	9
	Availability [%]	100	100	100	100	100	100	100	100	100	100	83.33	66.67	100	100	100	100
	CV	0.13	0.58	0.16	0.24	0.16	0.20	0.24	0.14	0.13	0.29	0.17	0.22	0.24	0.60	0.25	0.40
PM_{10}																	
Santiago	Number Stations	10	10	10	10	10	10	10	10	10	10	10	10	10	10	10	10
	Availability [%]	100	100	100	100	100	100	100	100	100	100	83.33	66.67	100	100	100	100
	CV	0.20	0.36	0.15	0.20	0.24	0.23	0.24	0.17	0.14	0.22	0.16	0.31	0.23	0.27	0.20	0.22
$PM_{2.5}$																	
Santiago	Number Stations	10	10	10	10	10	10	10	10	10	10	10	10	10	10	10	10
	Availability [%]	100	100	100	100	100	100	100	100	100	100	83.33	66.67	100	100	100	100
	CV	0.22	0.32	0.15	0.13	0.24	0.23	0.20	0.13	0.12	0.19	0.16	0.32	0.29	0.29	0.20	0.22
SO_2																	
Santiago	Number Stations	4	4	4	4	4	4	4	4	4	4	4	4	4	4	4	4
	Availability [%]	100	100	100	100	100	100	100	100	100	100	83.33	66.67	100	100	100	100
	CV	0.15	0.20	0.16	0.18	0.11	0.16	0.18	0.14	0.12	0.19	0.21	0.22	0.17	0.36	0.12	0.17

The observations availability refers to the percentage of days in each period when at least one station records enough data to construct their daily average (minimum of 18 hours). Additionally, only stations that maintain at least 75% of daily availability throughout the entire period are considered (at least 23 days with 18 hours minimum). The model availability refers to the percentage of days for which we have modeled data, being CHIMERE the only one with missing days, and USP missing information for México given their simulation domain did not include it.

Table B4. Stations availability and location for São Paulo

		Obs		ENSEMBLE		CAMS		MPI		EMEP		CHIM		SILAM		USP	
		Jan	Jul	Jan	Jul	Jan	Jul	Jan	Jul	Jan	Jul	Jan	Jul	Jan	Jul	Jan	Jul
CO																	
São Paulo	Number Stations	17	17	17	17	17	17	17	17	17	17	17	17	17	17	17	17
	Availability [%]	100	100	100	100	100	100	100	100	100	100	83.33	66.67	100	100	100	100
	CV	0.26	0.31	0.26	0.31	0.37	0.42	0.22	0.34	0.29	0.48	0.42	0.26	0.40	0.50	0.41	0.34
NO_2																	
São Paulo	Number Stations	18	18	18	18	18	18	18	18	18	18	18	18	18	18	18	18
	Availability [%]	100	100	100	100	100	100	100	100	100	100	83.33	66.67	100	100	100	100
	CV	0.35	0.31	0.28	0.27	1.13	0.87	0.27	0.33	0.26	0.36	0.34	0.20	0.45	0.53	0.49	0.45
O_3																	
São Paulo	Number Stations	20	20	20	20	20	20	20	20	20	20	20	20	20	20	20	20
	Availability [%]	100	100	100	100	100	100	100	100	100	100	83.33	66.67	100	100	100	100
	CV	0.37	0.38	0.35	0.44	0.32	0.36	0.33	0.48	0.35	0.57	0.38	0.43	0.47	0.85	0.43	0.41
PM_{10}																	
São Paulo	Number Stations	23	22	23	22	23	22	23	22	23	22	23	22	23	22	23	22
	Availability [%]	100	100	100	100	100	100	100	100	100	100	83.33	66.67	100	100	100	100
	CV	0.39	0.37	0.27	0.33	0.34	0.36	0.27	0.36	0.40	0.75	0.39	0.33	0.56	0.76	0.47	0.38
$PM_{2.5}$																	
São Paulo	Number Stations	9	9	9	9	9	9	9	9	9	9	9	9	9	9	9	9
	Availability [%]	100	100	100	100	100	100	100	100	100	100	83.33	66.67	100	100	100	100
	CV	0.49	0.45	0.29	0.37	0.34	0.36	0.26	0.38	0.35	0.60	0.40	0.32	0.61	0.88	0.47	0.37
SO_2																	
São Paulo	Number Stations	8	8	8	8	8	8	8	8	8	8	8	8	8	8	8	8
	Availability [%]	100	100	100	100	100	100	100	100	100	100	83.33	66.67	100	100	100	100
	CV	0.37	0.41	0.28	0.31	0.28	0.36	0.26	0.40	0.31	0.48	0.30	0.39	0.35	0.46	0.34	0.34

The observations availability refers to the percentage of days in each period when at least one station records enough data to construct their daily average (minimum of 18 hours). Additionally, only stations that maintain at least 75% of daily availability throughout the entire period are considered (at least 23 days with 18 hours minimum). The model availability refers to the percentage of days for which we have modeled data, being CHIMERE the only one with missing days, and USP missing information for México given their simulation domain did not include it.

Table B5. Stations availability and location for Quito

		Obs		ENSEMBLE		CAMS		MPI		EMEP		CHIM		SILAM		USP	
		Jan	Jul	Jan	Jul	Jan	Jul	Jan	Jul	Jan	Jul	Jan	Jul	Jan	Jul	Jan	Jul
CO																	
Quito	Number Stations	6	6	6	6	6	6	6	6	6	6	6	6	6	6	6	6
	Availability [%]	100	100	100	100	100	100	100	100	100	100	83.33	66.67	100	100	100	100
	CV	0.17	0.16	0.15	0.15	0.07	0.06	0.14	0.12	0.31	0.32	0.18	0.12	0.15	0.16	0.34	0.26
NO_2																	
Quito	Number Stations	5	5	5	5	5	5	5	5	5	5	5	5	5	5	5	5
	Availability [%]	100	100	100	100	100	100	100	100	100	100	83.33	66.67	100	100	100	100
	CV	0.24	0.18	0.16	0.28	0.49	0.46	0.20	0.16	0.26	0.31	0.22	0.27	0.18	0.18	0.37	0.32
O_3																	
Quito	Number Stations	7	7	7	7	7	7	7	7	7	7	7	7	7	7	7	7
	Availability [%]	100	100	100	100	100	100	100	100	100	100	83.33	66.67	100	100	100	100
	CV	0.17	0.20	0.13	0.13	0.08	0.07	0.21	0.21	0.26	0.20	0.20	0.12	0.24	0.27	0.33	0.18
PM_{10}																	
Quito	Number Stations	3	3	3	3	3	3	3	3	3	3	3	3	3	3	3	3
	Availability [%]	96.67	100	100	100	100	100	100	100	100	100	83.33	66.67	100	100	100	100
	CV	0.34	0.24	0.22	0.23	0.14	0.12	0.25	0.33	0.26	0.41	0.19	0.16	0.22	0.38	0.40	0.26
$PM_{2.5}$																	
Quito	Number Stations	5	5	5	5	5	5	5	5	5	5	5	5	5	5	5	5
	Availability [%]	96.67	100	100	100	100	100	100	100	100	100	83.33	66.67	100	100	100	100
	CV	0.19	0.24	0.20	0.19	0.14	0.12	0.21	0.24	0.23	0.32	0.19	0.13	0.23	0.33	0.40	0.26
SO_2																	
Quito	Number Stations	7	7	7	7	7	7	7	7	7	7	7	7	7	7	7	7
	Availability [%]	100	100	100	100	100	100	100	100	100	100	83.33	66.67	100	100	100	100
	CV	0.33	0.35	0.21	0.33	0.09	0.08	0.19	0.17	0.19	0.27	0.19	0.25	0.12	0.19	0.34	0.34

The observations availability refers to the percentage of days in each period when at least one station records enough data to construct their daily average (minimum of 18 hours). Additionally, only stations that maintain at least 75% of daily availability throughout the entire period are considered (at least 23 days with 18 hours minimum). The model availability refers to the percentage of days for which we have modeled data, being CHIMERE the only one with missing days, and USP missing information for México given their simulation domain did not include it.

Table B6. Stations availability and location for Medellín

		Obs		ENSEMBLE		CAMS		MPI		EMEP		CHIM		SILAM		USP	
		Jan	Jul	Jan	Jul	Jan	Jul	Jan	Jul	Jan	Jul	Jan	Jul	Jan	Jul	Jan	Jul
CO																	
Medellin	Number Stations	2	2	2	2	2	2	2	2	2	2	2	2	2	2	2	2
	Availability [%]	76.67	100	100	100	100	100	100	100	100	100	83.33	66.67	100	100	100	100
	CV	0.14	0.11	0.10	0.09	0.08	0.13	0.13	0.13	0.34	0.30	0.19	0.09	0.14	0.12	0.18	0.14
NO_2																	
Medellin	Number Stations	4	4	4	4	4	4	4	4	4	4	4	4	4	4	4	4
	Availability [%]	100	100	100	100	100	100	100	100	100	100	83.33	66.67	100	100	100	100
	CV	0.19	0.16	0.13	0.17	0.68	0.70	0.16	0.15	0.37	0.25	0.25	0.18	0.24	0.16	0.20	0.20
O_3																	
Medellin	Number Stations	4	3	4	3	4	3	4	3	4	3	4	3	4	3	4	3
	Availability [%]	100	100	100	100	100	100	100	100	100	100	83.33	66.67	100	100	100	100
	CV	0.21	0.17	0.13	0.10	0.12	0.14	0.13	0.18	0.17	0.21	0.11	0.11	0.18	0.26	0.30	0.17
PM_{10}																	
Medellin	Number Stations	1	1	1	1	1	1	1	1	1	1	1	1	1	1	1	1
	Availability [%]	100	100	100	100	100	100	100	100	100	100	83.33	66.67	100	100	100	100
	CV	0.16	0.20	0.14	0.15	0.17	0.29	0.32	0.39	0.22	0.33	0.13	0.16	0.22	0.18	0.31	0.37
$PM_{2.5}$																	
Medellin	Number Stations	5	5	5	5	5	5	5	5	5	5	5	5	5	5	5	5
	Availability [%]	100	100	100	100	100	100	100	100	100	100	83.33	66.67	100	100	100	100
	CV	0.15	0.14	0.14	0.15	0.18	0.30	0.27	0.30	0.18	0.25	0.14	0.13	0.22	0.20	0.27	0.35
SO_2																	
Medellin	Number Stations	1	1	1	1	1	1	1	1	1	1	1	1	1	1	1	1
	Availability [%]	10	100	100	100	100	100	100	100	100	100	83.33	66.67	100	100	100	100
	CV	0.20	0.19	0.26	0.20	0.20	0.23	0.28	0.22	0.74	0.52	0.17	0.15	0.27	0.31	0.22	0.25

The observations availability refers to the percentage of days in each period when at least one station records enough data to construct their daily average (minimum of 18 hours). Additionally, only stations that maintain at least 75% of daily availability throughout the entire period are considered (at least 23 days with 18 hours minimum). The model availability refers to the

percentage of days for which we have modeled data, being CHIMERE the only one with missing days, and USP missing information for México given their simulation domain did not include it.

Table B7. Stations availability and location for Lima

		Obs		ENSEMBLE		CAMS		MPI		EMEP		CHIM		SILAM		USP	
		Jan	Jul	Jan	Jul	Jan	Jul	Jan	Jul	Jan	Jul	Jan	Jul	Jan	Jul	Jan	Jul
CO																	
Lima	Number Stations	8	7	8	7	8	7	8	7	8	7	8	7	8	7	8	7
	Availability [%]	100	100	100	100	100	100	100	100	100	100	83.33	66.67	100	100	100	100
	CV	0.21	0.17	0.08	0.09	0.08	0.10	0.11	0.09	0.10	0.08	0.36	0.13	0.33	0.19	0.20	0.14
NO_2																	
Lima	Number Stations	2	6	2	6	2	6	2	6	2	6	2	6	2	6	2	6
	Availability [%]	93.33	96.67	100	100	100	100	100	100	100	100	83.33	66.67	100	100	100	100
	CV	0.23	0.16	0.10	0.13	0.38	0.70	0.08	0.11	0.14	0.10	0.25	0.12	0.20	0.19	0.20	0.19
O_3																	
Lima	Number Stations	3	6	3	6	3	6	3	6	3	6	3	6	3	6	3	6
	Availability [%]	100	100	100	100	100	100	100	100	100	100	83.33	66.67	100	100	100	100
	CV	0.47	0.29	0.14	0.13	0.18	0.15	0.17	0.08	0.12	0.10	0.12	0.12	0.19	0.18	0.31	0.25
PM_{10}																	
Lima	Number Stations	8	8	8	8	8	8	8	8	8	8	8	8	8	8	8	8
	Availability [%]	100	100	100	100	100	100	100	100	100	100	83.33	66.67	100	100	100	100
	CV	0.13	0.27	0.09	0.12	0.13	0.18	0.16	0.19	0.24	0.23	0.11	0.11	0.20	0.18	0.16	0.23
$PM_{2.5}$																	
Lima	Number Stations	9	8	9	8	9	8	9	8	9	8	9	8	9	8	9	8
	Availability [%]	96.67	100	100	100	100	100	100	100	100	100	83.33	66.67	100	100	100	100
	CV	0.16	0.22	0.12	0.13	0.13	0.18	0.18	0.14	0.20	0.11	0.18	0.13	0.28	0.23	0.16	0.23
SO_2																	
Lima	Number Stations	4	2	4	2	4	2	4	2	4	2	4	2	4	2	4	2
	Availability [%]	100	100	100	100	100	100	100	100	100	100	83.33	66.67	100	100	100	100
	CV	0.19	0.37	0.15	0.11	0.12	0.05	0.10	0.12	0.19	0.10	0.22	0.21	0.24	0.16	0.19	0.15

The observations availability refers to the percentage of days in each period when at least one station records enough data to construct their daily average (minimum of 18 hours). Additionally, only stations that maintain at least 75% of daily availability throughout the entire period are considered (at least 23 days with 18 hours minimum). The model availability refers to the percentage of days for which we have modeled data, being CHIMERE the only one with missing days, and USP missing information for México given their simulation domain did not include it.

Table B8. Stations availability and location for Guadalajara

		Obs		ENSEMBLE		CAMS		MPI		EMEP		CHIM		SILAM		USP	
		Jan	Jul	Jan	Jul	Jan	Jul	Jan	Jul	Jan	Jul	Jan	Jul	Jan	Jul	Jan	Jul
CO																	
Guadalajara	Number Stations	7	7	7	7	7	7	7	7	7	7	7	7	7	7		
	Availability [%]	96.67	100	100	100	100	100	100	100	100	100	83.33	66.67	100	100		
	CV	0.20	0.12	0.22	0.14	0.20	0.13	0.14	0.18	0.28	0.20	0.32	0.16	0.30	0.27		
NO_2																	
Guadalajara	Number Stations	8	8	8	8	8	8	8	8	8	8	8	8	8	8		
	Availability [%]	100	100	100	100	100	100	100	100	100	100	83.33	66.67	100	100		
	CV	0.25	0.17	0.30	0.17	0.64	0.88	0.16	0.18	0.34	0.24	0.39	0.28	0.32	0.33		
O_3																	
Guadalajara	Number Stations	8	8	8	8	8	8	8	8	8	8	8	8	8	8		
	Availability [%]	96.67	100	100	100	100	100	100	100	100	100	83.33	66.67	100	100		
	CV	0.16	0.31	0.16	0.16	0.28	0.24	0.22	0.27	0.22	0.16	0.18	0.12	0.26	0.27		
PM_{10}																	
Guadalajara	Number Stations	8	8	8	8	8	8	8	8	8	8	8	8	8	8		
	Availability [%]	96.67	100	100	100	100	100	100	100	100	100	83.33	66.67	100	100		
	CV	0.22	0.20	0.32	0.20	0.28	0.29	0.34	0.47	0.34	0.25	0.31	0.19	0.36	0.37		
SO_2																	
Guadalajara	Number Stations	8	8	8	8	8	8	8	8	8	8	8	8	8	8		
	Availability [%]	96.67	100	100	100	100	100	100	100	100	100	83.33	66.67	100	100		
	CV	0.52	0.41	0.33	0.12	0.26	0.17	0.20	0.21	0.26	0.16	0.28	0.23	0.30	0.28		

The observations availability refers to the percentage of days in each period when at least one station records enough data to construct their daily average (minimum of 18 hours). Additionally, only stations that maintain at least 75% of daily availability throughout the entire period are considered (at least 23 days with 18 hours minimum). The model availability refers to the percentage of days for which we have modeled data, being CHIMERE the only one with missing days, and USP missing information for México given their simulation domain did not include it.

Appendix C. Particular Hourly simulations

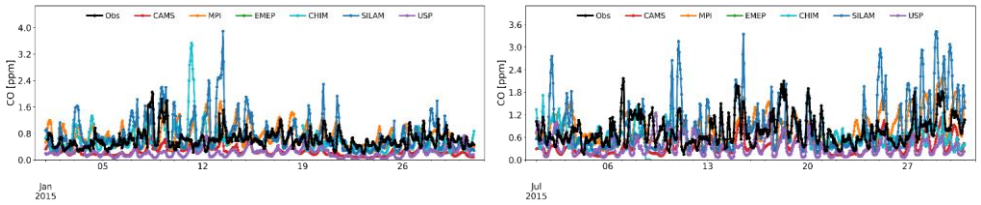

Figure C1. Hourly CO simulations in São Paulo for January and July of 2015

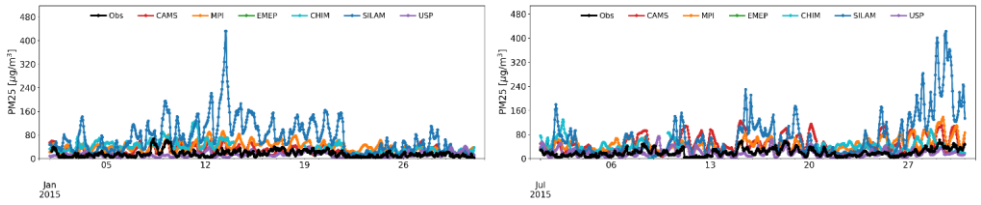

Figure C2. Hourly $PM_{2.5}$ simulations in São for January and July of 2015

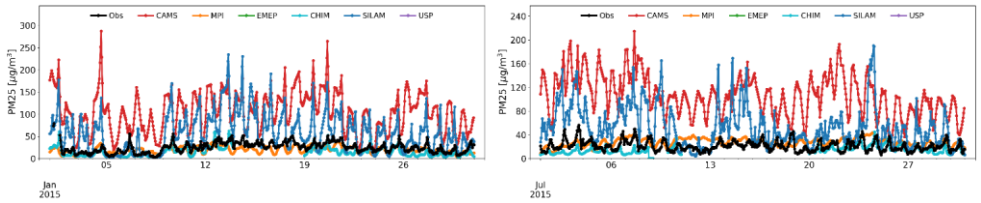

Figure C3. Hourly $PM_{2.5}$ simulations in México City for January and July of 2015

~~Table B1. Stations availability and location for Santiago~~

		Obs		ENSEMBLE		CAMS		MPI		EMEP		CHIM		SILAM		USP	
		Jan	Jul	Jan	Jul	Jan	Jul	Jan	Jul	Jan	Jul	Jan	Jul	Jan	Jul	Jan	Jul
CO																	
Santiago	Number Stations	8	9	8	9	8	9	8	9	8	9	8	9	8	9	8	9
	Availability [%]	100	100	100	100	96.67	96.67	100	100	96.67	96.67	83.33	66.67	100	100	96.67	96.67
	CV	0.10	0.34	0.10	0.16	0.30	0.29	0.17	0.14	0.14	0.14	0.17	0.27	0.15	0.22	0.11	0.18
NO_2																	
Santiago	Number Stations	9	9	10	10	10	10	10	10	10	10	10	10	10	10	10	10
	Availability [%]	100	100	100	100	96.67	96.67	100	100	96.67	96.67	83.33	66.67	100	100	96.67	96.67
	CV	0.23	0.31	0.14	0.14	0.36	0.32	0.22	0.19	0.18	0.13	0.14	0.21	0.17	0.23	0.21	0.25
O_3																	
Santiago	Number Stations	9	9	9	9	9	9	9	9	9	9	9	9	9	9	9	9
	Availability [%]	100	100	100	100	96.67	96.67	100	100	96.67	96.67	83.33	66.67	100	100	96.67	96.67
	CV	0.14	0.57	0.16	0.22	0.16	0.21	0.25	0.14	0.12	0.24	0.18	0.25	0.23	0.50	0.25	0.39
PM_{10}																	
Santiago	Number Stations	10	10	10	10	10	10	10	10	10	10	10	10	10	10	10	10
	Availability [%]	100	100	100	100	96.67	96.67	100	100	96.67	96.67	83.33	66.67	100	100	96.67	96.67
	CV	0.20	0.39	0.16	0.20	0.25	0.22	0.26	0.21	0.16	0.26	0.18	0.22	0.23	0.28	0.21	0.19
$PM_{2.5}$																	
Santiago	Number Stations	10	10	10	10	10	10	10	10	10	10	10	10	10	10	10	10
	Availability [%]	100	100	100	100	96.67	96.67	100	100	96.67	96.67	83.33	66.67	100	100	96.67	96.67
	CV	0.22	0.37	0.16	0.14	0.25	0.22	0.22	0.18	0.14	0.20	0.18	0.24	0.27	0.30	0.21	0.19
SO_2																	
Santiago	Number Stations	4	4	4	4	4	4	4	4	4	4	4	4	4	4	4	4
	Availability [%]	100	100	100	100	96.67	96.67	100	100	96.67	96.67	83.33	66.67	100	100	96.67	96.67
	CV	0.14	0.20	0.16	0.12	0.12	0.16	0.27	0.21	0.13	0.23	0.24	0.15	0.18	0.38	0.11	0.16

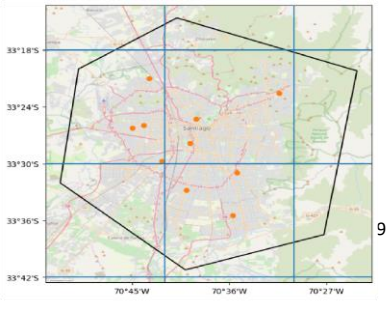

Table B2. Stations availability and location for Bogotá

		Obs		ENSEMBLE		CAMS		MPI		EMEP		CHIM		SILAM		USP	
		Jan	Jul	Jan	Jul	Jan	Jul	Jan	Jul	Jan	Jul	Jan	Jul	Jan	Jul	Jan	Jul
CO																	
Bogotá	Number Stations	7	8	7	8	7	8	7	8	7	8	7	8	7	8	7	8
	Availability [%]	100	100	100	100	96.67	96.67	100	100	96.67	96.67	83.33	66.67	100	100	96.67	96.67
	CV	0.28	0.15	0.16	0.15	0.10	0.13	0.17	0.12	0.24	0.18	0.21	0.15	0.17	0.22	0.32	0.27
NO_2																	
Bogotá	Number Stations	8	7	8	7	8	7	8	7	8	7	8	7	8	7	8	7
	Availability [%]	100	100	100	100	96.67	96.67	100	100	96.67	96.67	83.33	66.67	100	100	96.67	96.67
	CV	0.22	0.17	0.19	0.18	0.44	0.59	0.18	0.10	0.27	0.13	0.31	0.34	0.15	0.17	0.35	0.27
O_3																	
Bogotá	Number Stations	10	11	10	11	10	11	10	11	10	11	10	11	10	11	10	11
	Availability [%]	100	100	100	100	96.67	96.67	100	100	96.67	96.67	83.33	66.67	100	100	96.67	96.67
	CV	0.24	0.23	0.10	0.12	0.08	0.11	0.21	0.19	0.11	0.15	0.18	0.15	0.14	0.26	0.35	0.21
PM_{10}																	
Bogotá	Number Stations	10	10	10	10	10	10	10	10	10	10	10	10	10	10	10	10
	Availability [%]	100	100	100	100	96.67	96.67	100	100	96.67	96.67	83.33	66.67	100	100	96.67	96.67
	CV	0.27	0.22	0.30	0.20	0.15	0.21	0.31	0.52	0.34	0.19	0.25	0.12	0.24	0.24	0.32	0.31
$PM_{2.5}$																	
Bogotá	Number Stations	9	10	9	10	9	10	9	10	9	10	9	10	9	10	9	10
	Availability [%]	100	100	100	100	96.67	96.67	100	100	96.67	96.67	83.33	66.67	100	100	96.67	96.67
	CV	0.33	0.18	0.30	0.18	0.16	0.22	0.28	0.40	0.33	0.21	0.27	0.10	0.26	0.28	0.32	0.30
SO_2																	
Bogotá	Number Stations	7	6	7	6	7	6	7	6	7	6	7	6	7	6	7	6
	Availability [%]	100	100	100	100	96.67	96.67	100	100	96.67	96.67	83.33	66.67	100	100	96.67	96.67
	CV	0.29	0.34	0.17	0.14	0.10	0.14	0.21	0.16	0.34	0.21	0.24	0.35	0.20	0.15	0.29	0.35

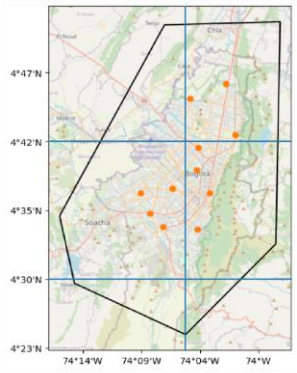

Table B3. Stations availability and location for México

		Obs		ENSEMBLE		CAMS		MPI		EMEP		CHIM		SILAM		USP	
		Jan	Jul	Jan	Jul	Jan	Jul	Jan	Jul	Jan	Jul	Jan	Jul	Jan	Jul	Jan	Jul
CO																	
México	Number Stations	21	24	21	24	21	24	21	24	21	24	21	24	21	24		
	Availability [%]	96.77	100	100	100	96.67	96.67	100	100	96.67	96.67	83.33	66.67	100	100		
	CV	0.21	0.26	0.28	0.20	0.25	0.19	0.22	0.13	0.35	0.26	0.48	0.15	0.33	0.33		
NO_2																	
México	Number Stations	24	24	24	24	24	24	24	24	24	24	24	24	24	24		
	Availability [%]	100	100	100	100	96.67	96.67	100	100	96.67	96.67	83.33	66.67	100	100		
	CV	0.24	0.22	0.28	0.19	0.44	0.50	0.21	0.13	0.29	0.21	0.37	0.12	0.36	0.35		
O_3																	
México	Number Stations	21	29	28	29	28	29	28	29	28	29	28	29	28	29		
	Availability [%]	96.77	100	100	100	96.67	96.67	100	100	96.67	96.67	83.33	66.67	100	100		
	CV	0.31	0.19	0.23	0.21	0.15	0.14	0.26	0.21	0.35	0.22	0.29	0.34	0.25	0.28		
PM_{10}																	
México	Number Stations	17	24	17	24	17	24	17	24	17	24	17	24	17	24		
	Availability [%]	96.77	100	100	100	96.67	96.67	100	100	96.67	96.67	83.33	66.67	100	100		
	CV	0.29	0.20	0.52	0.26	0.28	0.22	0.24	0.27	0.48	0.29	0.51	0.23	0.46	0.40		
$PM_{2.5}$																	
México	Number Stations	14	16	14	16	14	16	14	16	14	16	14	16	14	16		
	Availability [%]	96.77	100	100	100	96.67	96.67	100	100	96.67	96.67	83.33	66.67	100	100		
	CV	0.35	0.23	0.50	0.29	0.28	0.22	0.24	0.20	0.33	0.16	0.52	0.29	0.48	0.43		
SO_2																	
México	Number Stations	23	26	23	26	23	26	23	26	23	26	23	26	23	26		
	Availability [%]	96.77	100	100	100	96.67	96.67	100	100	96.67	96.67	83.33	66.67	100	100		
	CV	0.59	0.29	0.35	0.20	0.25	0.09	0.27	0.13	0.32	0.13	0.37	0.18	0.34	0.27		

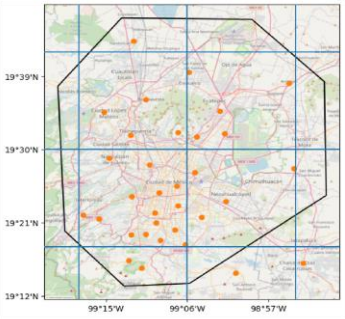

~~Table B4. Stations availability and location for Sao Paulo~~

		Obs		ENSEMBLE		CAMS		MPI		EMEP		CHIM		SILAM		USP	
		Jan	Jul	Jan	Jul	Jan	Jul	Jan	Jul	Jan	Jul	Jan	Jul	Jan	Jul	Jan	Jul
CO																	
São Paulo	Number Stations	17	17	17	17	17	17	17	17	17	17	17	17	17	17	17	17
	Availability [%]	100	100	100	100	96.67	96.67	100	100	96.67	96.67	83.33	66.67	100	100	96.67	96.67
	CV	0.26	0.31	0.28	0.29	0.39	0.43	0.25	0.33	0.31	0.38	0.38	0.27	0.40	0.47	0.41	0.36
NO_2																	
São Paulo	Number Stations	18	18	18	18	18	18	18	18	18	18	18	18	18	18	18	18
	Availability [%]	100	100	100	100	96.67	96.67	100	100	96.67	96.67	83.33	66.67	100	100	96.67	96.67
	CV	0.36	0.32	0.30	0.27	1.18	0.91	0.30	0.33	0.28	0.31	0.34	0.22	0.44	0.47	0.48	0.48
O_3																	
São Paulo	Number Stations	20	20	20	20	20	20	20	20	20	20	20	20	20	20	20	20
	Availability [%]	100	100	100	100	96.67	96.67	100	100	96.67	96.67	83.33	66.67	100	100	96.67	96.67
	CV	0.40	0.38	0.35	0.41	0.35	0.35	0.36	0.41	0.32	0.35	0.36	0.36	0.46	0.77	0.46	0.41
PM_{10}																	
São Paulo	Number Stations	23	22	23	22	23	22	23	22	23	22	23	22	23	22	23	22
	Availability [%]	100	100	100	100	96.67	96.67	100	100	96.67	96.67	83.33	66.67	100	100	96.67	96.67
	CV	0.42	0.39	0.29	0.31	0.34	0.37	0.28	0.37	0.40	0.64	0.40	0.35	0.53	0.74	0.46	0.41
$PM_{2.5}$																	
São Paulo	Number Stations	9	9	9	9	9	9	9	9	9	9	9	9	9	9	9	9
	Availability [%]	100	100	100	100	96.67	96.67	100	100	96.67	96.67	83.33	66.67	100	100	96.67	96.67
	CV	0.51	0.49	0.32	0.33	0.35	0.38	0.29	0.37	0.39	0.51	0.40	0.35	0.59	0.85	0.46	0.41
SO_2																	
São Paulo	Number Stations	8	8	8	8	8	8	8	8	8	8	8	8	8	8	8	8
	Availability [%]	100	100	100	100	96.67	96.67	100	100	96.67	96.67	83.33	66.67	100	100	96.67	96.67
	CV	0.40	0.41	0.29	0.30	0.28	0.38	0.32	0.42	0.34	0.42	0.31	0.43	0.35	0.45	0.33	0.36

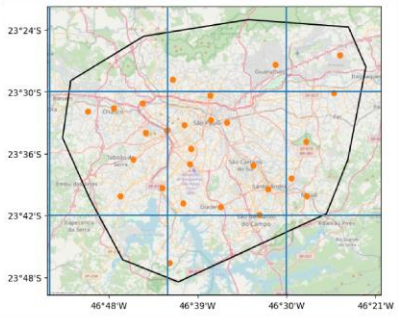

Appendix C. Hourly simulations

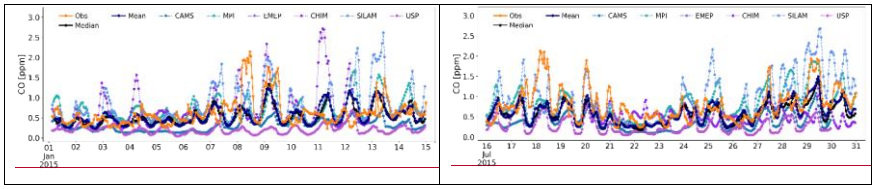

Figure C1. Hourly CO simulations in São Paulo during the first two weeks in January and the last two weeks in July of 2015

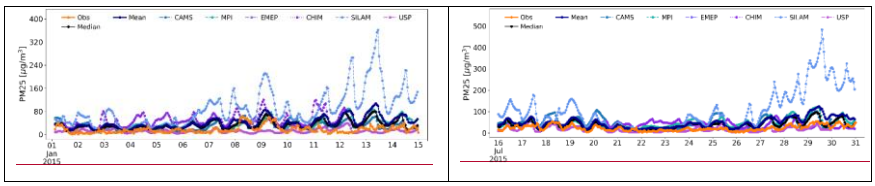

Figure C2. Hourly $PM_{2.5}$ simulations in São Paulo during the first two weeks in January and the last two weeks in July of 2015

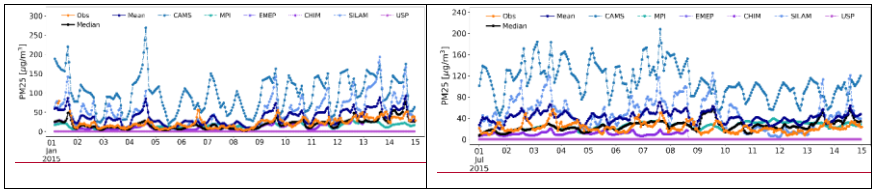

Figure C3. Hourly $PM_{2.5}$ simulations in México City during the first two weeks of January and July of 2015

Appendix D. Simulations by all models

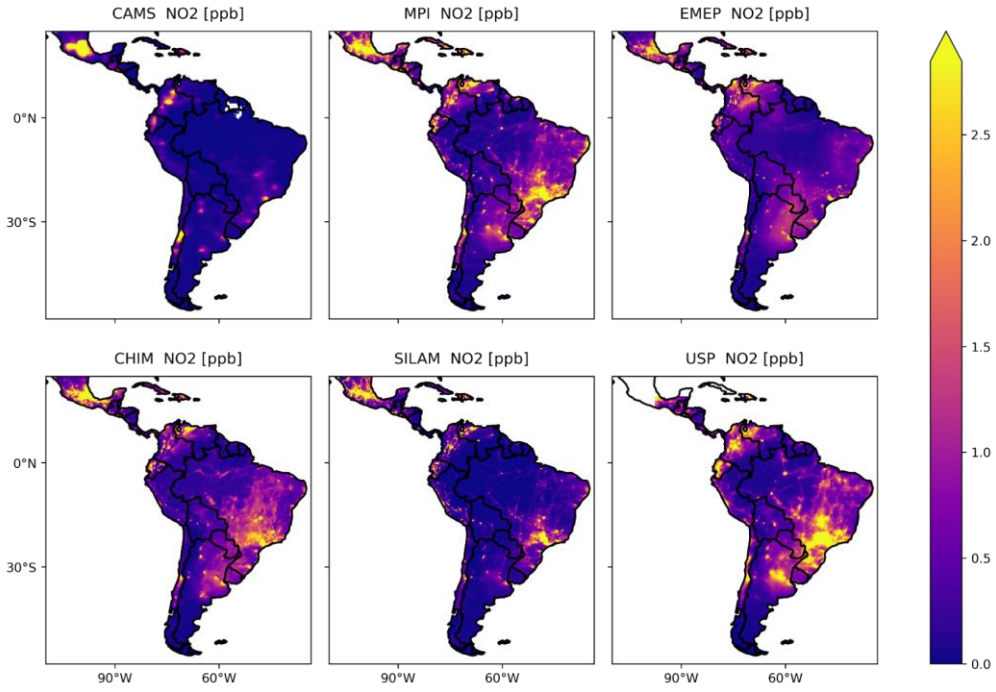

Figure D1. NO_2 simulations in January 2015 by all models

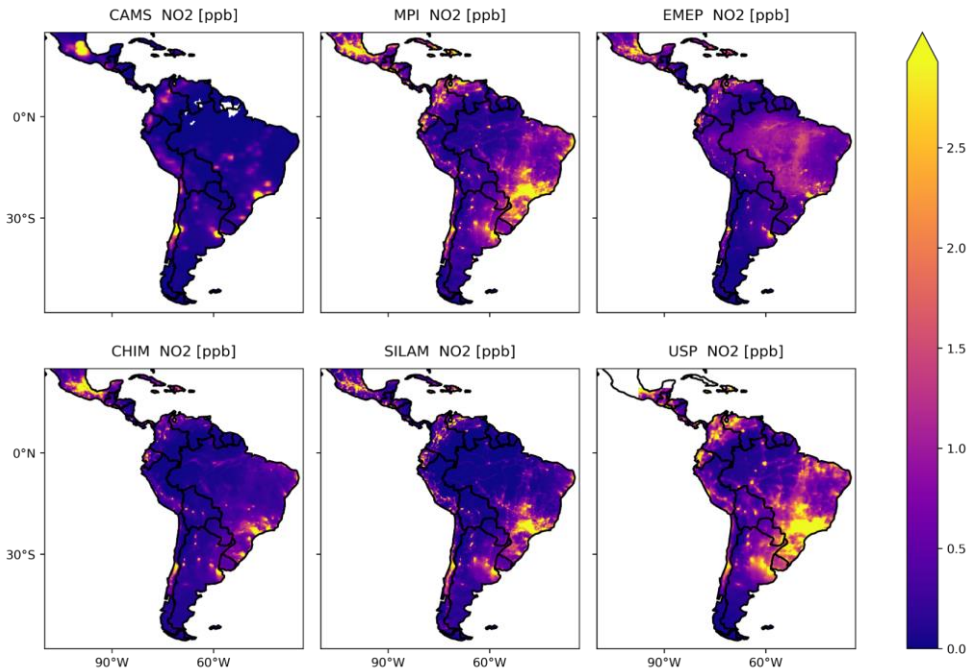

Figure D2. NO_2 simulations in July 2015 by all models

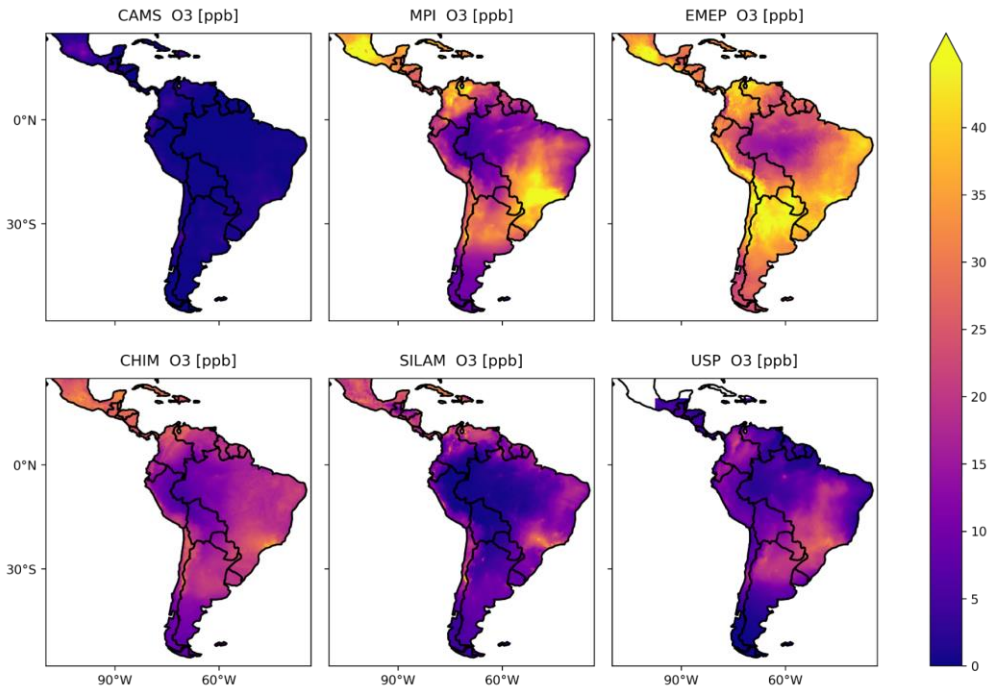

Figure D3. O_3 simulations in January 2015 by all models

1835

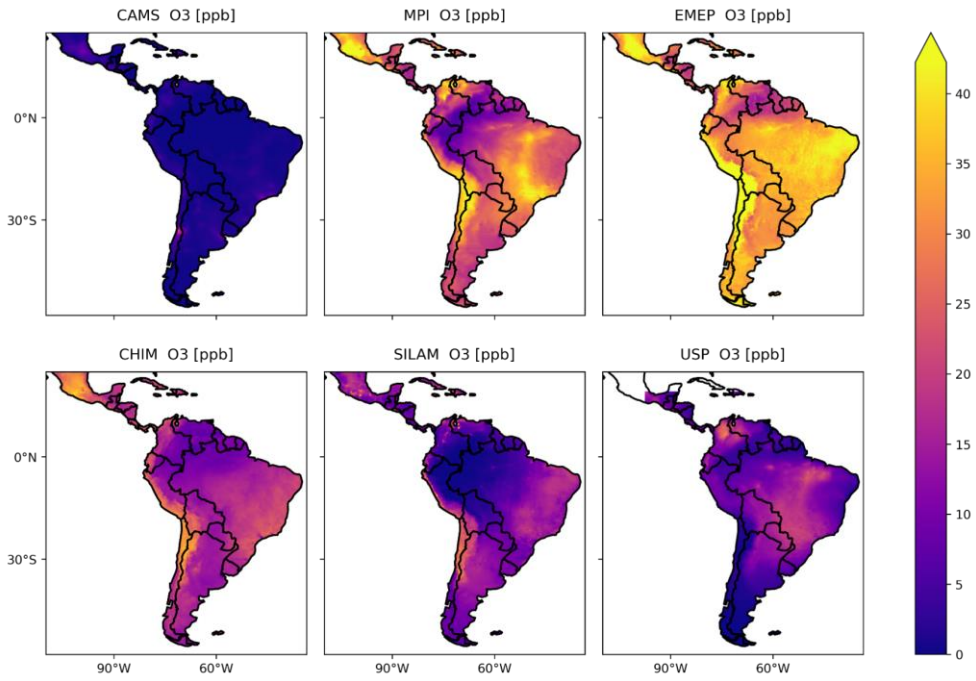

Figure D4. O_3 simulations in July 2015 by all models

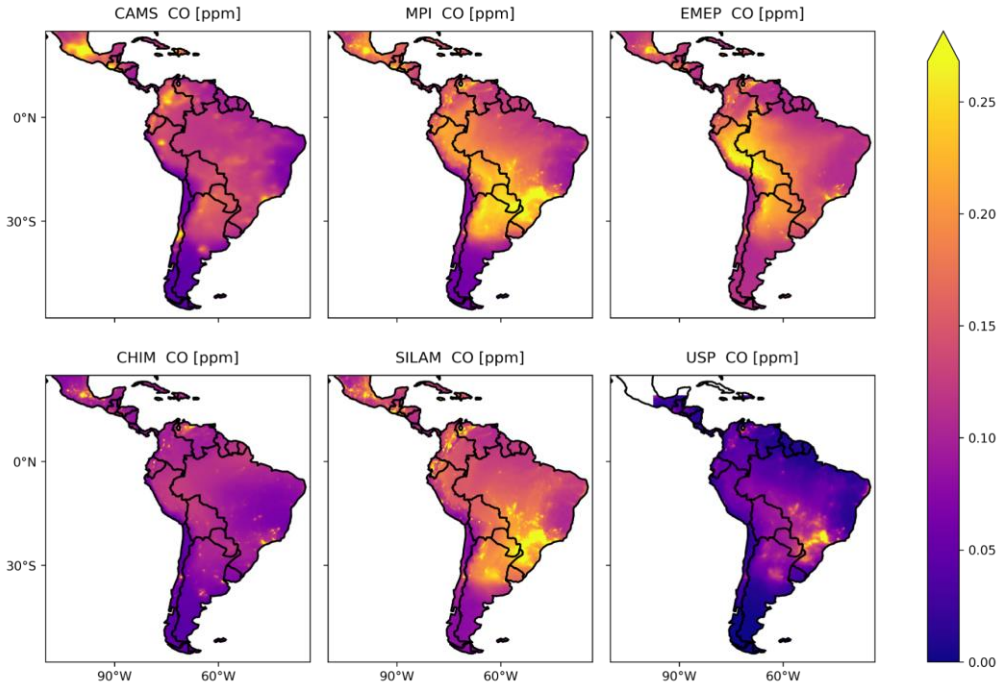

Figure D5. CO simulations in January 2015 by all models

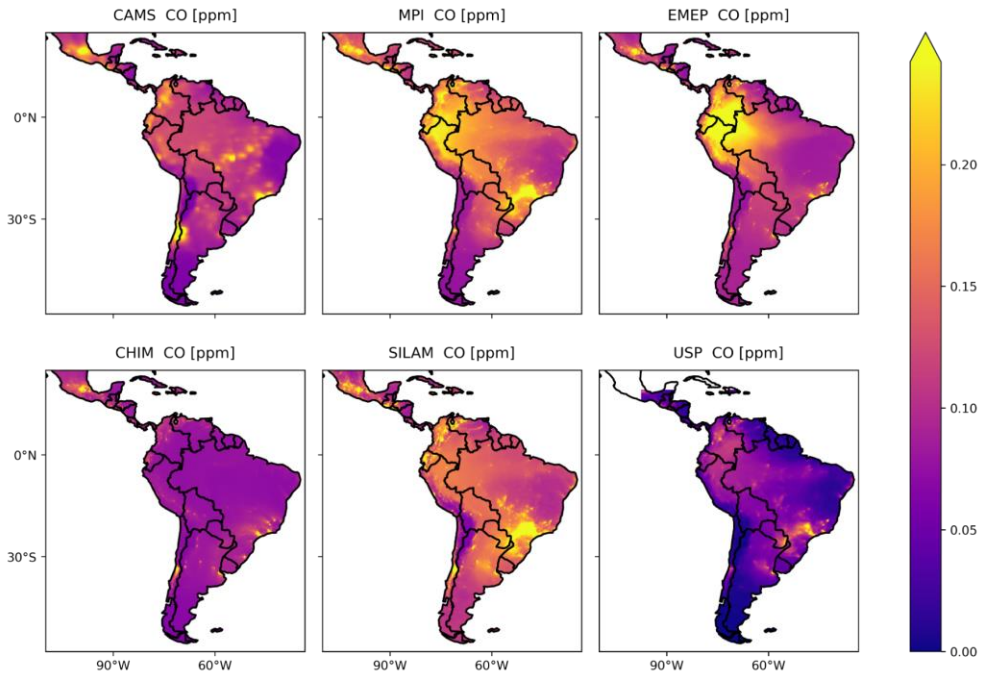

Figure D6. CO simulations in July 2015 by all models

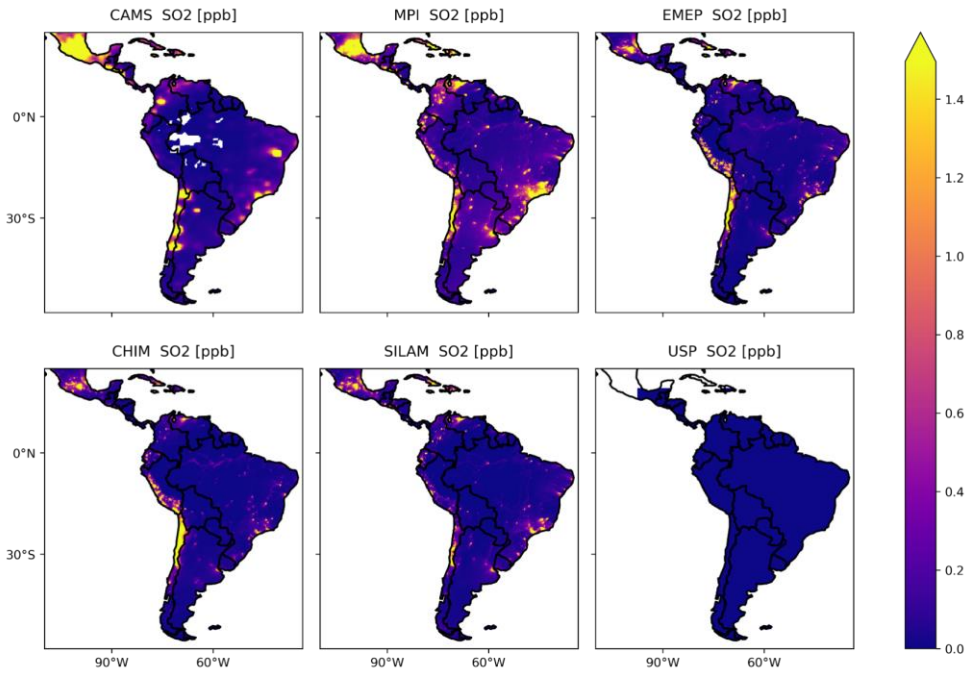

Figure D7. SO_2 simulations in January 2015 by all models

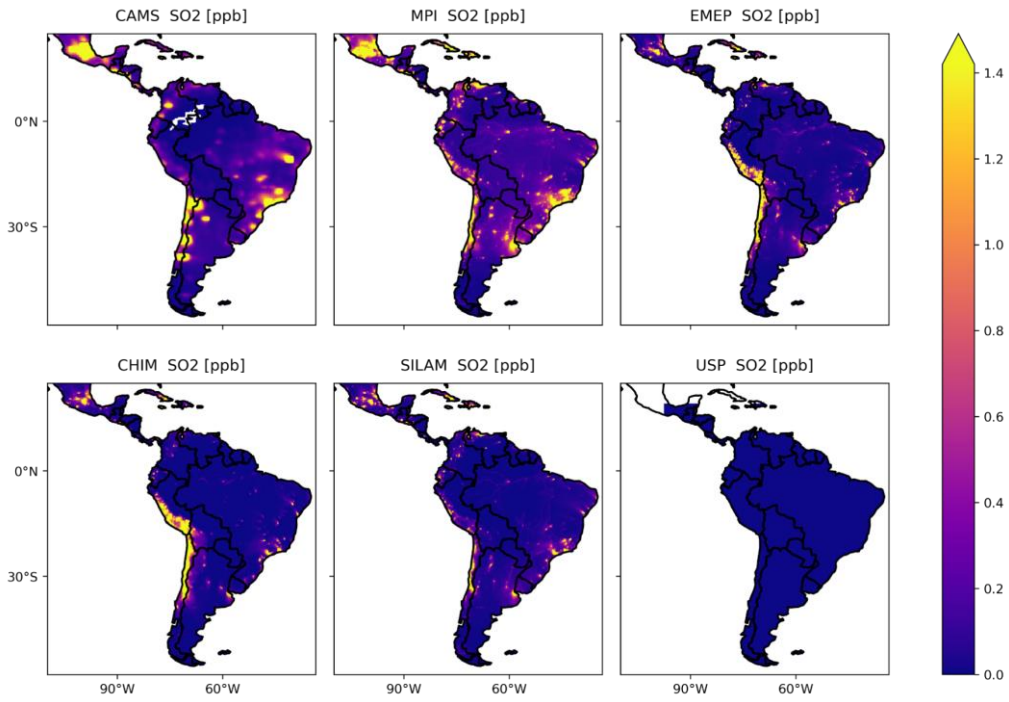

Figure D8. SO_2 simulations in July 2015 by all models

1850

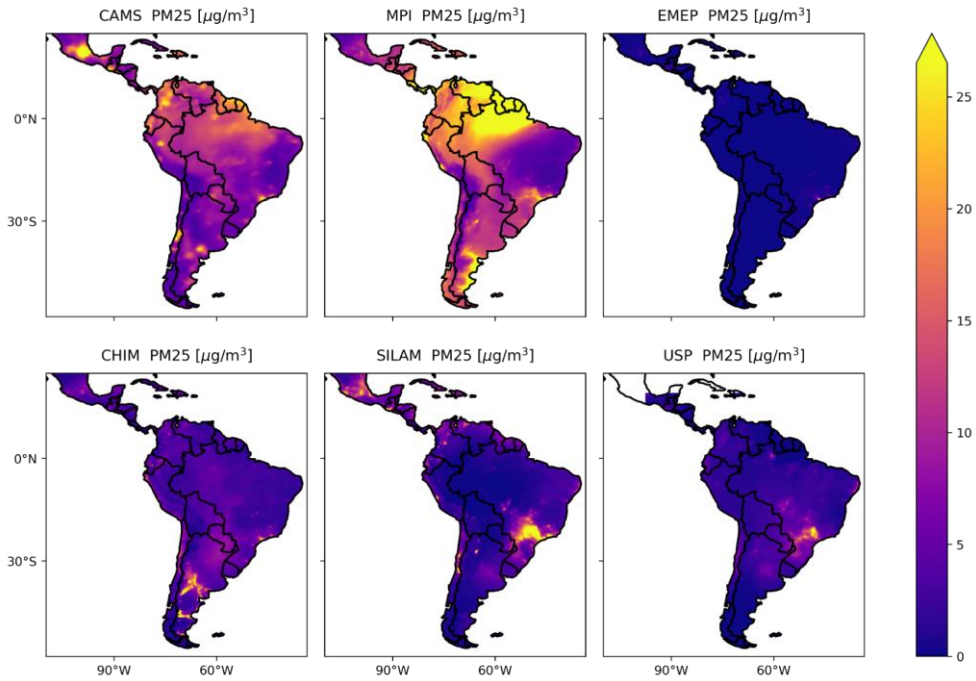

Figure D9. $PM_{2.5}$ simulations in January 2015 by all models

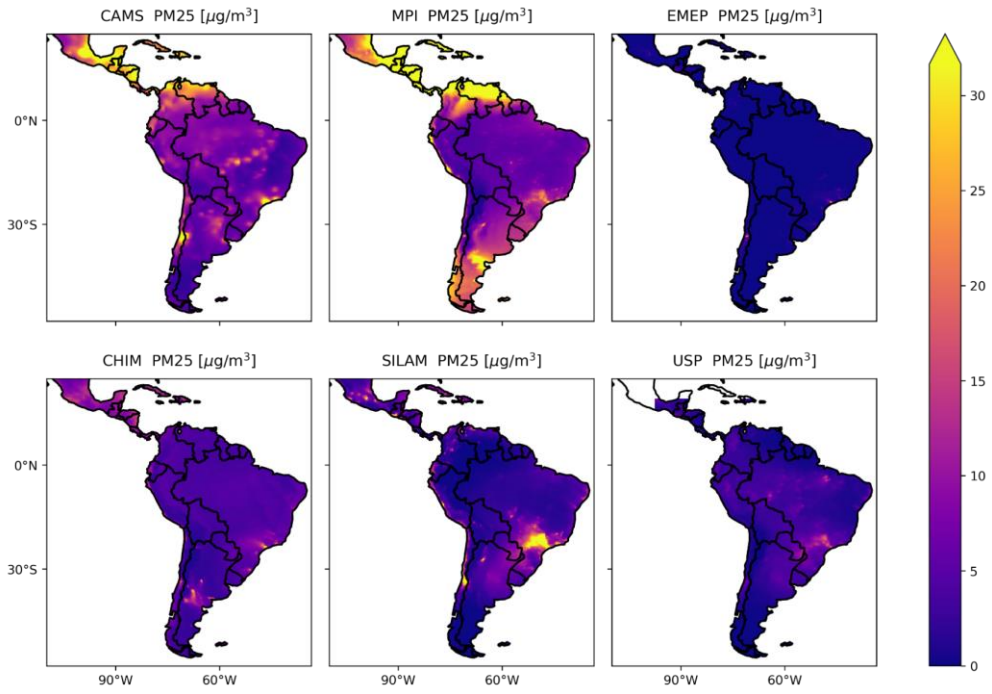

Figure D10. $PM_{2.5}$ simulations in July 2015 by all models

Appendix E. Model deviations

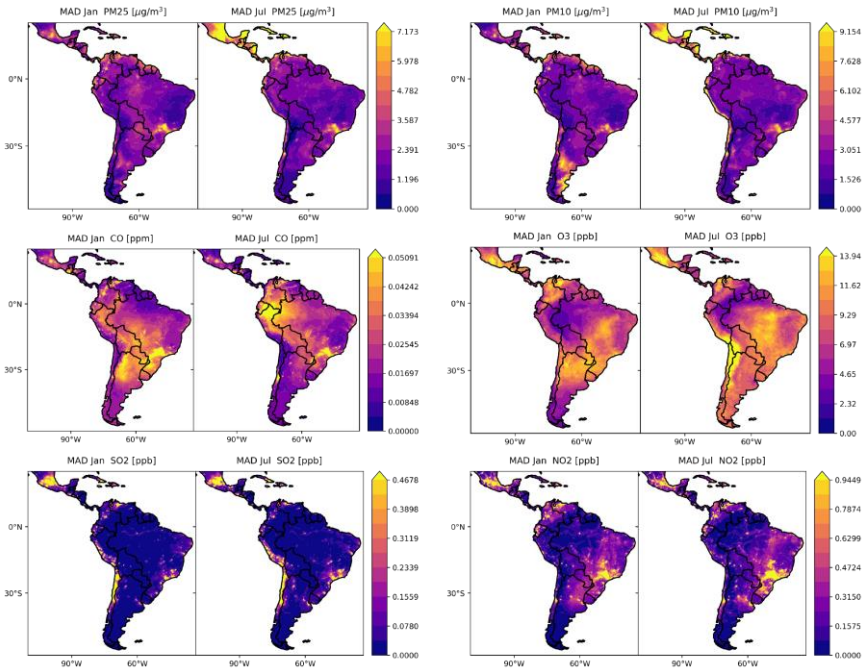

Figure E1. Median absolute deviation of the models with respect to the ensemble for PM_{10}, $PM_{2.5}$, O_3, CO in LAC for January and July 2015

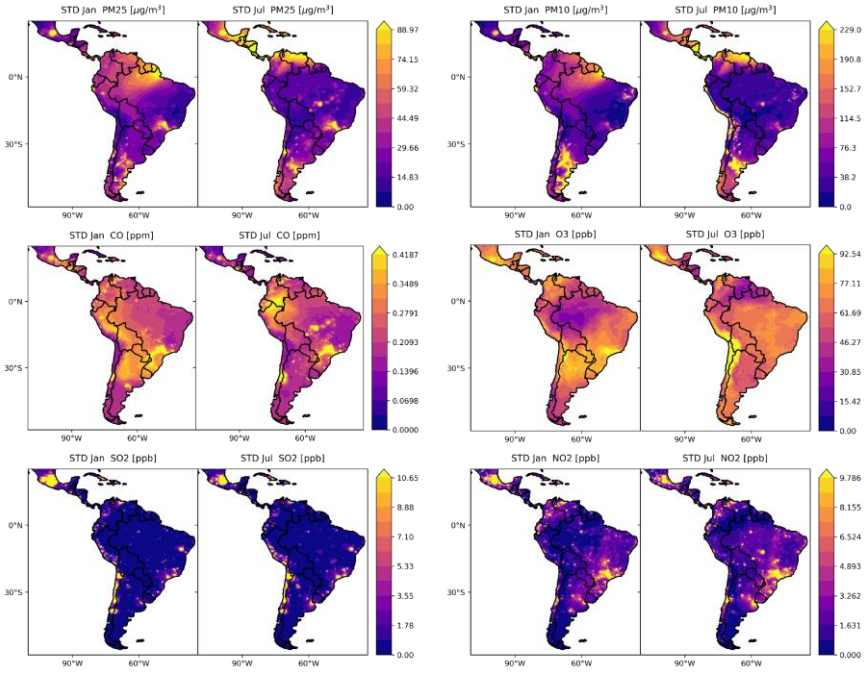

Figure E2. Standard deviation PM_{10}, $PM_{2.5}$, O_3, CO in LAC for January and July 2015 (based on the mean of the models)

1870